Identifying the Pathogenic Mechanisms of *Swiss-Cheese* Phenotypes to Understand Neuropathy Target Esterase Associated Disorders

By

Elizabeth Rosa Sunderhaus

A DISSERTATION

Presented to the Department of Molecular and Medical Genetics

and the Oregon Health & Science University

School of Medicine

in partial fulfillment of

the requirements for the degree of

Doctor of Philosophy

May 2018

Oregon Health and Science University

CERTIFICATE OF APPROVAL

This is to certify that the Ph.D. dissertation of

Elizabeth Rosa Sunderhaus

has been approved on May 4th, 2018

Advisor, Doris Kretzschmar, Ph.D.

Member and Chair, David B. Morton, Ph.D.

Member, Susan Hayflick, M.D.

Member, Mary Logan, Ph.D.

Member, Amanda McCullough, Ph.D.

"Two roads diverged in a wood, and I—
I took the one less traveled by,
And that has made all the difference."
Robert Frost

"Kick Butt,
Play Hard,
Have Fun"
Wisdom from my Father,
John Sunderhaus
Eternally sleeping, never far from my heart

TABLE OF CONTENTS

Index of Figures

Index of Figures (Continued)

Index of Figures (Continued)

List of Abbreviations

ADLI: Anterior Dorsal-Lateral Interneurons

AMPs: Antimicrobial peptides

BiP: Binding Immunoglobulin Protein

BNS: Boucher-Neuhauser Syndrome

CA: Cerebellar Ataxia

cDNA: complementary Deoxyribonucleic Acid

CHOP: CCAAT-Enhancer-Binding Protein Homologous Protein

CNB: Cyclic Nucleotide Binding

CS: Canton S

DN: Deutocerebral Neuropil

DNA: Deoxyribonucleic Acid

DPE: Days Post Eclosion

eIF2α: Eukaryotic Initiation Factor 2 α

EJP: Excitatory Junctional Potential

EMS: Ethylmethane Sulfonate

ER: Endoplasmic Reticulum

ERAD: ER Associated Degradation

GC: Great Commissure

List of Abbreviations

GFAP: Glial Fibrillary Acidic Protein

GHS: Gordon Holmes Syndrome

GRP78: 78 kDa Glucose-Regulated Protein

HSP: Hereditary Spastic Paraplegia

ICLI: Inferior Contralateral Interneurons

Imd: Immune Deficiency

LCA: Leber Congenital Amaurosis

LMS: Laurence-Moon Syndrome

LPC: Lysophosphatidylcholine

MAG: Myelin-Associated Glycoprotein

MBP: Myelin Basic Protein

mEPP: miniature End Plate Potential

MND: NTE Motor Neuron Disease

MRI: Magnetic Resonance Imaging

mRNA: messenger Ribonucleic Acid

NMJ: Neuromuscular Junction

Nt: Natalisin

NTE: Neuropathy Target Esterase

List of Abbreviations

OMS: Oliver McFarlane Syndrome

OP: Organophosphate

OPIDN: Organophosphate Induced Delayed Neuropathy

PC: Phosphatidylcholine

PE: Phosphatidylethanolamine

Per: Period

PLA_2: Phospholipase A_2

PKA: Protein Kinase A

PKA-C3: Protein Kinase A Catalytic Subunit 3

Pkare: PKA-related protein kinase

PKID: Protein Kinase A Interaction Domain

PND: Post-Natal Day

PNPLA: Patatin-like Phospholipase Domain-Containing

PNPLA6: Patatin-Like Phospholipase Domain-Containing Protein 6

PRKX: Protein Kinase X

Rel: Relish

RNA: Ribonucleic Acid

sATX: Spastic Ataxia

List of Abbreviations

SERCA: Sarco-Endoplasmic Reticulum Ca^{2+} ATPase

SLI: Schmidt-Lanterman Incisures

SWS: Swiss-Cheese

TAM: Tamoxifen

TM: Transmembrane

TOCP: tri-ortho cresyl phosphate

TUDCA: Tauroursodeoxycholic Acid

UAS: Upstream Activating Sequence

UPR: Unfolded Protein Response

WT: Widltype

XBP1: X-box binding protein 1

Acknowledgements

One of the questions I always receive during PMCB recruitment is what graduate school is really like? How did you prepare for it? And, I can honestly say, life happens in graduate school, and having a strong base of support is really the only way you can prepare. I was lucky to have the support of so many people along this journey, especially when my world came crashing down.

Firstly, I would like to thank Dr. Doris Kretzschmar, my mentor and Fearless Leader, without whom none of the work presented here would have been accomplished. Doris supported my crazy ideas and always encouraged me to think outside of the box. She wouldn't let me give up on experiments, even when they kept having hiccups, because she knew I could make them succeed. She gave me guidance and let me accomplish my science at my own pace. She was there for my emotional rants about science, administrative issues, and/or family issues. We shared laughs about craziness occurring at home, the strange antics of my cat, Gingee, and how Cincinnatians have butchered some of the German customs. I will be forever grateful for her support and guidance through this crazy ride called graduate school. I would never have found a more understanding mentor like her, or one that would come visit me in the hospital when I was medically confirmed as a freak of nature, as my mom proudly calls me. She made me into the scientist I am today.

Secondly, I have to thank my Dissertation Advisory Committee members—Dr. Susan Hayflick, Dr. Mary Logan, Dr. David Morton, and Dr. Amanda McCullough. Without their guidance and encouragement through the rough

patches, I honestly may have given up. Thank you for being there at the meetings to discuss my science and career goals. And, thank you for understanding the numerous delays that occurred. You all were wonderful to have on my committee and be sounding boards for my ideas.

Thirdly, I need to thank all of my past and present lab members. Thank you to Bonnie Bolkan, Scott Holbrook, and Sudeshna Dutta. They all trained me in the ways of the lab, and they gave me a strong science foundation to pursue my thesis work. Thank you to Marlene Cassar, who was an amazing lab mate, especially when it was only the two of us in the lab. She was my companion in the lab, and I miss her every day that she has been gone. She never judged my crazy, and she was an amazing scientist. Thank you to Alex Law and Subeena Chib, who are my current lab mates. They both have been supportive of my work, and I wish them luck in their future endeavors.

As I mentioned above, one cannot get through graduate school without a strong foundation of support, and I was lucky to have some of the best support a girl could ask for. Thank you to Jackie Wirz for being all around awesome. She always was willing to lend an ear, and she is constantly helping me to find a way to accomplish my goals. To Rick Goranflo is given my eternal gratitude for being amazing, even though he knows I can't say no when he asks a favor. Thank you to my fellow MMG'ers—Nichole, Ellie, Asia, Holly, John, Ryan, Kristof, Jimi, Daelyn, and Michael. They are all amazing scientists, and I never would have made it through graduate school without their encouragement. Nothing was off limits when someone needed advice, and they made me laugh at the times I just

wanted to have a good cry. They were always there when I needed a sounding board, just needed a drink, or just some excellent companionship. This group of students is special, and I will miss them all as I go forward into the world.

Thank you to all of the friends I have made throughout this journey. To Kayly Lembke, my co-conspirator, my movie buddy, and overall the bestest friend a girl could have. She has done so much for me, and if I were to describe her awesomeness, it would take too much of this thesis. She was my companion when I learned my Dad had passed away. She stayed with me the entire time, watching old movies on TCM, and just letting me cry. She took care of my cat, and she got me on the plane home to my family. She was there in the Emergency Room when I was having pain from my internal hernia, and she stayed with me up until they took me into the operating room. She is an amazing person, and our friendship is one of the most significant things I will take away from my time in graduate school. To Lauren Hablitz, the women who trained me in the ways of Hobbits and the importance of second breakfast. I do not know what my lab life would have been without her. Her and my crazy meshed from the first moment, and I still can't adequately describe what exactly our relationship is, but it works. Thank you to Shannon Liudahl, my fellow cohort member. We started this crazy time together, and without her, my time in graduate school would have been that much harder. Thank you to Sarah Wicher for being an astounding friend and source of advice. I treasure all of our outings together, and those times were some of the best I have ever had. To the rest of my friends, Marilyn Chow and Courtney Betts, thank you

for understanding and accepting me. Without out your support, I could never have accomplished as much as I have.

Lastly, thank you to the support of my family. To my cousins, near and far. You are all amazing individuals. When I see you, you are excited for me to be there, and I know I have your love and support. To my brother, Louis, our relationship has never been the easiest, and there are times when we really don't like each other. But, I know you always love me and have my back. Thank you for encouraging me throughout this journey.

To my grandpa. You always believed in me, no matter if it was basketball or science. I love you and miss you every day.

To my dad. You were taken away from us too early. Not a day goes by when I don't want to talk to you and tell you about my day. You were always there to support me in my endeavors, and I miss our talks so much.

Finally, to my mom, one of the strongest women I know. You are always there when I need you, and you are always supporting me. Our adventures are legendary, and I wouldn't want to see the world with anyone else. You are my best friend, and you are always pushing me to go further because you see the potential in me when I don't even know it's there. Please continue to push me, even when I sometimes resent it. My drive to pursue more has always come from you, and you really are the greatest mom in the world.

Abstract

Neuropathy Target Esterase (NTE) is an enzyme localized to the ER that regulates Protein Kinase A (PKA) signaling and maintains lipid homeostasis. Exposure to a neurotoxic organophosphate or mutations in NTE cause a spectrum of disorders with neurodegenerative symptoms ranging from blindness, hypogonadism, and cerebellar atrophy to motor neuron loss. Understanding how the functions of NTE are affected by a chemical or mutations and the mechanisms of pathology is important for the identification of pathways and development of therapeutic strategies. Loss of NTE's ortholog, Swiss-Cheese (SWS), in *Drosophila melanogaster* causes a dysregulation of PKA signaling, an increase in phosphatidylcholine (PC) and lysophosphatidylcholine (LPC) levels and eventual age-dependent neurodegeneration. The goal of this research was to use *Drosophila* to understand the etiology of NTE disorders. Chapter 3 presents work that furthers the understanding of how the dysregulation of PKA signaling affects the loss of motor coordination. We interpret that loss of PKA-C3 function is sufficient to cause impairment of coordinated movement. However, further research needs to be conducted to understand if the regulation of this kinase affects the etiology of NTE disorders. Chapter 4 presents work that shows how the loss of lipid homeostasis activates the Unfolded Protein Response (UPR). These data show that the UPR is a mechanism in the etiology of NTE disorders and provides therapeutic targets for patients. Overall, this work adds to the understanding of NTE disorder etiology and provides evidence that targeting UPR pathways could be a viable therapy for NTE disorder patients.

Chapter 1

Introduction and Background

The History of Neuropathy Target Esterase in Human Disease

"*When you see him coming, I am going to tell you, If you sell him jake, you'd better give him a crutch too"* (Jake Leg Blues 1931)

In 1930, during the Prohibition era, a strange illness, resulting in paralysis in thousands of victims, swept through the United States, eventually being linked to the drinking of Jamaica Ginger extract or "jake", a source of "illegal" alcohol at the time (Morgan et al. 1976, Baum 2003). Consumers of the corrupted "jake" reported cramping muscles and pain followed by weakness in their legs. Eventually, most victims experienced paralysis in one form or another, usually losing control of their hands and feet. (Morgan et al. 1976, Baum 2003). Their unusual gait and walk caused by the affliction became known as "jake leg," and was a theme widespread through blues and country music of the 1930's (Baum 2003). A minimum estimate of 35,000 individuals were affected by the adulterated drink (Morgan et al. 1976). An investigation into the cause revealed that, in the attempt to circumvent the regulations of the Prohibition Bureau, an adulterant known as tri-ortho cresyl phosphate (TOCP) was added to the mixture, and it was this once considered non-toxic organophosphate (OP) that caused permanent paralysis of thousands of victims (Morgan et al. 1976). The disease was medically termed organophosphate induced delayed neuropathy (OPIDN), and while there were outbreaks in other countries due to other contaminated sources, the identity of the targeted protein was not discovered until 30 years later (Morgan et al. 1976).

In the 1950's, studies conducted with chickens analyzed the effects and the types of lesions TOCP caused on the nervous system. The histological analysis of

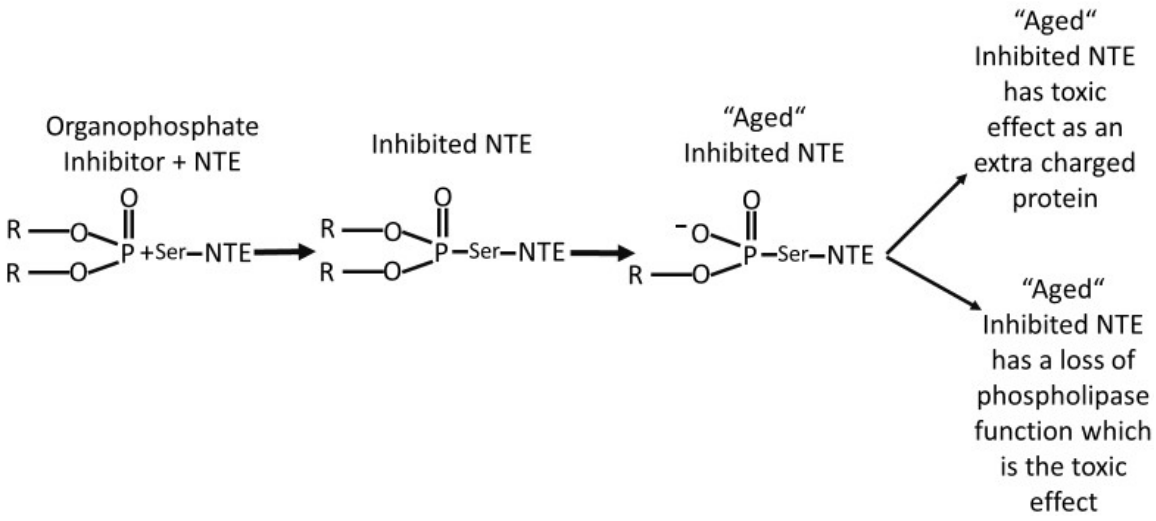

Figure 1-1: Hypothesized mechanisms for OP toxicity in OPIDN. Schematic of the "ageing" reaction originally described by Johnson 1974. When an organism is exposed to an organophosphate (OP) that will inhibit NTE function, the OP will target the catalytically essential serine in the phospholipase domain, making a covalent bond that inhibits the function of NTE. The "ageing" occurs when a side group of the OP is cleaved, permanently binding the OP to NTE. It was predicted that the modified NTE was toxic, damaging the nerves and glia. However, the loss of NTE function as a phospholipase in itself may be the toxic effect, as will be discussed later in this thesis.

exposed hens showed there was demyelination and damage of axon fibers in the peripheral nerves and spinal cord. It was noted that the larger nerves were more susceptible, and the sequence of events observed closely resembled Wallerian degeneration (Cavanagh 1954). It was further noted that treatment with organophosphates disrupted trafficking in the neuronal axons, causing a chemical transection of the nerves that resulted in the Wallerian-like degeneration (Cavanagh 1954, Johnson 1992). However, it wasn't until the 1960's and 1970's that a potential target and mechanism for TOCP poisoning was described. It was

shown that a "neurotoxic esterase" was targeted, causing its activity to be lost, which led to the nervous system lesions in chickens (Johnson 1970). In addition, an "ageing" reaction was proposed where the organophosphate covalently binds the esterase, resulting in an inhibited esterase enzyme with a charged group (Johnson 1974). This "aged" enzyme was thought to be toxic and cause a deleterious effect on metabolism, resulting in damage to nerves and glia and classic neuropathy symptoms described in patients (Figure 1-1) (Johnson 1974). By treating hens with different organophosphates, biochemists established a list of compounds that affected the hens, similar to TOCP. With this list and radioactivity assays to label proteins that these compounds bound to, researchers eventually isolated the protein that was affected, naming it Neuropathy Target Esterase (NTE) (Williams and Johnson 1981). The researchers then developed an assay to measure the esterase function of this protein using the use of phenyl-valerate as a substrate. The phenyl-valerate assay is still in use today to diagnose patients and understand how mutations affect the function of NTE (Johnson 1977, Hein et al. 2010). With cellular fractionation studies, researchers identified the location of NTE, showing that the protein is localized to the cell bodies and axons of the neurons, in particular with the membranous section, such as the endoplasmic reticulum (ER) (Glynn et al. 1997). While the studies with organophosphates helped to develop an activity assay and identify NTE's location in the neuron, the actual function of NTE as a phospholipase in the ER was not known until later with the advances in molecular technologies. It was not until this improvement of cloning and sequencing techniques that actual patients with mutations in NTE were

identified, taking this area of study from its roots in organophosphate exposures to genetic pedigrees.

Mutations in NTE cause a spectrum of disorders

In 2008, Rainier et al. published the first study of index families shown to have mutations in NTE that were genetically linked to childhood onset of weakness in the lower limbs followed by muscle wasting. Magnetic resonance imaging (MRI) studies showed atrophy of the spinal cord, all similar to what is seen in patients diagnosed with OPIDN (Rainier et al. 2008). However, it was also similar to a form of hereditary spastic paraplegia (HSP) caused by mutations in the *spartin* gene. Thus, a linkage analysis was conducted to identify the causal mutations (Rainier et al. 2008). A location on chromosome 19 that contained NTE was identified to have haplotype sharing by affected individuals, leading the researchers to suggest that these mutations deleteriously affected the function of NTE (Rainier et al. 2008). Sanger sequencing identified homozygous mutations in the affected individuals of the consanguineous family. In the other unrelated index family, all individuals affected were compound heterozygotes for NTE mutations (Rainier et al. 2008). These results led Rainier et al. to conclude that mutations in NTE can cause an autosomal recessive form of HSP, and the proposed mechanism in OPIDN of the "aged" enzyme being toxic was not sufficient to explain these cases. Thus, the researchers proposed that the altered activity of NTE alone was sufficient to cause the resulting neuropathies and ataxias. To investigate this hypothesis, investigators used the phenyl-valerate assay to assess the activity of NTE in primary fibroblasts from affected individuals and unaffected heterozygotes

(Hein et al. 2010). The assay uses a colorimetric technique to measure differences in the amount of phenyl-valerate catabolized into phenol in the conditions of one organophosphate that inhibits NTE and one that does not; the difference being the NTE specific activity. The assay showed that affected individuals did have lower NTE activity than their unaffected controls in most cases (Hein et al. 2010). However, there were some unaffected individuals that also had lower activity calculated by this assay, indicating that either the assay in fibroblasts does not reflect what happens in the nervous system or reduction in NTE activity alone is not sufficient to cause motor neuron disease that was similar to OPIDN (Hein et al. 2010). In the following years, with the occurrence of next generation sequencing, other patients with mutations in NTE were identified, and their diagnoses expanded the spectrum of NTE associated disorders. The earliest occurrence of this was in 2014 when clinical patients diagnosed with Boucher-Neuhauser (BNS) and Gordon Holmes syndrome (GHS) were identified to have mutations throughout the coding region of NTE, which is also called Patatin-Like Phospholipase Domain-Containing Protein 6 (PNPLA6) (Synofzik et al. 2014). These patients presented with a wide range of symptoms with onset of disease also being variable. The most common presentations of the affected individuals were early age onset of chorioretinal dystrophy with eventual blindness, hypogonadism, and ataxia that

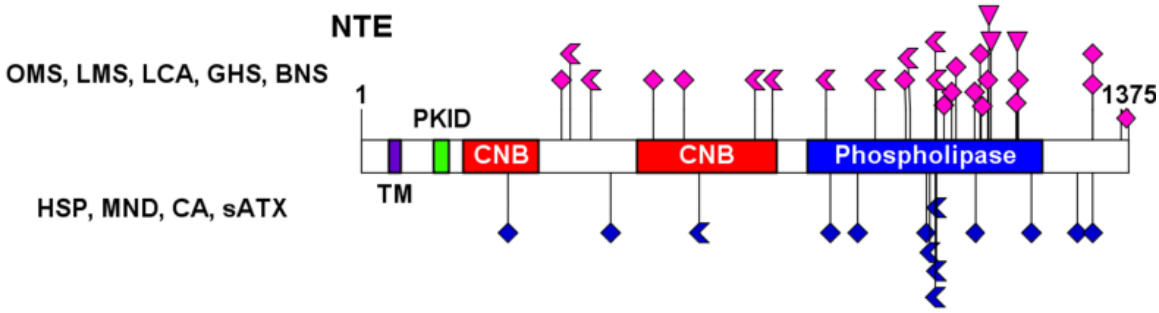

Figure 1-2: Pathogenic mutations of NTE identified in patients. Cartoon of NTE with all known mutations. Mutations marked above NTE have been found in patients diagnosed with the early age of onset diseases of OMS, LMS, LCA, GHS, and BNS. Mutations marked below NTE have been found in patients diagnosed with later age of onset diseases of HSP, MND, C, and sATX. The diamond shape markers indicate a missense mutation. The arrow heads indicate a mutation that led to a truncation of the protein. The upside-down triangles indicate an insertion mutation. It is clearly shown that there are mutations throughout NTE, and no genotype pattern for specific phenotypes is readily observed.

presented later in life (Synofzik et al. 2014). As the years have progressed, more patients with mutations throughout NTE have been identified, with the list of NTE-associated disorders growing to include Laurence-Moon (LMS), Oliver McFarlane (OMS), Leber Congenital Amaurosis (LCA), Cerebellar Ataxia (CA), NTE Motor Neuron Disease (MND), and spastic Ataxia (sATX) (Deik et al. 2014, Topaloglu et al. 2014, Kmoch et al. 2015, Koh et al. 2015, Wiethoff et al. 2017, Langdahl et al. 2017). (Figure 1-2). All of the patients found so far have been either homozygous or compound heterozygous for mutations in NTE with varying symptoms and age of onsets. All of the affected probands' symptoms include an eventual development of ataxia, further complicating a spectrum of neurodegenerative disorders with the only symptom able to be treated being the hypogonadism. These index families

can be found throughout the world, and currently, there is no genotype-phenotype correlation available for clinicians to determine which symptoms may arise in their patients. The work presented in this thesis investigated the basic mechanisms behind these disorders to provide guidance for potential therapy targets and determine if analyzing mutations in NTE could provide insight into a pattern that would be predictive of symptoms in patients.

The Function of Neuropathy Target Esterase

NTE was shown to be inhibited by organophosphates, and the studies done in hens and other animal models determined its activity and location. The data from these studies showed that NTE was associated with the ER, trafficked out into the axons, and that its most likely role was an involvement in the metabolism of a carboxylic acid, which includes phospholipids (Glynn et al. 1997, Glynn 2000). It was not until several years later, with the use of improved biochemical techniques to isolate the protein and sequence its primary structure, that it was discovered how conserved the protein's functional domain was and how similar it was to other serine hydrolases (Lush et al. 1998). The protein was isolated, and with the aid of proteolytic digests, the sequence of NTE was determined. While NTE was predicted to have four transmembrane domains, the one closest to the N-terminus had the strongest score, and thus, it was deemed that one that kept NTE in the ER membrane (Lush et al. 1998). In addition, the catalytic domain contained the GXSXG motif, which is found in similar esterases, indicating the serine at position 966 of the protein was likely the protein's catalytically essential serine (Figure 1-3) (Lush et al. 1998). However, when the sequence was submitted to databases,

NTE's sequence failed to find similarity to other hydrolases, leading the researchers to conclude that NTE is a new class of serine esterase (Lush et al. 1998, Atkins et al. 2000). Interestingly, the database search revealed that NTE's sequence was conserved in other organisms, and it was very similar to *Drosophila melanogaster*'s Swiss-Cheese (SWS), which will be discussed in the next section (Figure 1-3) (Lush et al. 1998). From this work, the researchers concluded that NTE was a conserved serine esterase that was embedded into membranes, but the actual substrates of NTE still remained elusive (Atkins et al. 2000).

Neuropathy target esterase is a phospholipase in the endoplasmic reticulum

Due to its similarity to Phospholipase A_2's (PLA_2) ability and need to associate with membranes to be fully functional, it was hypothesized that NTE was a serine esterase that catabolized membrane lipids, in particular phospholipids (Glynn 2000). To test this hypothesis, the truncated construct called NEST, which contained the membrane bound catalytic domain of NTE, was cloned into *E. coli* to determine if this simplified form was capable of releasing radioactive fatty acids from the lipids incubated with it (Tienhoven et al 2002). NEST catabolized phospholipids at rates similar to the PLA_2, although, its favored substrate was lysophospholipids (Tienhoven et al 2002). Notably, this study only used the truncated version of NTE, and it was also unknown if these results would replicate *in vivo*. As the ability to manipulate the genome in murine models improved, the

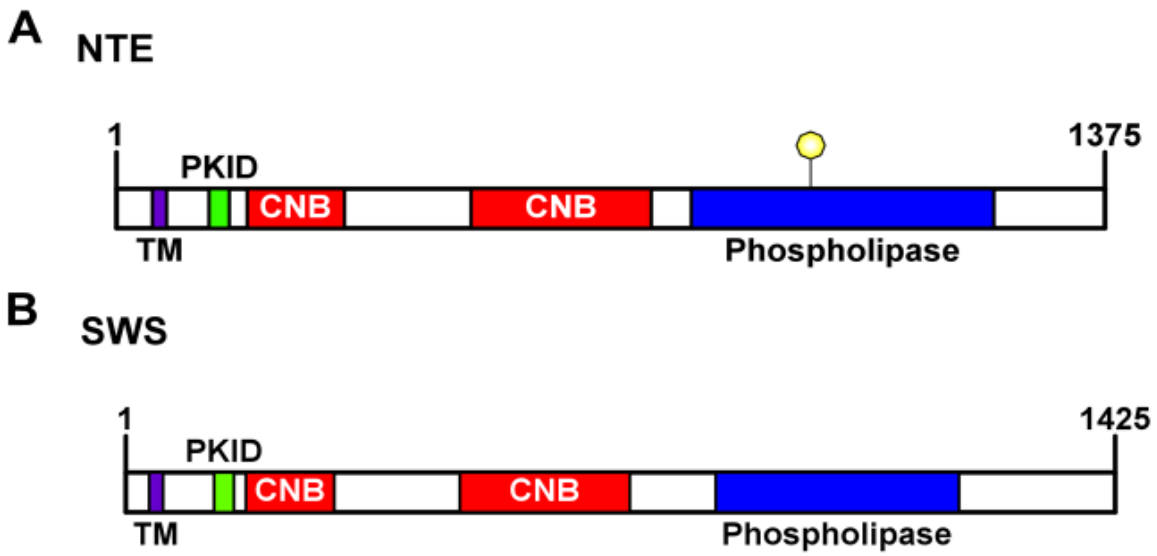

Figure 1-3: Protein domain structure of NTE and its homologue SWS. A. Cartoon of NTE's protein domain structure. The transmembrane (TM) domain localizes NTE to the ER, allowing the phospholipase domain to conduct its role in lipid homeostasis. The yellow marker indicates the location of the catalytically vital serine. There is a PKA Interaction Domain (PKID) that contains a pseudosubstrate site predicted to regulate the activity of PKA catalytic subunits. There are three cyclic nucleotide binding domains, one near the PKID and two that overlap in the middle of the protein, which are thought to regulate either the phospholipase domain or PKID regulatory activity. **B.** Cartoon of SWS's protein domain. SWS is the *Drosophila* homologue of NTE and its protein domain structure matches that of NTE. SWS has an overall 41% identity score when compared to NTE's primary structure, and the score is higher in the conserved domains (Lush et al. 1998, Atkins et al. 2000, Kretzschmar et al. 1997).

next logical step was to eliminate a copy of NTE to determine if NTE's role as a lysophospholipase held true in an animal model. In the first study, a LacZ construct was inserted to cause an inframe fusion that resulted in a truncated version of NTE that did not have the catalytic domain of the protein. However, the β-galactosidase activity assay showed that the expression pattern was consistent with previous

studies (Winrow et al. 2003). The researchers found that a homozygous deletion of NTE was embryonic lethal due to what was later shown to be placental failure, indicating NTE was vital for development (Winrow et al. 2003, Moser et al. 2004). Since they could not easily examine the effect of a complete NTE knockout using embryos, they decided to examine the activity of NTE in heterozygotes. Using the phenyl-valerate assay, with only one allele of NTE, the overall activity of NTE was reduced by 60% compared to wildtype (Winrow et al. 2003). The mice were also more sensitive to the effects of organophosphate treatments as shown by a higher mortality rate and reduction in movement when placed in an open field test. All of these data confirmed that NTE was highly expressed in the nervous system, essential for embryonic survival, and that having two alleles of NTE is protective against the effects of organophosphate exposure (Winrow et al. 2003). Using the same mouse model, the ability of murine NTE to act as a lysophospholipase was assessed with an adapted phenyl-valerate assay that instead used lysolecithin, a lysophospholipid that demyelinates neuronal sheaths and cause axonal lesions, similar to the ones see in OPIDN. With the use of this adapted assay and brain homogenates, it was shown that NTE catabolizes lysolecithin, and the heterozygous mice were again deficient in NTE activity when assayed (Quistad et al. 2003). All of these data established that NTE's function was to catabolize phospholipids, in particular lysophospholipids.

Confirming that NTE is indeed a phospholipase, while important, was not enough to understand the complete role of NTE in the nervous system. NTE needed to be deleted from the nervous system entirely, but a complete knockout

of NTE is embryonic lethal. Fortunately, a conditional knockout system was developed that involved the use of the Cre/Loxp system. A *Nestin* promotor was used to drive Cre-recombinase in the nervous system of mice, which when bred into a floxed NTE, deleted NTE in the nervous system (Akassoglou et al. 2004). These conditional knockout mice showed age dependent neurodegeneration, specifically in the hippocampus. In addition, the mice showed abnormal membranous whorls, which was similar to the phenotypes seen in the *Drosophila sws*^{1} mutational line that will be described further in the next section (Akassoglou et al. 2004). Because NTE is known to localize to membranous organelles, the researchers confirmed that NTE was localized to the ER with immunohistochemistry, and with the loss of NTE, abnormal ER aggregates were present in the hippocampal sections of the nervous system knockout (Akassoglou et al. 2004). This lead the researchers to believe that improper protein folding, transport, and degradation due to an impaired ER may be causing cellular damage. The researchers concluded that this cellular damage contributed to the neurological symptoms seen in the mice, including the loss of Purkinje cells in the cerebellum and the corresponding locomotor defects (Akassoglou et al. 2004). With the use of the same mice, it was also shown that the long axonal tracts of the spinal cord are equally affected by the loss of NTE. The researchers showed that the neurons of knockout mice had impaired secretion, which inhibited the maintenance of the long axons by preventing the export of neuronal materials (Read et al. 2009). In addition, it was discovered that lesions found in the lumbar spine axons were preceded by swelling, and when phosphatidylcholine (PC) was

assayed in brain homogenates of these mice, it was discovered that the knockout mice have an intrinsically higher level of PC that is never resolved (Read et al. 2009). These data along with the evidence of impaired secretion indicates that NTE is vital for the maintenance of lipid homeostasis and axonal maintenance, and its loss in the nervous system cannot be compensated for by other phospholipases (Read et al. 2009). However, how and why the loss of lipid homeostasis is causing the neurodegenerative phenotypes has never been adequately studied. It is the goal of this thesis to identify a mechanism that will explain why the loss of NTE function in the nervous system results in impaired ER function and the eventual loss of neurons.

Swiss-Cheese, a Model of Neuropathy Target Esterase Disorders

With the increase in life expectancy, neurodegenerative diseases like Alzheimer's disease have become an increasing health threat for the general population. Although significant progress has been made in identifying genes that impact the risk for disease, there is still much not understood about how and why these neurodegenerative diseases differ from patient to patient.

"Simple" invertebrate model organisms such as *Drosophila melanogaster* offer a variety of experimental advantages to study the mechanisms of neurodegenerative diseases, including a short life cycle, high fecundity, and the availability of molecular techniques that make the manipulation of the organism relatively easy, such as the GAL4/UAS system (Brand and Perrimon 1993, Greenspan 1997, Rubin et al. 2000, Jenett et al. 2012, McGurk et al. 2015). The GAL4/UAS system allows for the temporal expression of a choice construct in a

subset of cells (Brand and Perrimon 1993, Jenett et al. 2012). GAL4 is a yeast transcription factor that when expressed by a specific promotor can bind to the Upstream Activating Sequence (UAS) in front of the construct of interest to express it in a tissue specific manner (Brand and Perrimon 1993, Jenett et al. 2012). There are hundreds of these promotors and GAL4 combinations, known in the field as drivers, available that can be used to express UAS constructs of interest (Jenett et al. 2012). Even though *Drosophila* is considered a simpler system than other model organisms, it actually has a highly complex and conserved nervous system, with many similarities to the human nervous system. For example, it is organized into regions with particular subsets of neurons and glia with roles in the control of the circadian clock, locomotor functions, and learning and memory. In addition, the majority of disease causing genes, approximately 70%, have orthologues in *Drosophila*, such as the orthologue for NTE known as SWS (Rubin et al. 2000, McGurk et al. 2015).

SWS was first isolated in an unbiased screen that used ethylmethane sulfonate (EMS) to isolate mutants that upon histological sectioning of the head showed brain defects (Heisenberg and Bohl 1979, Kretzschmar 1997). Numerous central nervous system vacuoles were observed in these flies, and the mutational line was named *swiss-cheese* for obvious reasons (Heisenberg and Bohl 1979, Kretzschmar 1997). This vacuole phenotype was sex-linked, leading the researchers to conclude the mutations and the gene of interest were located on the X chromosome (Heisenberg and Bohl 1979, Kretzschmar 1997). At seven days post eclosion (dpe), neurodegeneration and apoptosis were detected in the

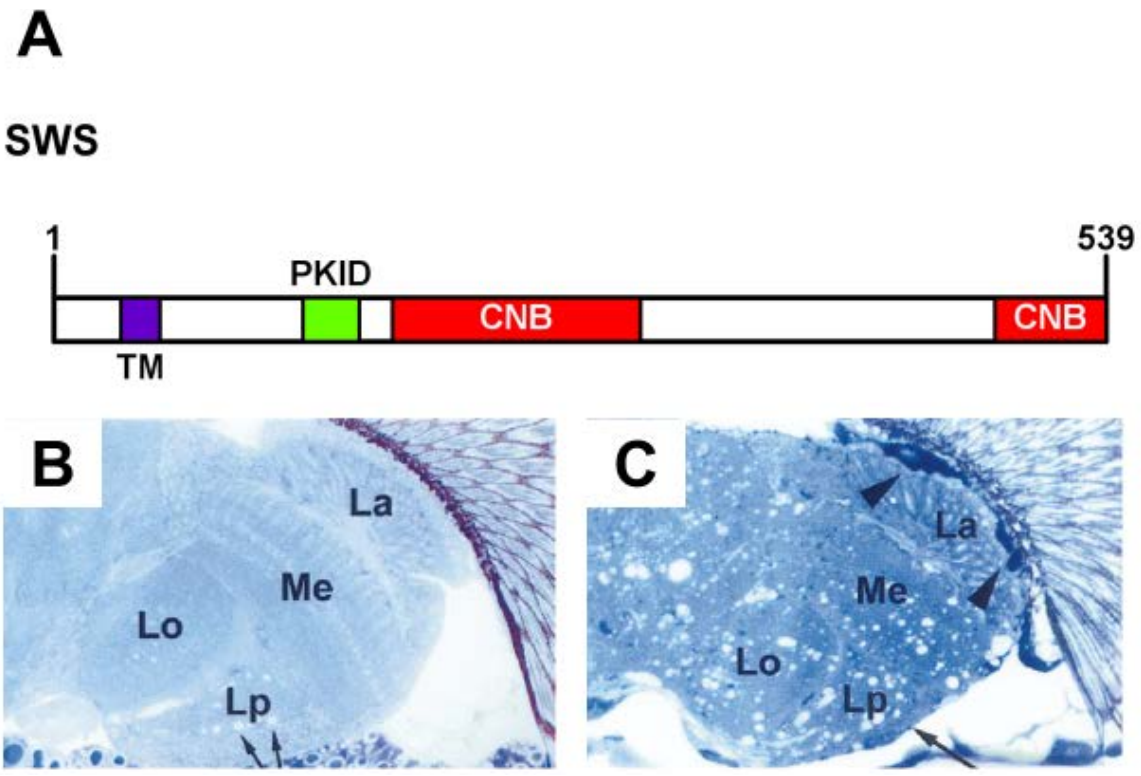

Figure 1-4: The *sws*^{1} mutation with phenotypes A. Schematic of the truncated form of the SWS protein in the *sws*^{1} mutant line. Based on negative western blots, *sws*^{1} is considered a null mutation. **B.** Cross section of a wildtype fly brain stained with toluidine blue at 20 dpe. (The arrows indicate white areas in the lobula plate that are cross sections of giant fibers, not vacuoles.) **C.** Section of a *sws*^{1} fly brain at 20 dpe, exhibiting the age dependent neurodegeneration and darkly stained structures that are indicative of *sws*^{1}'s glial phenotype. Recreated from Kretzschmar et al. 1997 with permission.

neuropil and cortex of the mutants respectively, and both were shown to increase with age. (Kretzschmar 1997). In addition to the neurodegenerative phenotype, a glial wrapping defect was detectable by EM in newly eclosed flies (Kretzschmar 1997). As with the neurodegeneration, the glial abnormalities progressed with age, including the formation of irregular membranous whorls. It was concluded that SWS

was required in both glia and neurons for nervous system maintenance, and possibly also for the proper interaction between the two cell types (Kretzschmar 1997).

One particular mutation designated as *sws*^{1} was the line used in this thesis. Therefore, a thorough description of the mutation and its phenotypes is required. *sws*^{1} was discovered to contain a nonsynonymous mutation in a predicted cyclic nucleotide binding motif that resulted in an early truncation of the protein at amino acid location 539, which would result in a protein one fourth of its usual size (Figure 1-4) (Kretzschmar 1997). However, this mutation has been classified as a null allele, since SWS protein was not detected in a western analysis (unpublished data). This mutant line displayed the age dependent neurodegeneration and reduced lifespan as seen in other *sws* mutation lines (Figure 1-4) (Kretzschmar 1997). Therefore, for this thesis it is assumed that when using the *sws*^{1} mutant line, that the flies are null for any SWS protein and function.

SWS and its conserved function as a phospholipase in the ER

Once it was known that SWS was the *Drosophila* orthologue of NTE, it was investigated whether the functional activity of NTE as a phospholipase was conserved with its orthologue SWS (Lush et al. 1998). Expression of SWS and murine NTE with the GAL4/UAS in either glial or neurons rescued the defects in that specific cell type, indicating a cell autonomous function of SWS/NTE and mammalian NTE expression could also rescue the *sws*^{1} mutant defects (Muhlig-Versen et al. 2005). SWS was shown to localize to the ER, and in *sws*^{1} flies, a number of abnormal membranous structures appeared in the cell body of neurons,

similar to those seen in the nervous system of knockout mouse, leading to the conclusion that SWS was needed for the maintenance of the ER (Muhlig-Versen et al. 2005). The phenyl-valerate assay was used to show that the *sws*^{1} line lacked NTE-like esterase activity, and there was an increase in the levels of phosphatidylcholine, which was rescued when SWS was reintroduced back into the neurons using the GAL4/UAS system (Muhlig-Versen et al. 2005). Although, how this increase in PC levels and lack of lipid homeostasis causes the phenotypes seen in the *sws*^{1} mutant line is unknown, all of these data led to the conclusion that SWS was indeed the functional orthologue of NTE, and *Drosophila* could be used as an animal model to study the effects of the loss of SWS/NTE in the nervous system.

SWS is a noncanonical regulator of PKA-C3

It was noted that SWS contained a N-terminus that showed homology to the regulatory subunits of Protein Kinase A (PKA) with cyclic nucleotide binding (CNB) sites and a pseudosubstrate site that was similar to the conserved R-R-X-S-X consensus site in other regulatory subunits of PKA (Figure 1-3) (Kretzschmar et al. 1997). With these molecular data, it was hypothesized that along with its role as a phospholipase, SWS could also be acting as a regulator of PKA signaling in the nervous system of *Drosophila.* To investigate whether the PKA interactive domain served a functional role, one of the conserved arginines, R133, was mutated to an alanine. Thus, if SWS is acting as a noncanonical regulator or PKA signaling, a mutation of this essential amino acid should impact the ability of SWS to rescue *sws*^{1} phenotypes (Bettencourt da Cruz et al. 2008). And, while we observed that

SWS^{R133A} rescued the *sws^{1}* neurodegeneration, the rescue was weaker in comparison to expression of wildtype SWS. This weaker rescue may be caused by a reduction in the mutated SWS's esterase activity, indicating that SWS rely on an interaction with the PKID to act as an esterase (Bettencourt da Cruz et al. 2008).

Knowing the mutation in SWS affected its function indicated that SWS most likely was a regulator of a catalytic PKA subunit. However, *Drosophila* has three catalytic subunits of PKA, and while PKA-C1 and its regulation had been widely studied at the time, the other two catalytic subunits' roles remain unknown. Thus, a yeast-two hybrid study was conducted to determine which of the catalytic subunits SWS interacted with and most likely regulated. With this study, a surprising result was found. SWS did not interact with the most well-known PKA-C1 subunit, but the unknown and understudied PKA-C3 subunit (Bettencourt da Cruz et al. 2008). To further confirm this finding, localization studies were conducted to ensure that *in vivo* SWS and PKA-C3 were found in the same locations within the nervous system. Upon immunohistochemistry of the brain, it was found that SWS and PKA-C3 were indeed localized in the same neurons of the brain (Bettencourt da Cruz et al. 2008). In addition, it was found that in the *sws^{1}* mutant PKA-C3, normally localized to membranes, was missing in the membrane fractions, indicating that PKA-C3 is mislocalized in neurons in the absence of SWS (Bettencourt da Cruz et al. 2008). To further support that deregulation of PKA-C3 activity contributed to the *sws^{1}* phenotypes, it was shown that overexpression of PKA-C3 in the neurons was sufficient to cause vacuoles to form in the brains of wildtype flies, indicating that

regulation of PKA-C3 activity is needed for the health of the nervous system (Bettencourt da Cruz et al. 2008).

Identifying Mechanisms that lead to SWS/NTE Related Phenotypes

NTE is the protein product of the PNPLA6 gene, and as mentioned above, studies have determined that mutations in the gene are responsible for several recessive neuronal diseases. In the last five years, over 40 index cases have been identified and it is highly likely that many more patients will be identified in the future. However, there are no therapies for the neurodegeneration observed in patients. And, with NTE being a target of toxic organophosphates that can be used in agriculture and chemical warfare, understanding the actual mechanisms behind the disease phenotypes is essential for developing potential therapies if a widespread exposure should occur. While the disease-causing gene is known, the cellular mechanisms leading to the pathologies are not. In this thesis, I have expanded upon several mechanisms that could account for the variation in the disorders as well as provide targets for future therapies.

From all of the reviewed literature so far, it is clear that SWS is indeed the orthologue of NTE, and through the use of *Drosophila* as an animal model, the mechanism involved in the death of neurons due to the loss of SWS/NTE can readily be investigated. From *Drosophila* studies, it is already known that SWS serves two functions in the neurons of *Drosophila*— one being the regulation of PKA signaling, and the second being the maintenance of lipid homeostasis in the ER (Figure 1-5). The following section introduces how the loss of these functions could be leading to the neurodegeneration seen in the flies, while providing

further background for experiments conducted in the remaining chapters of this thesis.

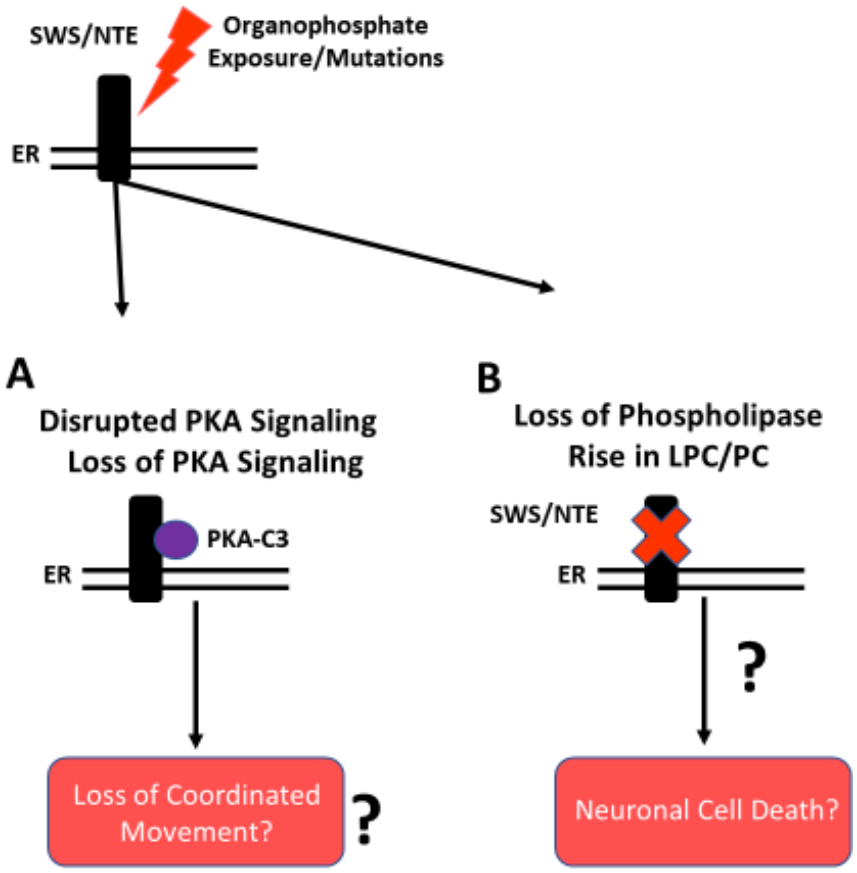

Figure 1-5: Identifying Mechanisms that lead to SWS/NTE Related Phenotypes. The two functions of SWS in the nervous system are to **A.** control PKA signaling by regulating the activity of PKA-C3 and **B.** maintain lipid homeostasis in the ER. **A.** Overactivation of PKA-C3 is sufficient to induce neurodegeneration in *Drosophila*, however, what the loss of PKA-C3 affects was unknown. In Ch. 3, I explore how the loss of PKA-C3 affects the coordinated movement of *Drosophila*. **B.** Loss of SWS/NTE function leads to a significant elevation of LPC/PC, which leads to neuronal cell death. However, why that elevation leads to neuronal death is unclear. In Ch. 4, I parse out what is affected and activated by the loss of lipid homeostasis and provide potential targets for therapies in the future.

Dysregulation of PKA-C3 leads to locomotor defects and neurodegeneration

Exposure to an organophosphate or mutations that affect the PKA interacting domain of NTE may play a role in the development of the neurological phenotypes associated with loss of NTE. Our lab has previously shown that SWS is able to interact with PKA-C3 in a yeast two-hybrid assay, and the pan-neuronal overexpression of PKA-C3 was sufficient to induce neurodegeneration in a wildtype background (Bettencourt da Cruz et al. 2008). It has also been shown that the disruption of SWS's regulatory function by treatment with TOCP contributes to neuronal degeneration in the fly model of OPIDN (Wentzell et al. 2014). When the flies were treated with TOCP, along with a decrease in esterase activity, there was also a decrease in PKA activity, indicating that the organophosphate prevented the release of PKA-C3 from SWS (Wentzell et al. 2014). This function of SWS appears to be conserved in the murine system as well. Murine NTE was capable of specifically interacting with PKA-C3 solely in a yeast two-hybrid screen (Wentzell et al. 2014). In addition, when murine hippocampal neurons were treated with TOCP, they too had a decrease in PKA activity, indicating that the treatment prevented NTE from releasing Pkare, the murine ortholog of PKA-C3 (Wentzell et al. 2014). This evidence indicates a toxic gain of function caused by organophosphate exposure, but it is unclear how mutations in NTE affect the regulatory function.

PKA-C3 is an unusual type of PKA catalytic subunit because its sequence homology is more closely related to murine Pkare and human Protein Kinase X (PRKX) than to any of the other catalytic subunit of PKA within *Drosophila*

(Blaschke et al. 2000, Huang et al. 2016). PKA-C3, Pkare, and PRKX comprise a phylogenetically distinct group of serine/threonine protein kinases that are regulated through binding to pseudosubstrate sites similar to the PKID found in SWS/NTE (Blaschke et al. 2000, Bettencourt da Cruz et al. 2008, Huang et al. 2016). Even though PKA-C3, Pkare, and PRKX have been shown to be expressed in the nervous system, there is no known information on the targets of the kinase function or how they affect their targets in the neurons (Kalderon and Rubin 1988, Li et al. 2005). Studies were conducted on PKA-C3 to determine if it could compensate for a PKA-C1 deficiency and if a knockout of PKA-C3 was lethal; however, once those studies did not reveal any effects, research into its role in the nervous system was no longer pursued (Melendez 1995). Thus, studies to elucidate the roles of PKA-C3 and its homologues are essential to further understand the implication in the nervous system when these kinases are deregulated. In Chapter 3 of this thesis, these studies were conducted in the hopes of further understanding functions of PKA-C3 and the implications of what occurs when its activity is dysregulated.

The Unfolded Protein Response is initiated with the loss of SWS function

Maintaining a healthy ER is vital for the activity and health of neurons. The ER is a major source of Ca^{2+} storage and signaling, as well as the initial step in the secretory pathway (Verkhratsky 2005). Neurons rely on the ER to control the Ca^{2+} pools in the dendrites and synapses, as well as to provide key nutrients to the axons, especially in larger neurons such as Purkinje cells (Verkhratsky 2005). A faulty ER leads to the impairment of important cellular signals as well as the

activation of the unfolded protein response (UPR) or ER stress response. The ER stress response has been shown to be involved in many different neurological diseases, and usually activation occurs by the elevation of unfolded proteins in the ER (Yoshida 2007, Hetz and Saxena 2017). The presence of unfolded proteins causes the chaperone GRP78 (BIP) to release the ER stress sensors IRE1α, PERK, and ATF6, activating their signal cascades (Yoshia 2007, Wang and Kaufman 2014, Hetz and Saxena 2017). These signal cascades then activate many responses such as lipogenesis, to enlarge the ER, or the translation of additional chaperones to aide in the folding process and reduce the burden on the ER (Figure 1-5) (Yoshia 2007, Wang and Kaufman 2014, Hetz and Saxena 2017). However, activation of the ER stress response will eventually trigger apoptosis and the longer the stress response continues, the more likely the cell will undergo programmed cell death.

It was previously mentioned that neurons in the *sws*^{1} line undergo apoptosis, supporting the hypothesis that ER stress could be playing a role in the neurodegenerative phenotype (Kretzschmar et al. 1997). Several papers have shown that an elevation in unfolded proteins is not the only way to activate the ER stress response; loss of lipid homeostasis can also cause ER stress (Lagace and Ridgway 2013, Mei et al. 2013, Roussel et al. 2013, Hetz and Mollereau 2014). It was observed that just affecting the saturation of the fatty acid tails was sufficient enough to initiate the ER stress response and eventually led to apoptosis when lipid homeostasis failed to be restored (Fu et al. 2011, Paran et al. 2015,). Our lab have shown that a loss of SWS in *Drosophila* causes a rise in PC levels and a

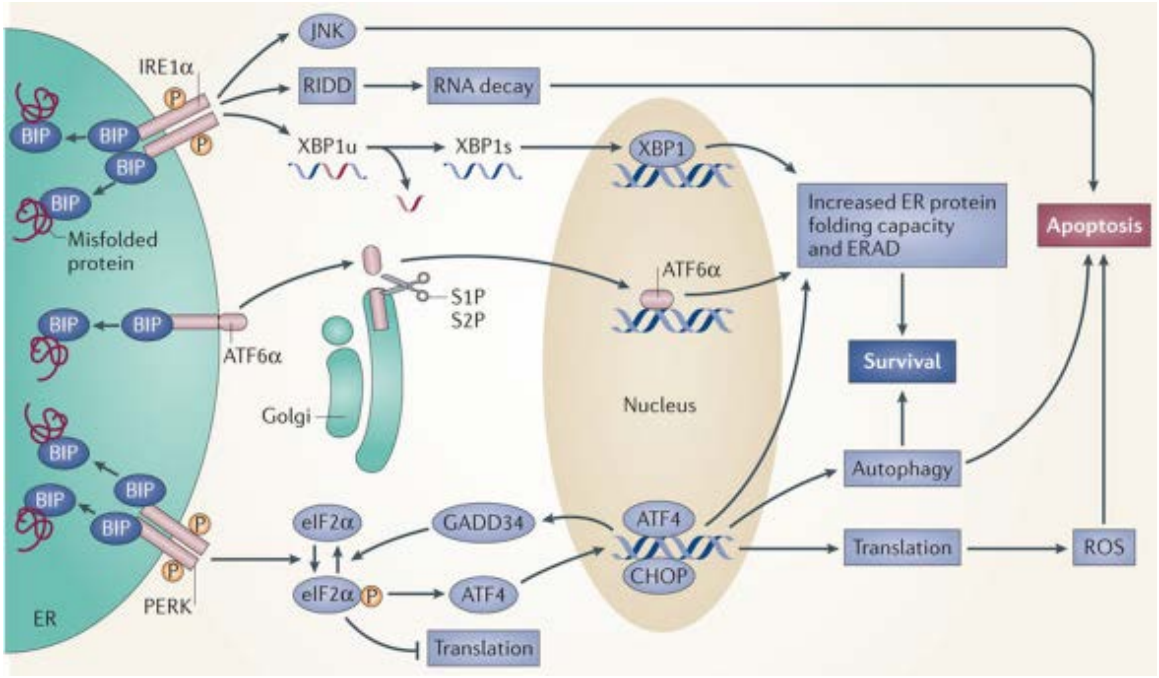

Figure 1-6: Diagram of the Unfolded Protein Response. Once an insult to the ER is sensed, BIP leaves the sensors IRE1α, PERK, and ATF6, resulting in the activation signal cascades. IRE1α dimerizes and auto-phosphorylates, allowing to splice the intron out of X-box binding protein 1 (XBP1u), so it can translocate to the nucleus to act as a transcription factor for UPR genes involved in expanding the ER and increase the number of chaperones. PERK also dimerizes to phosphorylate eukaryotic Initiation Factor 2 α (eIF2α) to inhibit translation. ATF6 translocated to the Golgi Apparatus, where it is cleaved to activate another transcription factor for chaperones and ER associated degradation (ERAD) pathways. If the insult to the ER fails to be resolved, apoptotic pathways will activate, resulting in cell death. Recreated from Wang et al. 2014 with the permission.

decrease in triacylglycerols, but phosphatidylethanolamine (PE) levels did not to change (Muhlig-Versen et al. 2005). As mentioned previously, the deletion of murine NTE also causes a rise in PC levels that other phospholipases fail to rectify (Read et al. 2009). In the ER, PC and PE are the primary phospholipids that make

up the membranous organelle. Multiple animal models, such as a rat obesity model and a mouse Duchene muscular dystrophy model, showed the ratio between the two phospholipid levels must be maintained for the Sarco/Endoplasmic Reticulum Ca^{2+} ATPase (SERCA) to function properly (Fu et al. 2014, Paran et al. 2015). SERCA is the pump that uses ATP to take Ca^{2+} from the cytosol and store it in the ER, where the Ca^{2+} can be used by chaperones to aide in protein folding. In neurons, it can also be used in the regulation of firing action potentials. In the two models, there was a higher PC/PE ratio in the cells causing SERCA activity to be inhibited, leading to the activation of the UPR (Fu et al. 2014, Paran et al. 2015). Currently, agonists of SERCA are being developed to determine if the activation of SERCA could be a potential therapy to attenuate ER stress when loss of lipid homeostasis is the suspected instigator (Kang et al. 2016). When one of the afore mentioned agonists was used, activation of SERCA reduced the ER stress markers and the expression of lipogenesis markers in a mouse model of type 2 diabetes (Kang et al. 2016). In Chapter 4 of this thesis, whether the UPR is playing a role in the locomotor defects and neurodegeneration seen in the *sws*^{1} mutant is investigated.

Chapter 2

Materials and Methods

MAINTENANCE FOR FLIES IN ALL CHAPTERS

Flies were maintained on standard fly food (Caltech media) under a 12:12h light:dark cycle. Stocks were maintained at 18ºC while crosses and aging flies were maintained at 25ºC.

DROSOPHILA STOCKS

Chapter 3

Canton S, *elav*-GAL4, and UAS-PKA-C1 were obtained from the Bloomington Stock Center. Pka-C3$^{NIG.6117R}$ was obtained from the National Institute of Genetics (NIG-Fly), Japan. *natalisin*-GAL4 was kindly provided by Y. Park and Y-J. Kim and is described in Jiang et al. 2013 and *Appl*-GAL4 by L. Torroja (Universidad Autonoma de Madrid, Spain). PBacf07226 and PBacPka-C3^{f00695} were obtained from the Exelixis Collection at the Harvard Medical School. UAS-PKA-C3 is described in Bettencourt da Cruz et al. 2008.

Chapter 4

The *sws*^{1} allele has been described in (Kretzschmar et al., 1997). Appl-GAL4 was kindly provided by L. Torroja (Universidad Autonoma de Madrid, Spain), CaLexA by Jing W. Wan (University of California, San Diego), and UAS-m-XBP1s by D. Rincon-Limas (University of Florida College of Medicine, Gainesville, FL). Canton S, elav-Gal4, UAS-XBP1-EGFP, UAS-SERCA, and UAS-Relish RNAi were obtained from the Bloomington Stock Center.

Appendix A

The *sws*^{1} allele and Appl-GAL4 were obtained from sources mentioned above. UAS-NTE D376GfsX18 was made by M. Cook and previously studied in the laboratory.

Appendix B

The *sws*^{1} allele and Appl-GAL4 were obtained from sources mentioned above. UAS-SERCA^{S495P} was obtained from the Bloomington Stock Center.

Appendix C

The TIM-GAL4 and UAS-Relish lines were given to the lab by Jaga Giebultowicz (Oregon State University). The Antimicrobial Peptides lines were a gift from Barry Ganetzky (University of Wisconsin). UAS-Relish RNAi was obtained from Bloomington Stock Center.

RT-qPCR-Chapter 3 and Appendix C

RNA extraction from *Drosophila* heads and cDNA synthesis was performed as previously described in (Cassar et al. 2015). Fold changes were calculated using the Pfaffl method for all of the analyses (Pfaffl 2001).

Chapter 3

For quantitative PCR, the PerfeCTa FastMix II (Quantabio) was used and samples were analyzed on a Bio-Rad iCycler iQ. We used 5'-CGAGCGGCCCAATTTGAATGT-3' and 5'-AAACGGAAGCGGCAACACGA-3' as primers for PKA-C3 and 5'-GGCGGCGAGAAGAAGATAGT-3' and 5'-CTTGGCCTTGTCCTTGAAGT-3' for the control reaction using the dTau gene.

Appendix C

For quantitative PCR, the Maxima SYBR Green qPCR system (Thermo Scientific) was used and samples were analyzed on a Bio-Rad iCycler iQ. This experiment was done in collaboration with Jaga Giebultowicz's lab at Oregon State University.

Primers used for quantification

Actin-Control 5'-CGAAGAAGTTGCTGCTCTGGTTGT-3' and 5'-GGACGTCCCACAATCGATGGGAAG-3'

Attacin C- 5'-CTGCACTGGACTACTCCCACATCA-3' and 5'-CGATCCTGCGACTGCCAAAGATTG-3'

CecropinA1- 5'-CATTGGACAATCGGAAGCTGGGTG-3' and 5'-TAATCATCGTGGTCAACCTCGGGC-3'

Diptericin B- 5'-AGGATTCGATCTGAGCCTCAACGG-3' and 5'-TGAAGGTATACACTCCACCGGCTC-3'

Drosomycin- 5'-AGTACTTGTTCGCCCTCTTCGCTG-3' and 5'-CCTTGTATCTTCCGGACAGGCAGT-3'

Metchnikowin- 5'-CATCAATCAATTCCCGCCACCGAG-3' and 5'-AAATGGGTCCCTGGTGACGATGAG-3'

FAST PHOTOTAXIS- Chapter 3, Appendix A

Fast phototaxis assays were conducted in the dark using the countercurrent apparatus described by Benzer 1967 and a single light source. A detailed description of the experimental conditions can be found in Strauss and Heisenberg

1993. Flies were starved overnight but had access to water and were tested the following morning. Five consecutive tests were performed in each experiment with a time allowance of 6 seconds to make a transition towards the light and into the next vial. The short time renders the paradigm sensitive for walking speed. Flies were tested in groups of 5-10 flies. Males and females were tested separately but did not show significant differences and were therefore combined to one value. GraphPad Prism was used to perform one-way ANOVA, two-way ANOVA, Kruskal-Wallis, or Mann-Whitney tests to determine significance when several experimental groups were compared with and without two sources of variation and when only two groups were compared, respectively.

WESTERN BLOT ANALYSES- Chapter 3, Chapter 4

Western blot analyses were performed as described in (Carmine-Simmen et al., 2009). Lysates of 3-4 heads were loaded on 10% SDS gels and blotted onto Chapter 3-PROTRAN Nitrocellulose transfer membranes (Whatman) or Chapter 4-PVDF. Chapter 3-Anti-PKA-C3 was used at 1:5000 and anti-Tubulin (1:2000) or anti-Actin (1:200) was used as a loading control (obtained from the Developmental Studies Hybridoma Bank, DSHB, developed under the auspices of the NICHD and maintained by the Department of Biology, University of Iowa). Chapter 4- Primary antibodies used were anti-GRP78 1:2000 (StressMarq SPC-180D), anti-GFP 1:2000 (ThermoFisher Scientific A-11122), anti-Actin 1:200 (Hybridoma JLA20) and anti-GAPDH (G-9) 1:333 (Santa Cruz- 365062) as a loading control. Antibodies were diluted in TBS-T supplemented with 5% milk powder and incubated overnight at 4ºC. Bands were visualized using horseradish peroxidase-

conjugated secondary antibodies (Jackson ImmunoResearch) at 1:10000 at RT for 1.5 hours and the SuperSignal West Pico chemiluminescent substrate (ThermoScientific). Chapter 4- At least three replicates were performed. Statistical analysis was done using GraphPad Prism. The GRP78 western was analyzed with a Kruskall Wallis test with a Dunn's multiple comparison test respectively. The CaLexA GFP western was analyzed with an unpaired two tailed student t-test.

CRAWLING ASSAYS- Chapter 3

Third instar larvae were rinsed in diH_2O and placed on 3% agar plates at room temperature. The crawling paths of the larvae were recorded for 5 minutes using a moticam 1000 connected to a PC and using the MIPlus07 software (Motic Images). The distance traveled in each video was traced and quantified using the segmented line tool in ImageJ software (http://imagej.nih.gov/ij/). GraphPad Prism was used to perform one-way ANOVA or Mann-Whitney tests to determine significance when several experimental groups were compared or when only two groups were compared, respectively.

ELECTROPHYSIOLOGICAL METHODS- Chapter 3

Intracellular recordings were made from the larval body wall muscle 6 in abdominal segment 3 using glass microelectrodes as previously described (Engel, 2008). Recordings were carried out at room temperature in extracellular HL3 saline which contained (in mM): 70 NaCl, 5 KCl, 20 $MgCl_2$, 10 $NaHCO_3$ 115 sucrose, 5 trehalose, 5 HEPES, and either 0.5, 1.0, or 2.0 $CaCl_2$ (as specified in text). Membrane potentials were recorded using an Axoclamp-2A amplifier (Axon Instruments), digitized at 10 kHz and stored with a Digidata 1440A digitizer (Axon

Instruments) connected to a PC (Dell). Excitatory junctional potentials (EJPs) were generated by injecting current into severed axons, at 0.5 Hz, via a suction electrode and an A310 Accupulser (World Precision Instruments) through an isolation transformer. The average single EJP amplitude of each recording was taken from 30-35 EJPs, whose amplitudes were measured using Clampfit 10.2 software (Molecular Devices, Axons Instruments). Spontaneous miniature end plate potentials (mEPPs) were recorded over 3 minutes and analyzed using Mini Analysis 6.0.0.7 (Synaptosoft Inc.). This experiment was done in collaboration with K. Lembke of the Morton lab at OHSU.

NEGATIVE GEOTAXIS ASSAY- Chapter 4, Appendix B

For each genotype tested, at least 10 flies were placed into an empty vial, and allowed to recover from CO_2 anesthetization for two hours. The flies were then banged down to the bottom of the vial, allowed to ascend, and the number of flies that cross 3 cm by 5 seconds was counted. The percentage of flies crossing the marker was calculated for each trial, averaged, and used for statistical comparisons. Statistical analysis was done using GraphPad Prism. When only two genotypes or treatments were compared, the data were analyzed with an unpaired two tailed student t-test. A one-way ANOVA was used to compare across multiple genotypes, and when a significant difference was found among the means, a multiple comparisons test was conducted comparing the means to *sws*^{1} Appl-GAL4 with a Dunnett's correction for multiple comparisons.

TISSUE SECTIONS AND MEASUREMENTS OF VACUOLES- Chapter 4, Appendix A, B, and C

Paraffin sections for light microscopy were prepared and analyzed for vacuole formation as described in (Sunderhaus and Kretzschmar, 2016). Briefly, whole flies were fixed in Carnoy's solution and dehydrated in an ethanol series followed by incubation in methyl benzoate before embedding in paraffin. Sections were cut at 7 µm and analyzed with a Zeiss Axioscope 2 microscope using the auto-fluorescence caused by the dispersed eye pigment. To quantify the vacuolization, we photographed sections at the level of the great commissure and numbered the pictures for a double-blind analysis. The area of the vacuoles in the deutocerebral neuropil was then calculated in ImageJ as total pixel number, converted into μm^2, and the genotype/treatment determined. Statistical analyses were done using GraphPad Prism. When only two genotypes or treatment were compared, the data were analyzed with an unpaired two tailed student t-test. A one-way ANOVA was used when multiple groups were compared, and when a significant difference was found among the means, a multiple comparisons test was conducted comparing the means to *sws*^{1} Appl-GAL4 with a Sidak's correction for multiple comparisons.

LIPID ANALYSIS- Chapter 4

Forty *Drosophila melanogaster* heads were collected and to each genotype sample 5 uL of Lipidomix™ was added as an internal standard. Cold methyl tert-butyl ether: methanol: water was added. Heads were pulverized using a ceramic bead blaster, centrifuged and the top layer was collected for UPLC-HDMS and UPLC-SWATH analysis. Samples were analyzed in duplicate in positive and

negative ion modes. Acquired data were searched by Peakview's™ XIC Manager and LPC, PC and PE XIC (extracted ion chromatograms) lists were searched based on formula, accurate mass, isotope ratio and MSMS fragmentation. This experiment was conducted by JT Morré at Oregon State's Mass Spectrometry Facility.

Analysis of the lipid results sent to us from Oregon State was done in collaboration with Michael Lasarev (M.S. degree in Statistics, Research Associate at the Oregon Institute of Occupational Health Sciences). Totals for LPC, PC, and PE were each divided by 50,000 prior to analysis to improve scale. Technical duplicates from the same batch were summarized by taking the geometric mean of the two (scaled) totals. These geometric means served as the response in a two-way analysis between batch and genotype. The range of values across genotypes within any given batch differed by more than a factor of 5, suggesting a log scale more appropriate for analysis. PC and PE were analyzed assuming a Gaussian distribution with log-link, while LPC was more appropriately modeled as a Gamma distribution, also with a log-link. The ratios between LPC:PE and PC:PE were also analyzed assuming Gaussian distribution with log-link. Three specific contrasts of interest (comparing NTE, SERCA, and XBP1 each against *sws*^{1} alone) were tested at the 0.017 level (usual 0.05 level Bonferroni-adjusted for three tests) for each response

TUDCA TREATMENTS- Chapter 4

Tauroursodeoxycholic acid was obtained from EMD Millipore (Cat #: 580549-5GM) and was added to regular *Drosophila* food at a final concentration of 15 mM

(Debattisti et al. 2014.) Flies were reared on the drugged food and were flipped to a new vial of food at 7dpe.

SITE-DIRECTED MUTAGENESIS- Appendix A

To create flies carrying human mutations, we used a pCMV6_XL6 expression vector (SC115919; Origene) containing a human cDNA encoding PNPLA6 (NTE) transcript variant 2 (NM_006702.2). Each of the mutations found in patients were introduced into this cDNA by site-directed mutagenesis using the Quikchange Lightning site-directed mutagenesis kit according to the instructions of the manufacturer (Stratagene). NTE A1064T was made by Alejandro Lomniczi in Dr. Sergio Ojeda's lab. The mutations were confirmed to be present in the plasmid by Sanger Sequencing.

Primers for Site-Directed Mutagenesis

NTE L524P 5'-GGAGGACGTGTGCCCGTTCGTAGCGCA-3'

NTE G530W 5'-CCACCAGTTCCCAGGGCTGCGCTAC-3'

NTE T581R 5'-CTGCCACCCTGTGCGCCGCACTCA-3'

NTE R1135Q 5'-GGCTGCTGTGGAATGAATCCCTGGGC-3'

Once the mutations in the construct had been confirmed, the Infusion HD Cloning Kit (Clontech Laboratories Inc.) was used to clone the NTE constructs into the p-UASt-attb plasmid. Once a clone was obtained, it was again confirmed using Sanger sequencing. Finally, the DNA was shipped to Best Gene Inc. to be injected into embryos.

INFUSION CLONING PRIMERS

F 5'-AGGGAATTGGGAATTCGAATCAACCGATGGAGGCTC-3'

R 5'-ATCTGTTAACGAATTCGGGCTGGTCAAGTCATCAGT-3'

Chapter 3

The PKA-C3 Catalytic Subunit is Required for Coordinated Movement in *Drosophila*

Adapted from and with additional data added:

Cassar, M., Sunderhaus, E., Wentzell, J.S., Kuntz, S., Strauss, R., Kretzschmar, D., 2018. The PKA-C3 catalytic subunit is required in two pairs of interneurons for successful mating of *Drosophila*. Sci. Rep. 8, 2458. https://doi.org/10.1038/s41598-018-20697-3

Abstract

Protein kinase A (PKA) has been shown to play a role in a plethora of cellular processes ranging from development to memory formation. Its activity is mediated by the catalytic subunits whereby many species express several paralogs. *Drosophila* encodes three catalytic subunits (PKA-C1-3) and while PKA-C1 has been well studied, the functions of the other two subunits were unknown. PKA-C3 is the orthologue of mammalian PRKX/Pkare and they are structurally more closely related to each other than to other catalytic subunits within their species. PRKX is expressed in the nervous system in mice but its function is also unknown. We now show that loss of PKA-C3 in *Drosophila* leads to phototaxis and crawling deficits, though the animals are still able to move. These phenotypes are specifically due to the loss of PKA-C3 because expression of PKA-C1 cannot compensate. In addition, knocking down PKA-C3 in all neurons or even in just restricted subsets is sufficient to induce phototaxis and crawling deficits, indicating that PKA-C3's activity is required for proper motor coordination. Understanding PKA-C3's role in the nervous system may provide further insight into the roles of PRKX/Pkare in the nervous system.

Introduction:

Protein kinase A (PKA) is a key regulator in many processes, including cellular growth, embryonic patterning, and learning and memory formation in flies and mammals (Skoulakis, EM et al. 1993, Walsh and Patten 1994, Lane and Kalderon 1994, Pan and Rubin, 1995, Mayford et al. 1995, Roman and Davis, 2001). PKA is a tetramer of two regulatory and two catalytic subunits, whereby several paralogs for these subunits are found in mammals as well as *Drosophila* (Beebe 1994). Flies encode three catalytic subunits, PKA-C1-3, but functional studies have only been performed with PKA-C1 and the functions of PKA-C3 were unknown (Kalderon and Rubin 1988, Inoue and Yoshioka 1997). PKA-C3 transcripts have been detected in a Northern blot analyses, which revealed expression in pupae and adult heads while weak expression was found in embryos and larvae (Kalderon and Rubin 1988). To address a functional redundancy with PKA-C1, PKA-C3 was induced in PKA-C1 mutants by fusing its coding region to the PKA-C1 promoter however, this did not rescue the phenotypes caused by the loss of PKA-C1 (Melendez et al. 1995). This suggested that the different catalytic subunits have specific functions that cannot be fulfilled by other subtypes. PKA-C3 is evolutionarily highly conserved and interestingly it is structurally more closely related to its mammalian orthologue PRKX (also called Pkare) than to PKA-C1 or PKA-C2 (Klink et al. 1995, Blaschke et al. 2000, Huang et al. 2016). PRKX is expressed in the developing and adult mouse brain, whereby the pattern during development is restricted to differentiating neurons in the first ganglion, the dorsal root ganglia, and the mantle layer of the telencephalon (Blaschke et al. 2000, Li et

al. 2005). How the regulation of PRKX occurs and its role in the nervous system is still unknown.

Our lab had previously shown that SWS acts as a non-canonical regulatory subunit that binds to PKA-C3, tethers it to membranes, and inhibits its activity (Bettencourt da Cruz et al. 2008). SWS specifically interacts with PKA-C3 and does not bind to PKA-C1 or PKA-C2, again supporting unique roles of this unusual PKA complex. The murine orthologue of SWS, NTE, was also able to interact and regulate PKA-C3 activity, indicating that regulation of this unique group of catalytic subunits may be a conserved function across species (Wentzell et al. 2014). In addition, it has been shown that overexpression of PKA-C3 on its own is capable of initiating neurodegeneration, indicating that deregulation of these catalytic subunits could have devastating consequences on the nervous system (Wentzell et al. 2014). If NTE is capable of regulating the activity of PRKX in the nervous system, understanding PKA-C3's function may be able to elucidate how dysregulation of PRKX could be involved in the spectrum of phenotypes associated with NTE related disorders. Unfortunately, what the roles are of these subunits and what consequences the loss of PKA-C3 activity has for neuronal integrity and function remained unknown. This chapter describes what the consequences are for *Drosophila* when PKA-C3 activity is lost in nervous system, in particular the loss of coordinated movement.

Results:

To identify functions of PKA-C3, we first knocked it down pan-neuronally using the Pka-C3$^{NIG.6117R}$ RNAi construct and the *Appl*-GAL4 driver line. The knockdown was confirmed by performing RT-qPCRs from head homogenates (Figure 3-1A). The knockdown flies were viable and did not show any overt defects. To determine whether brain development or survival was affected, we performed paraffin head sections of 3d and 30d old flies but neither revealed detectable changes compared to age-matched controls *(data not shown).* This suggests that the loss of PKA-C3 does not interfere with the development of the brain or with the maintenance of brain integrity during aging. We then tested whether the knockdown may affect behavior using fast phototaxis assays in which the flies are startled and react with a flight response by running towards a light source (Strauss and Heisenberg 1993). Using this assay, we found that significantly less of the pan-neuronal knockdown flies made successful transitions towards the light compared to control flies only carrying Pka-C3$^{NIG.6117R}$ or *Appl*-GAL4 when 14d old (Figure 3-1B) and this was even more prominent when using 30d old flies (Figure 3-1C).

To understand the role of PKA-C3 in the nervous system and because no classical allele was available, we generated a deletion in the *PKA-C3* gene using two piggyBac insertions and FLP/FRT-mediated recombination (Golic and Golic 1996). Two alternative transcripts, RA and RB, using different first exons are predicted to be transcribed from the PKA-C3 locus (Gramrates et al. 2017) and the deletion removes all coding exons of the RA transcript and all coding exons

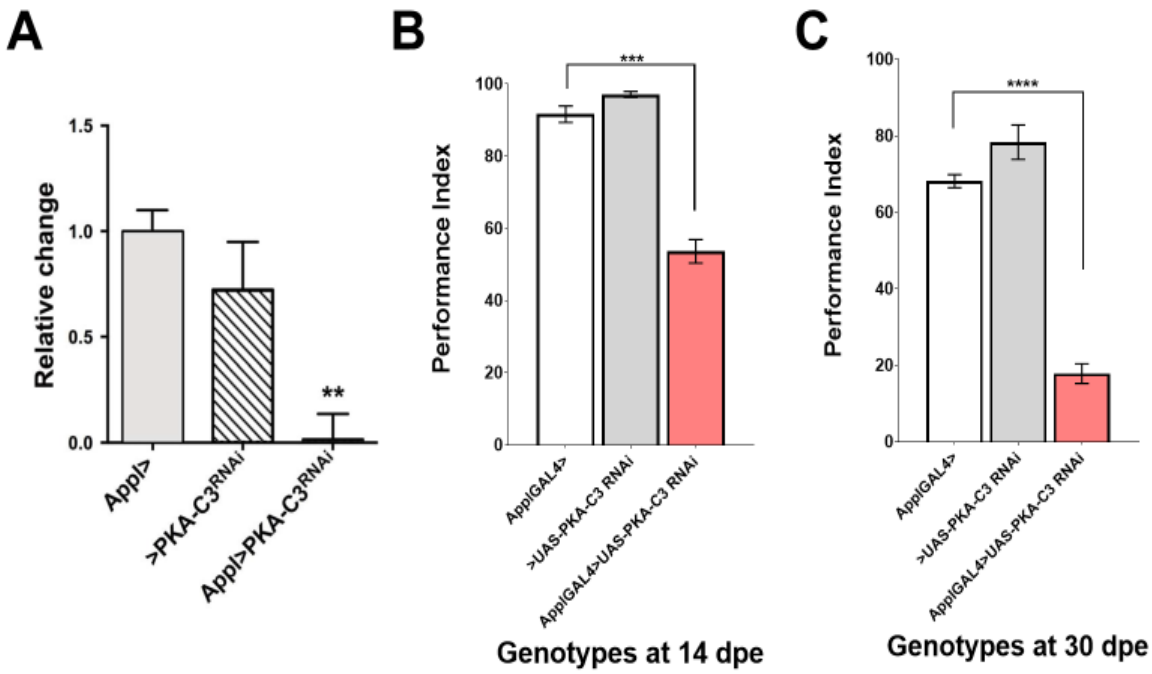

Figure 3-1: Knocking down PKA-C3 results in a fast phototaxis deficit. A. A qRT-PCR analysis showing the reduction in the PKA-C3 transcript when an RNAi is expressed pan-neuronally with Appl-GAL4. **B.** Fast phototaxis results at 14 dpe showing a significant deficit when PKA-C3 is knocked down by RNAi. **C.** Fast phototaxis at 30 dpe showing a continued deficit in phototaxis assays, which appears to be further exacerbated by age. qRT-PCR data represent three independent experiments and means with SEM (** $p<0.01$). Phototaxis data represent the mean and SEM of at least 10 independent trials of 6 or more flies. The data were analyzed by a Kruskall Wallis test with a Dunn's multiple comparison test (*** $p<0.001$, **** $p<0.0001$). Recreated from Cassar et al. 2018 with permission. Experiments conducted by D. Kretzschmar.

besides the first for RB (Figure 3-2A). The first exon of RB encodes 13 amino acids, which do not contribute to any known functional domain. The deletion was confirmed by Western blots that verified that no PKA-C3 protein was detectable in

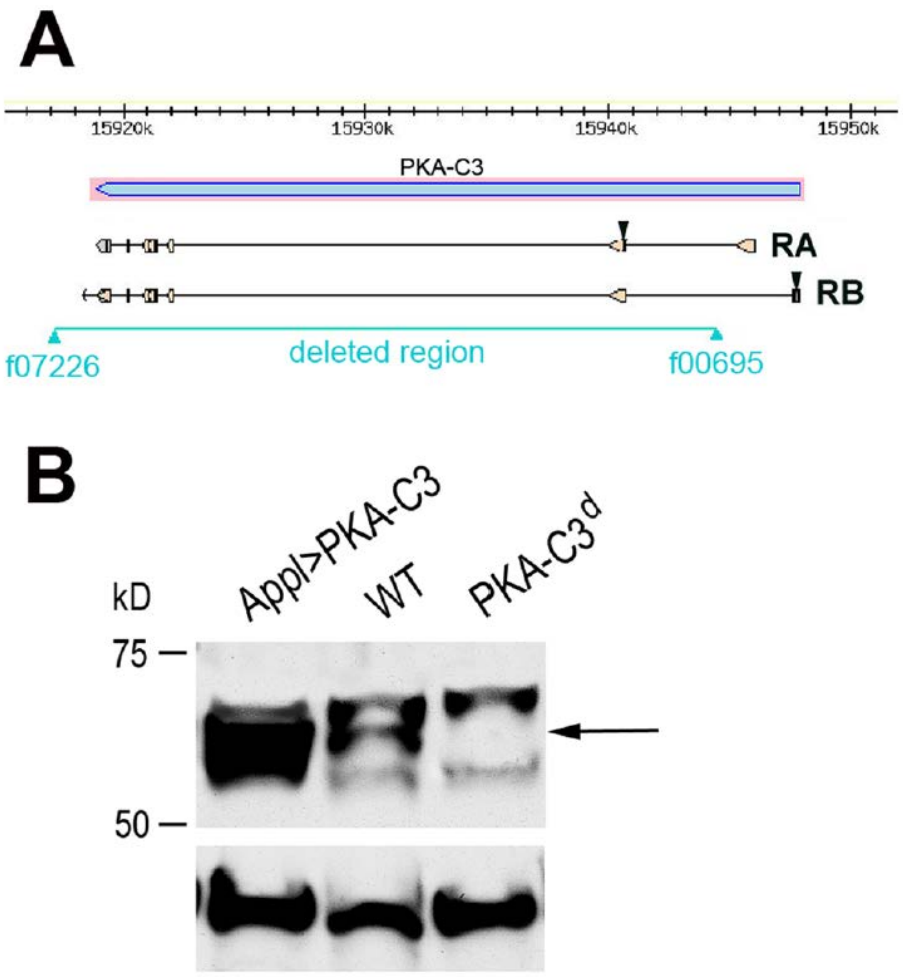

Figure 3-2: Making a PKA-C3 null fly. A. Genomic region of PKA-C3 showing the intron-exon structure of the two alternative PKA-C3 mRNA transcripts. The position of the two insertion lines PBac[1]Pka-C3f00695 and PBac[1]f07226 that were used for a FLP/FRT-mediated recombination is indicated by the light blue arrowheads and the created deletion by the light blue line. **B.** Western blot using the PKA-C3 antisera and head homogenates. Three bands around 60 kD, the predicted size of the two PKA-C3 isoforms is 57 kD and 65 kD, are detectable in wild type (WT) flies. The levels of the protein corresponding to the band in the middle (arrow) are strongly increased in flies expressing additional PKA-C3 pan-neuronally with *Appl*-GAL4, validating that this band corresponds to PKA-C3. The PKA-C3 band is missing in PKA-C3^{d} flies whereas the unspecific bands are still present. A loading control using anti-tubulin is shown below. Recreated from Cassar et al. 2018 with permission.

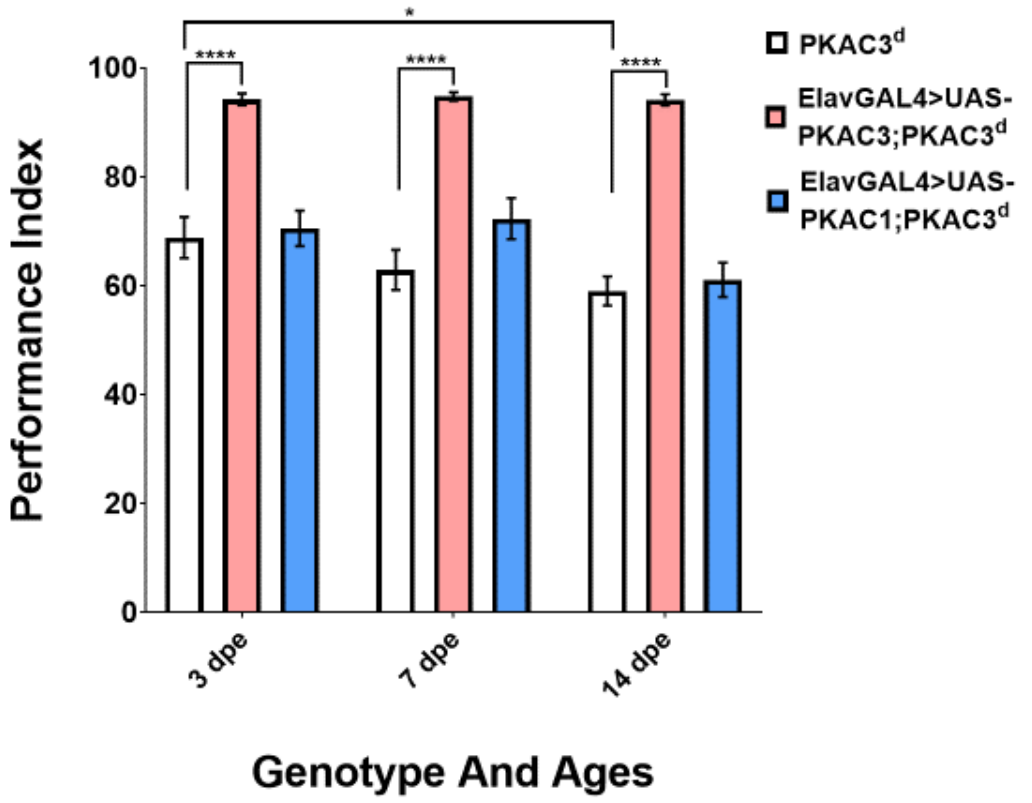

Figure 3-3: PKA-C3^{d} are deficient in fast phototaxis assays. A significant reduction in fast phototaxis performance is already detected in 3 dpe *Pka-C3^{d}* mutants and is also age dependent. This behavioral deficit is significantly rescued by the expression of PKA-C3. However, when PKA-C1 is expressed in an attempt to rescue the phototaxis phenotype there is no significant difference indicating PKA-C1 cannot compensate for a loss of PKA-C3. Data represent the mean and SEM of at least 10 independent trials of 6 or more flies. The data were analyzed with a two-way ANOVA where genotype and age were factors of variation with no significant interaction. Age and genotype were both a source of significant variation. Multiple comparisons testing was conducted on genotypes with a Dunnett's test and on age with a Tukey's test (*p<0.05, ****p<0.0001).

the deletion line (Figure 3-2B). Using this mutant, called Pka-C3^{d}, we confirmed that the loss of PKA-C3 causes a significantly reduced performance in the fast phototaxis assay in 7 and 14d old flies (Figure 3-3). We then addressed whether the behavior deficits only occur with aging or are already present in young flies. As

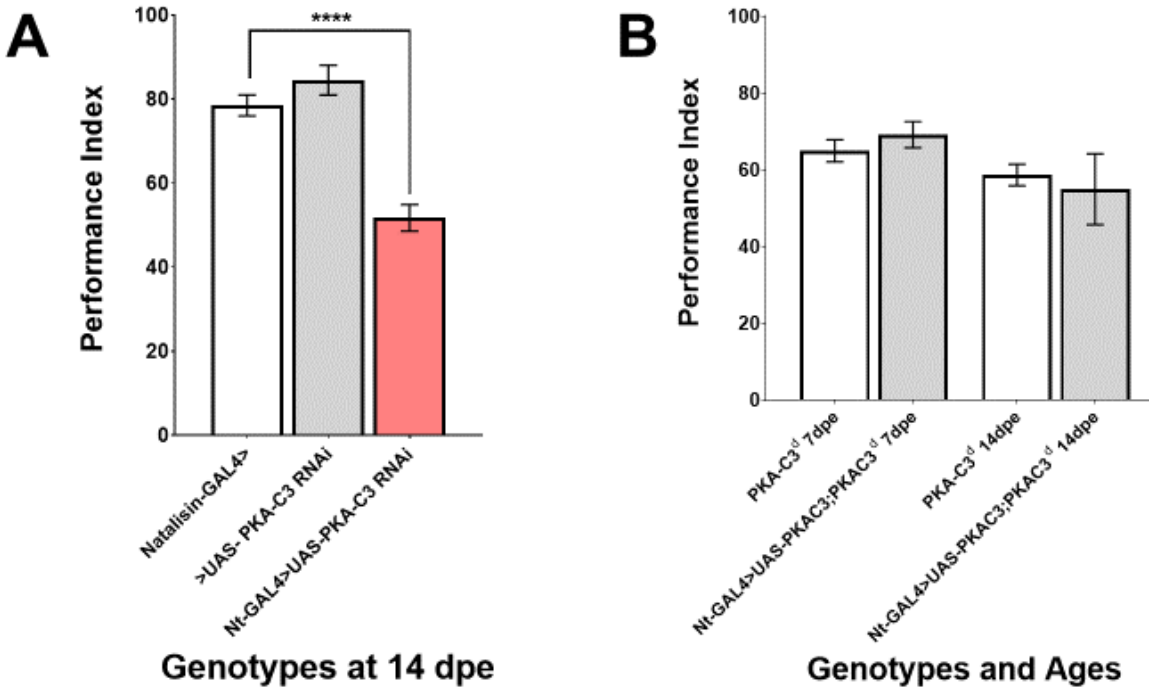

Figure 3-4: PKA-C3 expression is necessary in Natalisin positive neuronal subsets for cooridinated movevement, but not sufficient to rescue the phototaxis defect of PKA-C3^{d} A. A significant reduction in fast phototaxis performance is detected when PKA-C3 is knocked down in a subset of Natalisin positive neurons at 14 dpe. **B.** However, expressing PKA-C3 in those neurons is not sufficient to rescue defects of PKA-C3^{d} at 7 or 14 dpe. Data represent the mean and SEM of at least 8 independent trials of 6 or more flies. The data were analyzed by a one-way ANOVA test with a Sidak's multiple comparison test (**** $p<0.0001$).

shown in Figure 3-3, even 3d old Pka-C3^{d} mutants performed significantly worse than controls, showing that this phenotype does not develop with aging but is already present in young flies. Next, we determined whether the phototaxis deficits are specifically due to the loss of PKA-C3 by performing rescue experiments. As expected, pan-neuronal expression of PKA-C3 via elav-GAL4 in Pka-C3^{d} mutants restored the performance in the fast phototaxis assay at both ages (Figure 3-3). In contrast, expressing PKA-C1 did not improve the behavior (Figure 3-3), showing that PKA-C3 has specific functions that cannot be compensated by PKA-C1, although they show conservation in their catalytic domain (Cassar et al. 2018). This further supports that PKA-C3 and its mammalian orthologues may form a unique subclass of PKA catalytic subunits.

We have previously shown that PKA-C3 is expressed in a certain subset of neurons in the brain of adults, in particular the anterior dorsal-lateral interneurons (ADLIs) and inferior contralateral interneurons (ICLIs) (Cassar et al. 2018). PKA-C3 colocalized with the expression of Natalisin (Nt), which is a peptide involved in mating behavior. We showed that the expression of PKA-C3 is necessary in these neurons for copulation, and its activity must be tightly regulated as well, since overexpression of wildtype PKA-C3 with a Nt-GAL4 induced copulation deficits as well (Cassar et al. 2018). Using the same GAL4 line, knocking down PKA-C3 was sufficient to induce a significant phototaxis deficit, indicating PKA-C3 is necessary in these neurons (Figure 3-4A). However, when we attempted to rescue the PKA-C3^{d} line with the same GAL4 promoter, expression of PKA-C3 in these particular

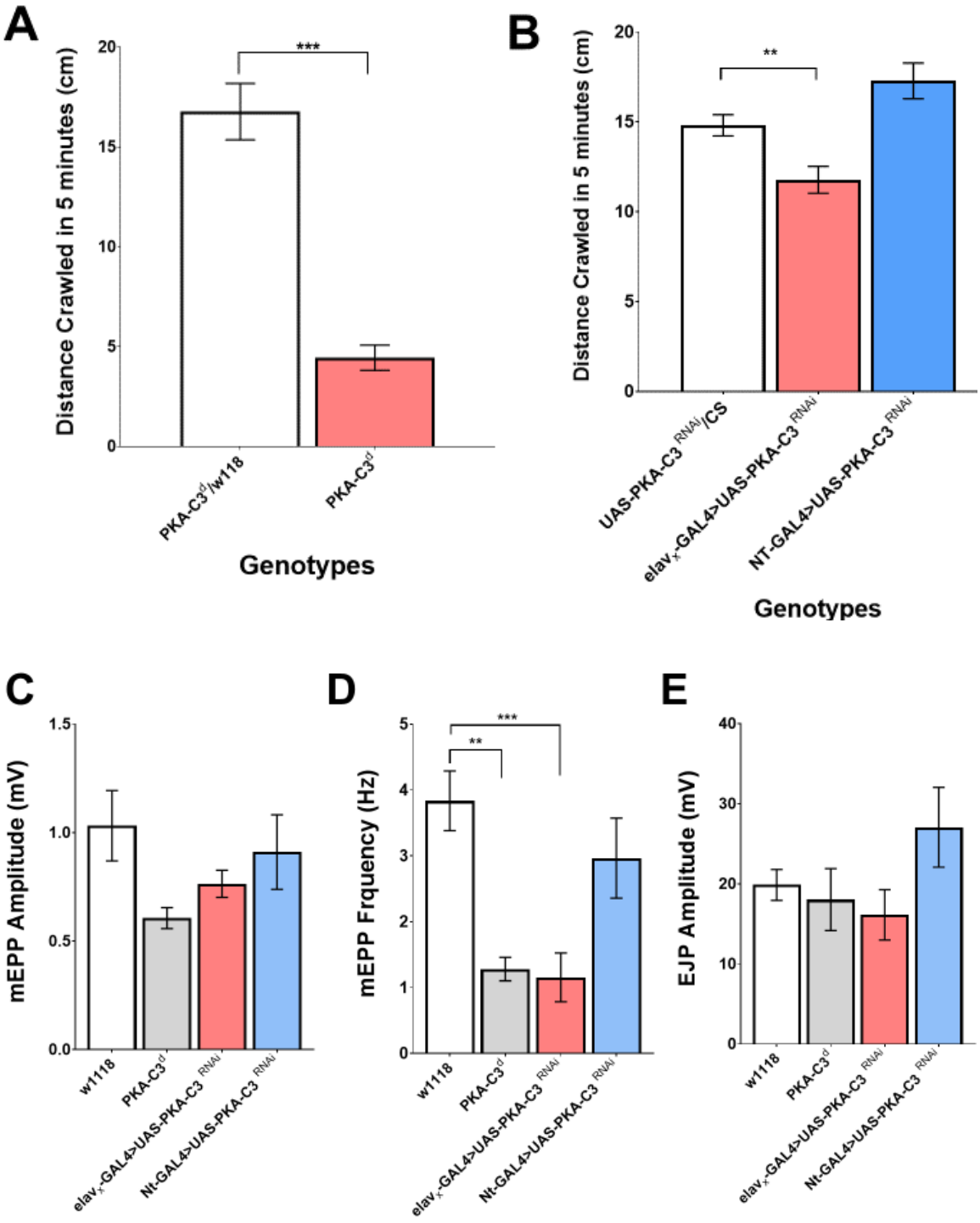
A
Distance Crawled in 5 minutes (cm)
***
PKA-C3d/w118
PKA-C3d
Genotypes
B
Distance Crawled in 5 minutes (cm)
**
UAS-PKA-C3 RNAi/CS
elavx-GAL4>UAS-PKA-C3 RNAi
NT-GAL4>UAS-PKA-C3 RNAi
Genotypes
C
mEPP Amplitude (mV)
w1118
PKA-C3d
elavx-GAL4>UAS-PKA-C3 RNAi
Nt-GAL4>UAS-PKA-C3 RNAi
D
mEPP Frquency (Hz)
***
**
E
EJP Amplitude (mV)

Figure 3-5: Loss of PKA-C3 expression results in defective crawling and synaptic physiology at the larval NMJ. A. A significant reduction in crawling is detected in the PKA-C3 mutant. **B.** Knocking down PKA-C3 in all neurons resulted in a significant crawling defect, however only knocking it down in Natalisin neurons had no effect. **C.** Although reduced in the PKA-C3 deficiency line, there is no signficant difference in minature End Plate Potential (mEPP) Amplitude among the genotypes. **D.** The mEPP frequency is significantly reduced at the larval NMJ in the PKA-C3 deficiency line and in the pan-neuronal knockdown. **E.** There is no significant difference detected when the EJP Amplitudes are measured. Crawling data represent the mean and SEM of at least 11 larva and were analyzed using a Mann-Whitney test (**A**) or an ordinary one-way ANOVA with a Dunnett's multiple comparisons test. (**B**). All electrophysiology experiments were carried out in 1 mM calcium. Data represent the mean and SEM of at least 8 animals and were analyzed using ordinary one-way ANOVA with a Dunnett's multiple comparisons test (*** $p<0.01$, ** $p< 0.05$). Electrophysiology experiments conducted by K. Lembke.

subsets of neurons was not sufficient to rescue the deficiency line's fast phototaxis deficit (Figure 3-4B), indicating that expression of PKA-C3 is required in other neurons besides the ADLIs and ICLIs.

Finally, we wanted to study whether the movement defect was also detectable at earlier stage of development. Crawling assays were conducted to determine if the deficiency line even at the larval stage exhibited a movement defect. Measuring the crawling of PKA-C3^{d} third instar larvae showed a significant decrease in distance crawled compared to wildtype (Figure 3-5A). This result was confirmed when PKA-C3 expression was knocked down pan-neuronally (Figure 3-5B). We had previously shown that the ADLIs and ICLIs connect to the motor

neurons, and it was also shown that PKA-C3 was localized to those synapses. Therefore, we wanted to determine if crawling defects could be explained by changes in synaptic dynamics. To learn if there was a defect in synaptic activity, evoked and spontaneous neurotransmitter release were measured at the neuromuscular junction (NMJ) of third instar larva. While there was a decrease in the miniature End Plate Potential (mEPP) amplitudes, only the mEPP frequency was significantly decreased in the PKA-C3 deficiency and pan-neuronal knockdown lines (Figure 3-5C, D). Loss of PKA-C3 had no impact on the amplitudes of Evoked Junction Potentials (EJP) measured at the NMJ. While the targets of PKA-C3 at the synapse are unknown, all of the data presented indicates that PKA-C3 could have an unknown function in synaptic signaling that is unique to its family of catalytic subunits.

Discussion

In *Drosophila*, as in other species, there are several catalytic subunits for PKA signaling, and while the C1 subunit has been studied extensively for its role in development and cellular signaling, the C3 component's role in the nervous system is relatively unknown. Whereas the loss of PKA-C1 is lethal during development, we have shown that the deletion of C3 is viable and has no anatomical defects. However, PKA-C3 mutants exhibit behavioral defects, in particular fast phototaxis and crawling defects, in early development stages, which persists even into the adult stages of *Drosophila*. Even though PKA-C1 and C3 have similar primary sequences in their catalytic domain, expression of C1 is not

sufficient to rescue the PKA-C3 mutant indicating that the catalytic subunits have different functions.

We have previously shown that the ADLIs and ICLIs are interneurons that can connect the sensory system to glutamatergic motor neurons (Cassar et al. 2018). We detected PKA-C3 at the synapses of the ADLIs and ICLIs to the motor neurons, indicating PKA-C3 may have a role in regulating those synapses. Here we show that by knocking down PKA-C3 in those neurons, a deficit in fast phototaxis behavior is elicited, however, expression of PKA-C3 just in those neurons to rescue the mutant line is not sufficient, indicating either the level of expression was not sufficient or PKA-C3 may be required in other neurons as well. The movement defect is detected even in larval stages of development with the mutant line having a significant deficit in timed crawling distance. These data are corroborated by the knockdown in all neurons with the ELAV-GAL4 driver, but knockdown in the Natalisin neurons was not sufficient to cause a crawling defect. To determine the cause of the crawling defect, electrophysiology was conducted. It was found that the mEPP frequencies were significantly reduced in the PKA-C3 mutant and RNAi knockdown lines, even though PKA-C3 expression has yet to be detected in motor neurons. These data indicate one of PKA-C3's functions could be to regulate synaptic signaling, most likely in interneurons. However, since PKA-C3 and its orthologs' targets have failed to be identified, the mechanism for this regulation still remains unknown.

Although we have shown that loss of PKA-C3 can lead to locomotor defects and electrophysiology in larva, we still have to confirm that they are PKA-C3

dependent, by performing rescue experiments. In adults, PKA-C3 rescued the movement defects when expressed in all neurons, but, while its expression in the Natalisin interneurons is necessary, it is not sufficient to rescue the mutant line. In addition, experiments should be conducted to determine if expression of PKA-C3's orthologs, Pkare and PRKX, could rescue the mutant line's locomotor defects, to determine whether the subunits' functions in the nervous system could be conserved across species (Cassar et al. 2018).

Further research also needs to be conducted to determine how the loss of PKA-C3 causes a defect in the synaptic physiology and what the potential targets are for its kinase activity. Preliminary data in the lab indicate that Synapsin may be one of those targets, but further experiments are needed to substantiate this result.

Although not much is known about this unique group of catalytic subunits, it is obvious that PKA-C3 plays a role in regulating coordinated movement. PRKX, according to the Human Protein Atlas, is expressed at high levels in the brain, in many similar locations as NTE. Since it is known that they are located in similar areas of the brain, and we have previously shown that murine NTE is capable of interacting with PKA-C3, it indicates that NTE could be acting as a regulator of PRKX. If NTE is indeed able to regulate PRKX activity, then dysregulation of this function through organophosphate exposure or mutations in NTE, could have devastating and vast effects on the activity of PRKX. To fully understand the etiology of NTE associated disorders, further research into the relationship of these two proteins is required.

Chapter 4

The Unfolded Protein Response in Age-dependent *Swiss-Cheese* Neurodegeneration

Adapted from and with additional data added:

Sunderhaus, ER and Kretzschmar, Doris. 2018. The Unfolded Protein Response in Age-dependent *Swiss-Cheese* Neurodegeneration. *In preparation*

Abstract

Mutations in Neuropathy Target Esterase (NTE), a phospholipase and regulator of PKA signaling, have been shown to cause a spectrum of disorders in humans. Loss of NTE's ortholog, Swiss-Cheese (SWS), in *Drosophila melanogaster* has been shown to cause an increase in lysophosphatidylcholine (LPC), phosphatidylcholine (PC), and age-dependent neurodegeneration. SWS is localized to the Endoplasmic Reticulum (ER), and recently, it has been shown that perturbing the membrane composition of the ER leads to the activation of the ER stress response through the inhibition of the Sarco/Endoplasmic Reticulum Ca^{2+}-ATPase (SERCA). To investigate whether ER stress could be causing the neurodegeneration and other symptoms of NTE associated disorders, the *sws*^{1} null allele line was used. This line showed an activated ER stress response through an elevation of GRP78, a chaperone known to be elevated in cells undergoing ER stress. The next step was to address whether manipulating ER stress genetically and chemically can prevent *sws*^{1}-related phenotypes. Overexpressing XBP1, an ER transcription factor, or SERCA suppressed the degeneration and locomotion defects in *sws*^{1} as detected by histology and negative geotaxis assays. In addition, expressing these constructs rescued the LPC composition of the fly brains. Feeding the flies tauroursodeoxycholic acid (TUDCA), a chemical known to reduce ER stress, also significantly improved the locomotor deficits and neurodegeneration in *sws*^{1}. Understanding how ER stress contributes to SWS/NTE etiologies provides potential for therapeutic targets to alleviate the neurodegeneration seen in NTE associated disorders.

Introduction

Patatin-like phospholipase domain-containing proteins (PNPLA) form a family of hydrolases that consists of at least eight members in mammals (Kienesberger et al. 2009). PNPLA family members show specific activity against diverse substrates, including phospholipids, triacylglycerols, and retinol esters, and they are expressed in various tissues. One of them, PNPLA6, also called Neuropathy Target Esterase (NTE), preferably hydrolyzed phosphatidylcholine (PC) and lysophosphatidylcholine (LPC) (Lush et al. 1998, van Tienhoven et al. 2002, Quistad et al. 2003). NTE is widely expressed in the developing and adult nervous system, but its expression becomes more restricted to large neurons with age (Glynn et al. 1998; Moser et al. 2000). Loss of NTE in mice causes lethality during embryogenesis, most likely due to placental defects and impaired vasculogenesis (Moser et al. 2004). A brain specific deletion is viable, but when the animals are aged they show neuronal degeneration and defects in motor coordination (Akassoglou et al. 2004). In humans, mutations in NTE have been connected with a variety of diseases including NTE-related motor neuron disorder, Spastic Paraplegia 39, Boucher-Neuhäuser, Gordon-Holmes syndrome, and Oliver McFarlane Syndrome to name a few (Deik et al. 2014, Kmoch et al. 2015, Rainier et al. 2011, Synofzik et al. 2014, Topaloglu et al. 2014). These are complicated autosomal recessive diseases with varying clinical symptoms such as hypogonadism, chorioretinal dystrophy, ataxia, and spasticity. While mutations in NTE have been shown to be the cause of the symptoms in the patients, the mechanism for the neurodegeneration seen in these patients is unknown.

As mentioned previously, NTE is an evolutionary conserved protein also found in *Drosophila*, where it is called Swiss-Cheese (SWS). This name is due to the formation of numerous vacuoles that develop in the nervous system of adult flies when SWS is lacking or mutated (Kretzschmar et al. 1997). While the brain appears to develop normally in these flies, the first vacuoles and neuronal cell death become evident around day 5 of adulthood and this increases with age. In addition, *sws* mutant flies show defects in the ensheathment of neurons by glia, followed by glial degeneration, which is accompanied by locomotion deficits and finally premature death (Kretzschmar et al. 1997, Dutta et al. 2016). Like murine NTE, SWS is expressed in all or most neurons but seems to become more restricted with age, and it is also expressed in glial cells, specifically ensheathing glia (Muhlig-Versen et al. 2005, Dutta et al. 2016). SWS and NTE are not only structurally well conserved, but also functionally, because expressing mouse NTE in flies lacking SWS can prevent the neuronal as well as glial phenotypes (Muhlig-Versen et al. 2005).

Like NTE, SWS contains an esterase domain that mediates phospholipase activity, and *sws* mutant flies show an increase in PC and LPC (Muhlig-Versen et al. 2005, Kmoch et al. 2015). PC is a major component of all cell membranes, and, like other phospholipids, it is mostly synthesized in the ER (Kienesberger et al. 2009, Lagace and Ridgway 2013). Substantial amounts of a cell's PC are localized in the ER, which forms a large membranous network within the cell, but also transfers and secretes lipids to other cellular compartments and to the extracellular environment. Therefore, it is not surprising that both SWS and NTE are enriched

in the ER, and that a loss of SWS or NTE causes disruptions of the ER in flies and mice (Glynn et al. 1998, van Tienhoven et al. 2002, Akassoglou et al. 2004, Muhlig-Versen et al. 2005). The ER is the site of a crucial cellular response called the unfolded protein response (UPR), which is activated by stress situations such as the accumulation of unfolded or misfolded proteins in the ER but also by changes in lipid composition (Lagace and Ridgway 2013, Mei et al. 2013, Roussel et al. 2013, Hetz and Mollereau, 2014). When induced, the UPR inhibits protein translation, promotes protein degradation pathways, and increases the production of chaperones. In addition, it upregulates proteins required for lipid synthesis and ER function to deal with the increasing demand for the ER. While these responses are aimed at decreasing stress and promoting cell survival, sustained activation of the UPR triggers apoptosis pathways. Due to these functions, disturbances in the ER have been connected to a variety of neurodegenerative diseases (Paschen and Mengesdorf 2005, Roussel et al. 2013, Hetz and Mollereau 2014). In regards to the neurodegeneration associated with NTE disorders, it has been shown that disturbances in lipid composition, such as an increase in PC, inhibit SERCA, resulting in a decrease of ER Ca^{2+} stores (Fu et al. 2011, Paran et al. 2015). However, if SERCA activity is restored either through over-expression of SERCA or the use of agonists, the UPR is deactivated and lipid composition is almost returned to normal levels (Fu et al. 2011, Kang et al. 2015). Together with the role of SWS/NTE as a phospholipase and evidence that SERCA is inhibited by a loss of lipid homeostasis, we investigated whether ER stress is playing a role in the degenerative and behavioral phenotypes caused by the loss of SWS.

Results

Loss of SWS results in induction of the Unfolded Protein Response

While the loss of SWS/NTE function in the nervous system has been known to cause behavior deficits and neurodegeneration in flies, mice, and humans, the mechanism by which the neurons lose their function and eventually die has not been determined. We have previously shown that with a loss of SWS in flies, there is a rise in LPC and PC levels, which could initiate the ER stress response and lead to the neurodegeneration.

To determine if the ER stress response is activated, male control flies carrying Appl-GAL4, the promotor construct used for the following rescue experiments, and *sws*^{1} Appl-GAL4 males were aged to 7 days post eclosion (dpe). The heads of the flies were collected and western analyses were used to determine if there was a difference in the levels of GRP78/BiP, a chaperone in the ER whose levels have been shown to be elevated during initiation and progression of the UPR. GRP78 levels were significantly elevated in the *sws*^{1} mutants, indicating loss of SWS function is sufficient to initiate the UPR (Figure 4-1A, B).

Due to the evidence that the ER stress response is activated, we then determined if reintroduction of SWS could alleviate the stress response seen in the

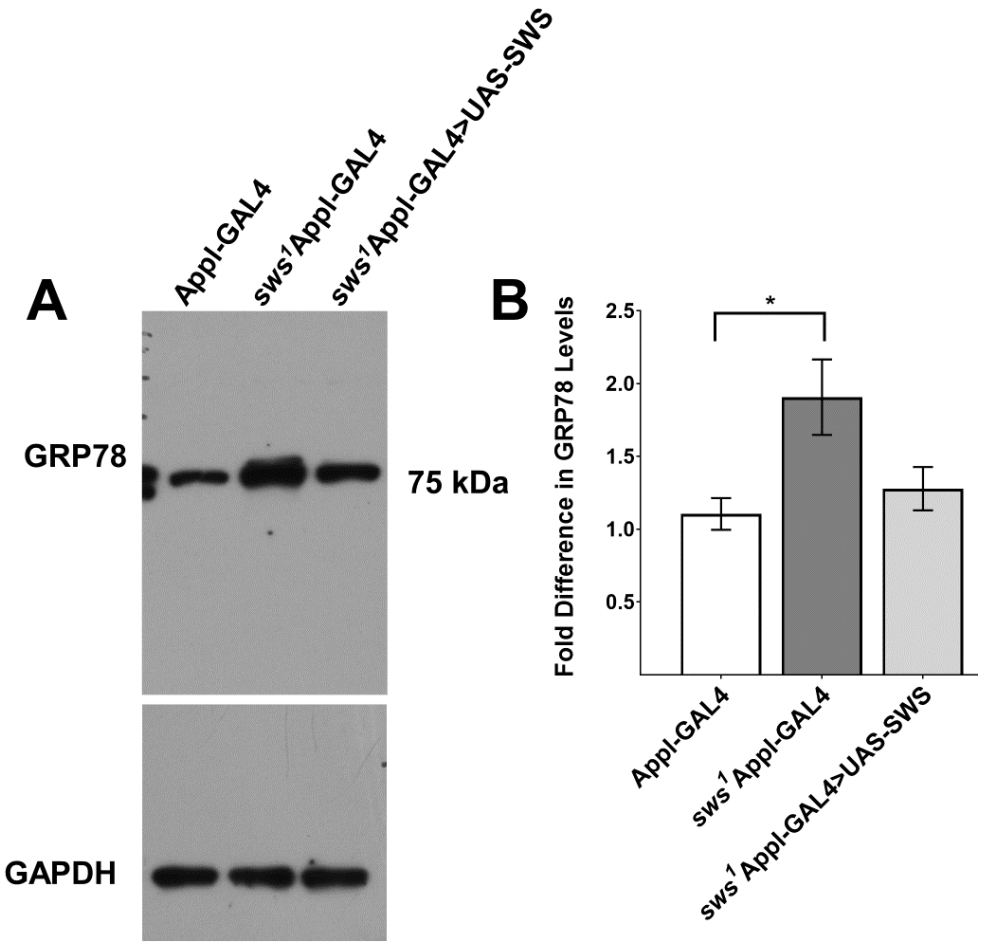

Figure 4-1: Loss of SWS activates the UPR. A. Western blot using the GRP78/BiP antisera and head homogenates. A single band appears for GRP78 at about 78 kDa, and GAPDH was used as a loading control. **B.** Quantification of the GRP78 band. There is a significant increase in GRP78 levels in *sws*^{1}, indicating activation of the UPR. Expression of SWS in neurons, while reducing the levels of GRP78, does not result in a significant difference from the mutant, most likely due to the glia phenotype that is not rescued with the expression of SWS in neurons. However, it was also not significantly different from wildtype as well. Data represent the mean and SEM of 3 independent trials. The data were analyzed with a Kruskall Wallis test with a Dunn's multiple comparison test respectively (* $p<0.05$).

flies. This result would indicate that expression of SWS in neurons is sufficient to

attenuate the UPR. Expressing wildtype SWS in the neurons using Appl-GAL4, the levels of GRP78 were reduced (Figure 4-1A, B). However, the difference failed to reach significance when compared to *sws*^{1}, most likely due to the glia phenotype in *sws*^{1}, which is not rectified with expression of SWS in neurons. However, the value in the rescue flies was also not significantly different from wildtype, indicating that there was an improvement.

As a final confirmation of the activation of the UPR, we genetically manipulated another component of the UPR pathways, X-Box Binding Protein (XPB1). XBP1 is a transcription factor that is spliced when the UPR becomes activated, and once translated, it translocates to the nucleus to upregulate the UPR genes associated with lipogenesis, ER associated protein degradation, chaperones, and ER remodeling proteins. In other *Drosophila* models of neurodegeneration, expression of XBP1 attenuated ER stress, improved the eclosion rate, and rectified a locomotor defect (Debattisti et al. 2014). It is thought that expression of XBP1 is able to improve secretion from the ER, allowing for continued signaling of the neuron. In a knockout NTE murine model, the neurons of knockout mice had impaired secretion, which inhibited the maintenance of the long axons by preventing the export of neuronal materials (Read et al. 2009). Because XBP1 is able to initiate lipogenesis and its activation improves secretion, this pathway was chosen as another confirmation of ER stress activation.

To determine if XBP1 expression rescues the *sws*^{1} locomotor defects, negative geotaxis was performed at 7 dpe. By expressing fly XBP1-EGFP or an already activated murine version (UAS-m-XBP1-s) pan-neuronally with the

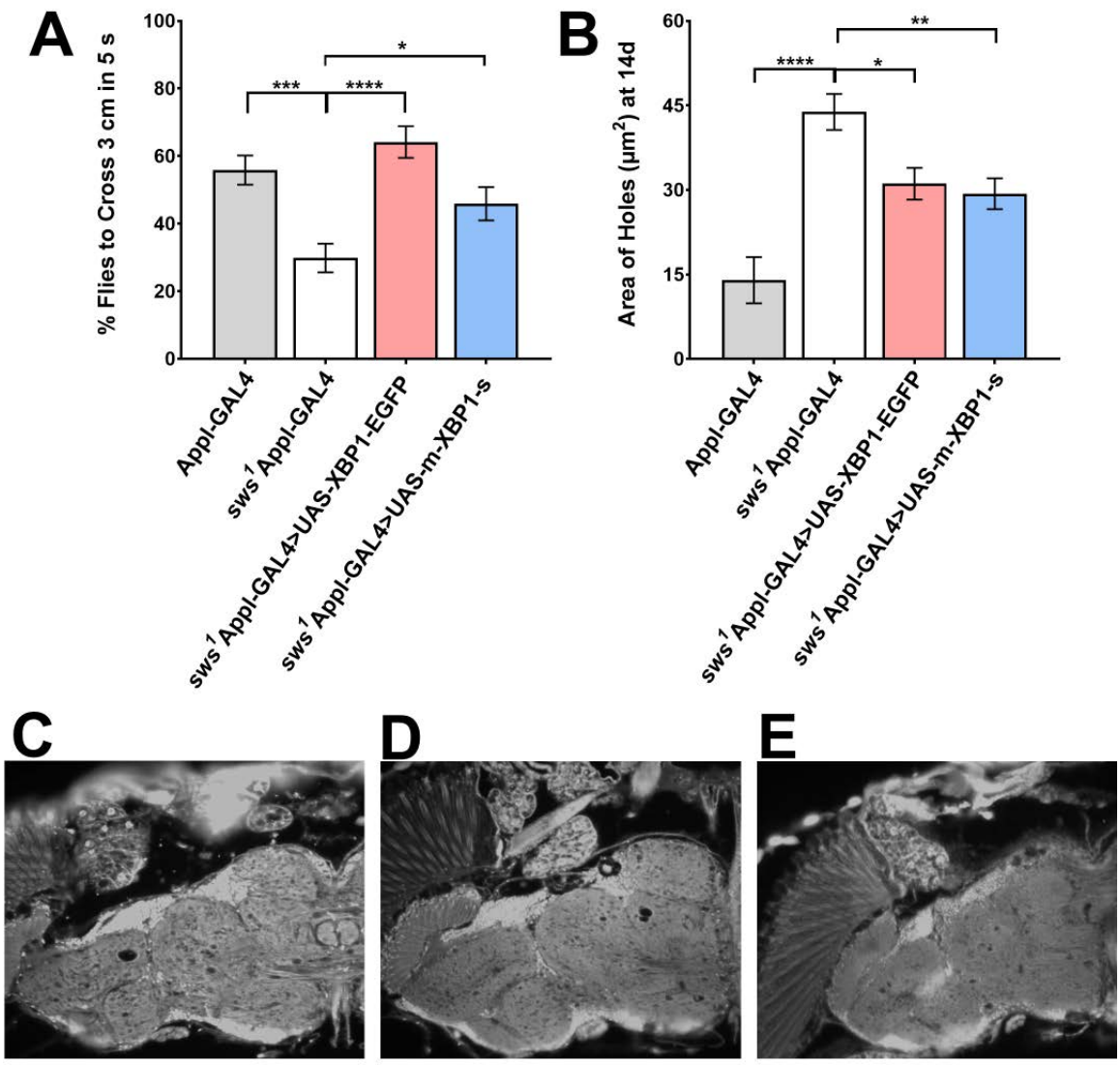

Figure 4-2: XBP1 expression rescues *sws*^{1}. A. Expression of different forms of XBP1 significantly rescues *sws*^{1} locomotor deficits at 7 dpe. **B.** Quantified neurodegeneration showing that expression of XBP1 significantly rescues *sws*^{1} at 14 dpe. Horizontal sections of **C.** *sws*^{1}Appl-GAL4 **D.** *sws*^{1}Appl-GAL4>UAS-XBP1-EGFP **E.** *sws*^{1}Appl-GAL4>UAS-m-XBP1-s taken at 14 dpe. Data represent the mean and SEM of **A.** 20 independent trials of 8 or more flies or **B.** at least 20 independent heads for each genotype. The data were analyzed with a one-way ANOVA test with a Sidak's multiple comparison test respectively (* p<0.05, **p<0.01, ****p<0.0001).

Appl-GAL4 driver, the locomotor defect was significantly rescued (Figure 4-2A). Because of this result, neurodegeneration was measured at 14 dpe to determine if expression of the constructs could also alleviate this phenotype as well. At 14 dpe, the expression of XBP1 and m-XBP1-s significantly rescued the neurodegeneration seen in the *sws*^{1} line, further indicating that the UPR is playing a role in the neurodegeneration phenotype (Figure 4-2B, C, D, E).

Expression of Sarco-Endoplasmic Reticulum Ca^{2+} *ATPase alleviates sws*^{1} *deficits*

SERCA is the pump that balances calcium between the ER and the cytosol by pumping Ca^{2+} into the ER to ensure proper protein folding and chaperone function. In neurons, a healthy ER is vital for the transport of materials within axons and to act as a Ca^{2+} pool to ensure folding of proteins and firing of action potentials along the axon (Verkhratsky 2005). The ER is also a major storage site of Ca^{2+} to prevent the initiation of the apoptotic pathways that are activated when levels of Ca^{2+} in the cytosol rise too high (Verkhratsky 2005). Loss of lipid homeostasis, namely the elevation of PC in the ER, can result in the inhibition of SERCA and activation of the UPR. However, if SERCA levels are increased, the UPR activation is attenuated (Fu et al. 2011). Knowing that the UPR is activated in *sws*^{1}, the GAL4/UAS system was used to express additional wildtype SERCA to determine if the inhibition of SERCA due to elevated levels of PC might be the mechanism initiating the ER stress response.

Appl-GAL4 was again chosen to express the UAS construct pan-neuronally in the *sws*^{1} mutant line, and negative geotaxis and neurodegeneration assays were

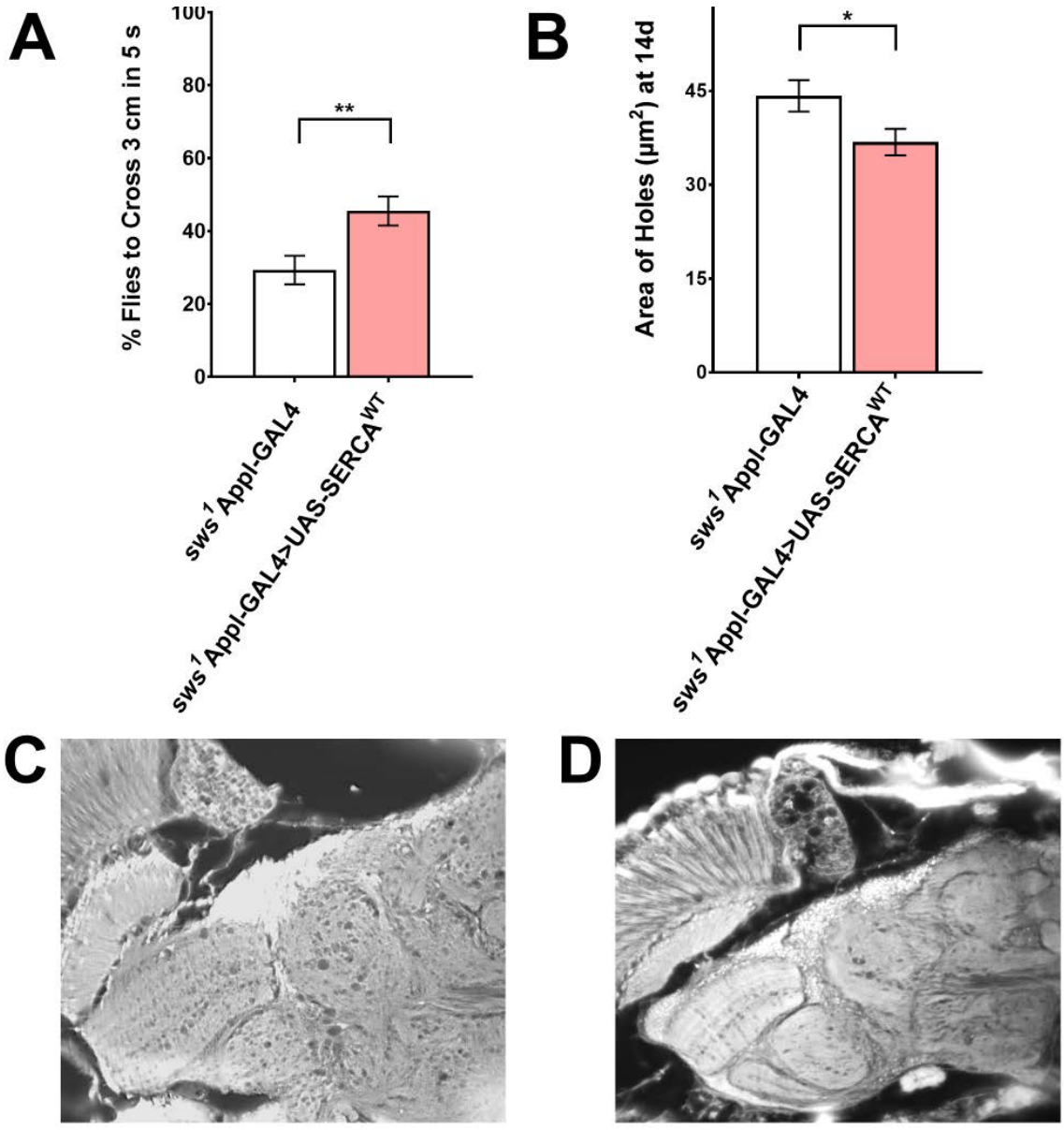

Figure 4-3: SERCA expression rescues *sws*^{1}. A. SERCA expression significantly rescues *sws*^{1} negative geotaxis deficits at 7 dpe. **B.** Quantified neurodegeneration showing that expression of SERCA significantly rescues *sws*^{1} at 14 dpe. Horizontal sections of **C.** *sws*^{1}Appl-GAL4 **D.** *sws*^{1}Appl-GAL4>UAS-SERCA^{WT} taken at 14 dpe. Data represent the mean and SEM of **A.** 20 independent trials of 8 or more flies or **B.** at least 20 independent heads for each genotype. The data were analyzed with an unpaired two tailed student t-test (*$p<0.05$, **$p<0.01$).

conducted at 7 and 14 dpe, respectively. When wildtype SERCA was expressed in neurons, there was a significant improvement in the locomotor deficits (Figure 4-3A). In addition, when neurodegeneration was quantified, wildtype SERCA significantly improved the neuronal integrity, indicating that inhibition of SERCA function plays a role in *sws[1]*'s neurodegeneration (Figure 4-3B, C, D).

To further confirm a loss of Ca^{2+} balance through inhibition of SERCA, the CaLexA system was used by driving it with the pan-neuronal Elav-GAL4 driver in the *sws[1]* mutant line. This system is a combination of the GAL4/UAS and LexA systems to drive a GFP construct in response to increased levels of Ca^{2+} in the cytosol (Figure 4-4A). We hypothesized that with the chronic inhibition of SERCA, Ca^{2+} rises steadily, and thus, using the CaLexA system at 7dpe, an increase in the levels of GFP should be seen in *sws[1]*. Using an antibody to detect GFP, a significant increase in GFP levels was detected in the *sws[1]* background versus the control, indicating more Ca^{2+} in the cytosol to activate the LexA transcription factor (Figure 4-4B, C). From this evidence and the rescue by SERCA expression, it was concluded that SERCA activity is inhibited with a loss of SWS/NTE function, leading to the activation of the ER stress response, and unless rectified, eventual cell death.

Lipid Homeostasis is Improved with Expression of NTE, XBP1, and SERCA

Loss of SWS/NTE, results in a rise in PC/LPC levels and SERCA inhibition, which would then lead to the activation of the ER stress response. Restoration of SERCA activity rescued the *sws[1]* mutant, and it is known that SERCA activity

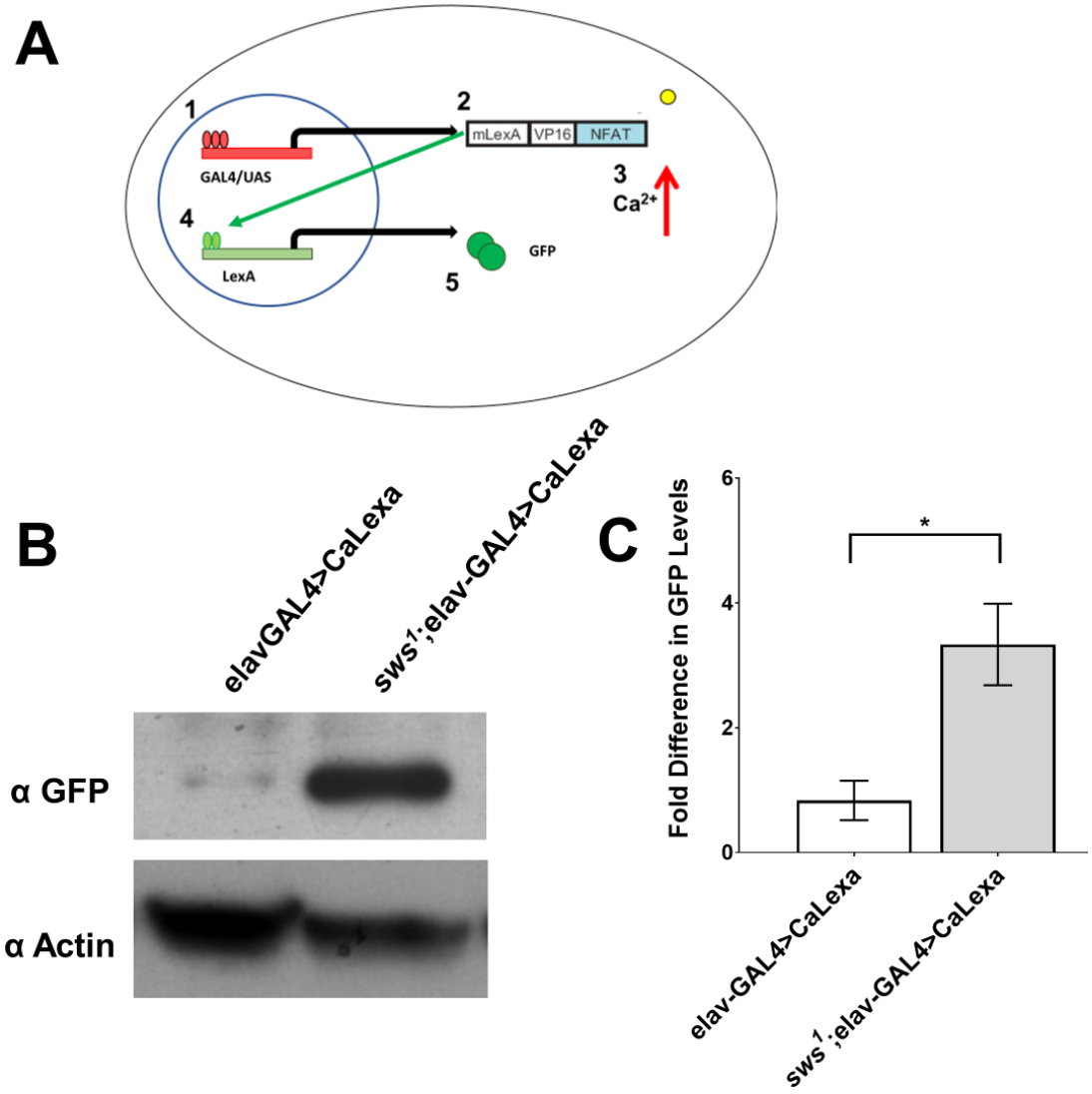

Figure 4-4: Higher levels of GFP are detected in *sws*^{1} when the CaLexA system is used. A. Schematic of CaLexA system. 1) GAL4/UAS expresses the LexA/NFAT transcription factor. 2) The LexA/NFAT transcription factor translocates to the cytosol. 3) Ca^{2+} levels rise causing the LexA/NFAT factor to be dephosphorylated. 4) The LexA/NFAT factor translocates back to the nucleus to activate the LexA operon, causing GFP to be expressed. **B.** Western blot using GFP antisera and head homogenates. Actin was used as a loading control. **C.** Quantification of GFP expression. Significantly higher levels of GFP in *sws*^{1} indicates higher levels of Ca^{2+} in the cytosol activating the CaLexA system. Data represent the mean and SEM of 3 independent trials. The data were analyzed with an unpaired two-tailed student t-test (*$p<0.05$).

influences the expression levels of lipogenesis pathways. Due to this evidence and the fact that activated XBP1 stimulates lipogenesis, the lipid composition in the heads of the flies was assessed through liquid chromatography and mass spectrometry.

Flies were frozen at 3-5 dpe, heads collected, and sent for UPLC-HDMS analysis. The data were analyzed to obtain quantified lipids measurements for LPC, PC, and phosphatidylethanolamine (PE). Although PE is a major phospholipid in the ER, we chose to normalize LPC and PC to PE because PE levels are not altered in *sws*^{1} (Muhlig-Versen et al. 2005). The totals of each lipid species were calculated and used to generate ratios used for statistical analyses. Expressing human NTE, XBP1-EGFP, or SERCA pan-neuronally with Appl-GAL4 significantly rescued the LPC/PE ratio (Figure 4-5A). However, only the expression of NTE significantly rescued the PC/PE ratio compared to *sws*^{1} Appl-GAL4 (Figure 4-5B). These results indicate that expression of NTE is capable of rescuing the loss of lipid homeostasis in *sws*^{1}, which had never been shown before. In addition, these results confirm that the expression of XBP1 and SERCA are capable of restoring LPC levels, indicating that manipulations of UPR pathways, such as AAV treatment with XBP1-s or agonists of SERCA, should be considered for future experiments to restore the aberrant lipid levels in patients.

Tauroursodeoxycholic Acid Treatment alleviates sws^{1} *phenotypes*

TUDCA is a bile salt that attenuates ER stress and inhibits apoptosis pathways, in particular pathways that involve the release of Ca^{2+} from the mitochondria. TUDCA has been shown to promote the activation of survival

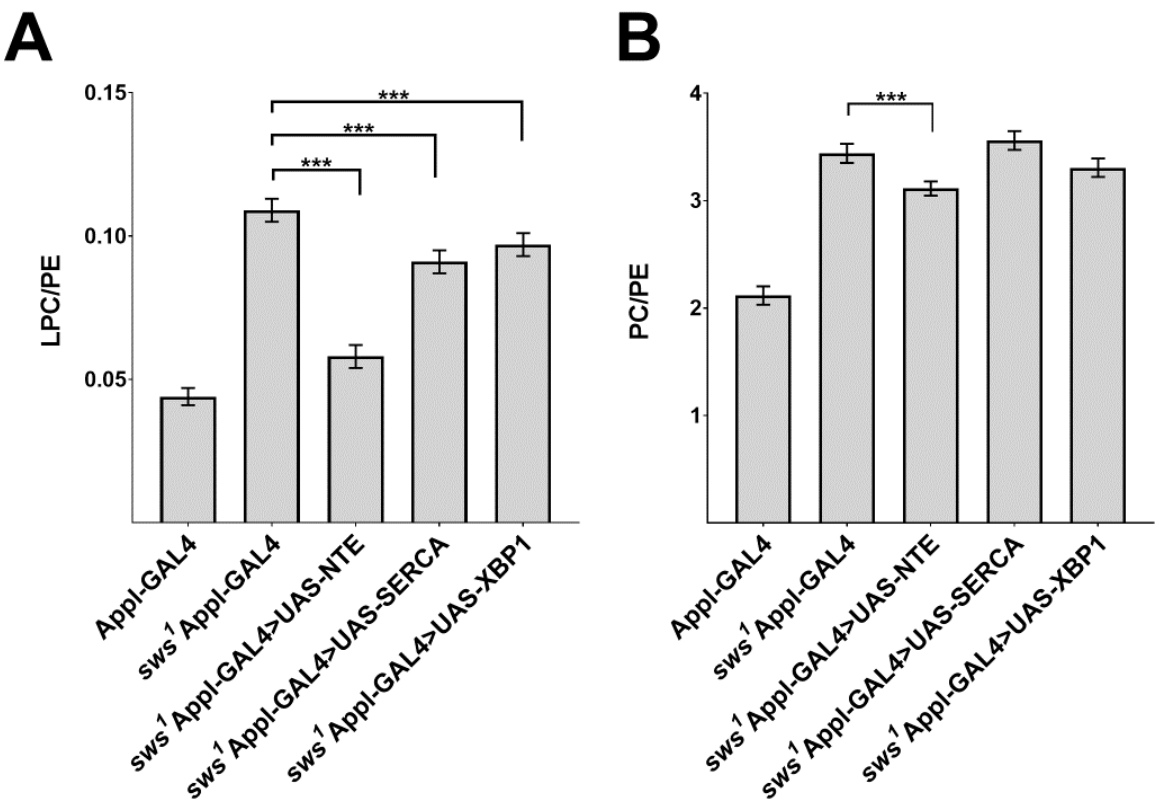

Figure 4-5: Lipid homeostasis in *sws*^{1} is altered with expression of NTE, SERCA, and XBP1. A. Expression of NTE, SERCA, and XBP1 significantly reduce the LPC/PE ratio. **B.** Only expression of NTE significantly rescues the PC/PE ratio. Data represent the mean and 95% intervals of 2-3 independent batches. The ratios between LPC:PE and PC:PE were also analyzed assuming Gaussian distribution with log-link with a two-way analysis that treated batch number and genotype as different factors. Three specific contrasts of interest, comparing *sws*^{1}Appl-GAL4 to lines expressing NTE, SERCA, and XBP1, were tested at the 0.017 level, due to a Bonferroni correction for multiple tests (***p<0.001).

pathways such as the p38 and ERK MAPK and the PI3K pathway, and it has also been reported to stabilize mitochondria membranes to prevent the release of cytochrome c and initiation of apoptosis by preventing Bax from binding to the mitochondrial membrane (Rodrigues et al. 2003, Schoemaker et al. 2004). TUDCA

is currently being used in human clinical trials to treat neurodegenerative disorders such as Amyotrophic Lateral Sclerosis (Elia et al. 2016).

Because of our results connecting *sws*^{1} phenotypes to ER stress and TUDCA's known efficacy in attenuating ER stress, flies were raised on food treated with 15 mM TUDCA, a concentration previously shown to be effective in a *Drosophila* Chacot-Marie Tooth disease model (Debattisti et al. 2014). The flies were reared and kept on the food before performing behavioral and histological assays as done in Figure 4-2. Treating the flies with TUDCA significantly improved the locomotor defect (Figure 4-6A). Neurodegeneration was assessed at 14 dpe as well and was also found to be significantly improved (Figure 4-6 B, C, D). These results indicate that treatment with TUDCA is able to alleviate the *sws*^{1} phenotypes and should be further investigated as a potential treatment option for the ataxia and neurodegeneration seen in patients with mutations in NTE.

Discussion

Loss of SWS/NTE function has been shown to cause an increase in lysophosphatidylcholine and phosphatidylcholine, however, why a rise in LPC and PC levels may cause the neurodegeneration and other symptoms of NTE-associated disorders was unknown. Here we provide evidence that a loss of SWS leads to a loss of lipid homeostasis and activates the UPR; these data are consistent with the model that the rise in LPC and PC inhibits SERCA leading to UPR activation.

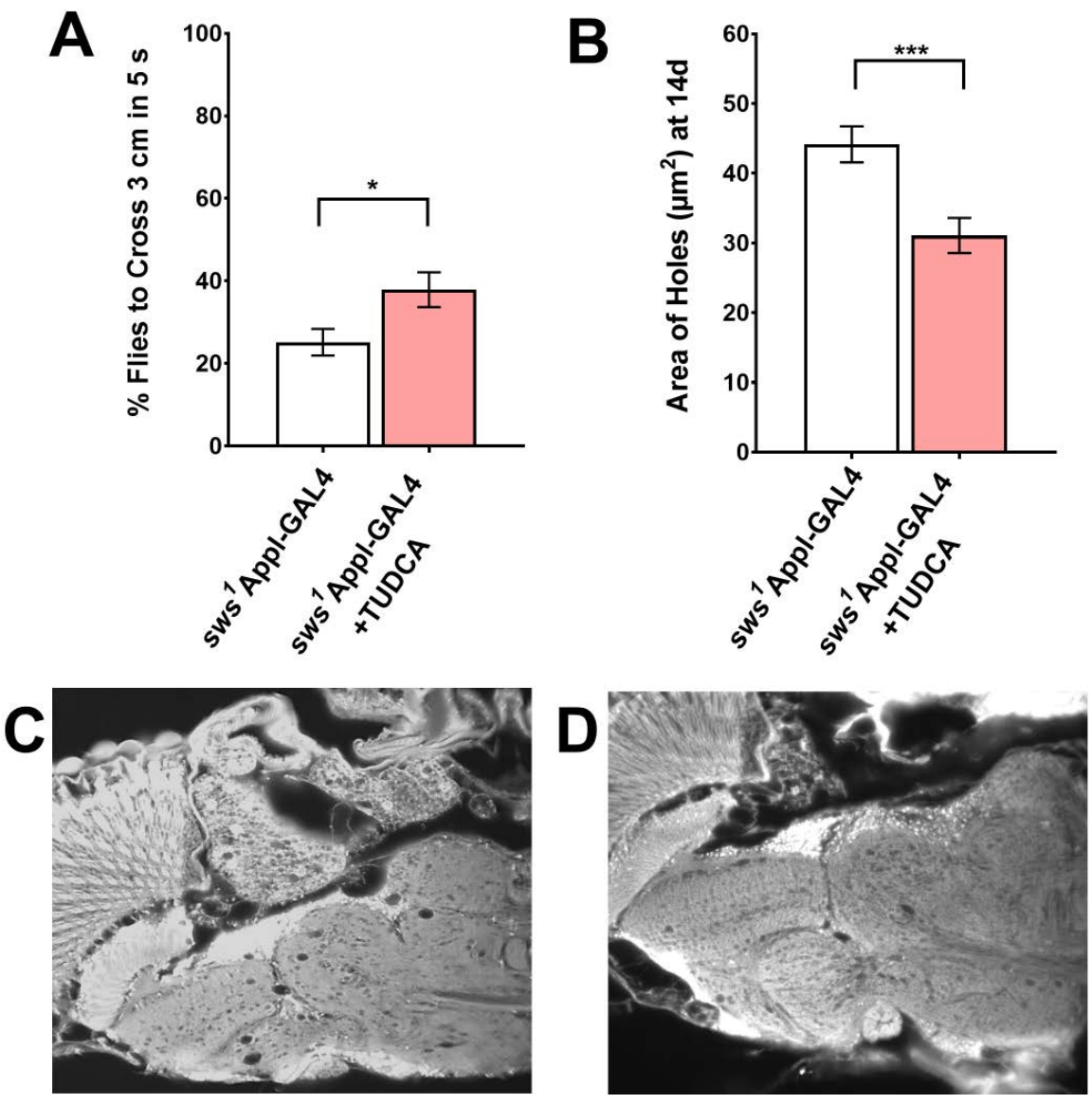

Figure 4-6: Rearing flies on TUDCA treated food rescues *sws*^{1}. A. Treating flies with TUDCA significantly rescues *sws*^{1} negative geotaxis deficits at 7 dpe. **B.** Quantified neurodegeneration showing that rearing flies on TUDCA significantly rescues *sws*^{1} at 14 dpe. Horizontal sections of **C.** *sws*^{1}Appl-GAL4 **D.** *sws*^{1}Appl-GAL4 + 15mM TUDCA taken at 14 dpe. Data represent the mean and SEM of **A.** 20 independent trials of 8 or more flies or **B.** at least 20 independent heads for each genotype. The data were analyzed with an unpaired two tailed student t-test (*$p<0.05$, ***$p<0.001$).

First, it had to be determined if the activation of the UPR was actually occurring in our *sws*^{1} line, which was confirmed by detecting the elevated levels of GRP78/BiP in the heads of *sws*^{1} flies. It was also shown that by reintroducing SWS back into the neurons, GRP78 levels were reduced, indicating that the activation of the UPR is dependent on the loss of SWS. Although, the reduction of GRP78 in the rescue failed to be significant when compared to *sws*^{1}, the reduction was also not significantly different from wildtype levels; the fact we did not achieve wildtype GRP78 levels is most likely due to the glial phenotype in the *sws*^{1} line that is not rescued by this approach. We have previously shown that the glia in *Drosophila* do require SWS, and we suspect that the glia may be undergoing UPR activation as well, explaining why expression of SWS only in neurons failed to completely rescue GRP78 levels.

To further support the evidence that the UPR is activated, XBP1 was targeted to alleviate the *sws*^{1} deficits as seen in other *Drosophila* neurodegenerative models. And, indeed, overexpression of XBP1 significantly rescued the phenotypes. With XBP1 being a transcription factor for lipogenesis, the lipids in the heads were analyzed to determine if the expression of XBP1 rectified the loss of lipid homeostasis. Expression of XBP1 rescues the elevation of LPC in the *sws*^{1} line but fails to rescue PC levels. These data indicate that XBP1 expression may be rescuing *sws*^{1} through effects on LPC levels, but it might also affect other pathways. It has been shown that XBP1 expression is able to improve secretion from the ER, thus allowing for transportation of neuronal materials. It is therefore hypothesized that XBP1 expression is improving the overall "health" of

the ER by upregulating chaperones and expanding the ER to allow for better secretion of neuronal materials needed for the maintenance of axons in addition to reducing LPC levels.

The activation of the ER stress response by loss of lipid homeostasis has been shown to occur in many models, and recently, there is evidence that elevation of PC in the ER is able to inhibit the function of SERCA. Our experiments show that overexpression of SERCA is able to significantly rescue the locomotor deficit and neurodegeneration seen in our null line. Also interesting was the fact that SERCA expression also altered the ratio of the lipids in *sws*^{1}. These data suggest that SERCA expression suppresses *sws*^{1} phenotypes by partially rescuing lipid levels, however, it is still possible another mechanism could be involved in the rescue. Agonists of SERCA haven been developed, and another future study should be to determine if these agonist drugs could improve locomotor deficits and delay the progression of the neurodegeneration, thus providing a feasible avenue of treatment for patients with NTE associated disorders.

Finally, we wished to determine if known attenuators of ER stress could also be a beneficial avenue of further research. In this study, TUDCA was used due to its previous use in a *Drosophila* model of ER stress, and its ability to prevent Ca^{2+} induced apoptosis. It was determined that TUDCA treatment significantly rescued the phenotypes in the flies, indicating that the bile salt may have a future as a potential therapy. Its use as a therapy in other ER stress related diseases, such as diabetes, is currently being investigated, and, while its use would not be curative,

it could serve as a primary or co-treatment due to its already proven ability to be tolerated in other clinical trials.

Overall, there is clear evidence that the activation of the Unfolded Protein Response contributes to the neurodegeneration seen in *sws*^{1} and targeting these pathways could be a viable avenue of therapy to consider. Unfortunately, while the major components of the UPR are conserved across species, the UPR in *Drosophila* differs in some aspects from its mammalian counterpart, such as *Drosophila* does not have an orthologue for CCAAT-enhancer-binding protein homologous protein (CHOP), which is a major factor in inducing apoptosis in vertebrates when the UPR is not alleviated. There being differences in the pathways does suggest these experiments should be repeated in a mammalian system, but this fact also allows for more potential targets to be exploited as well.

Another avenue of research should be if activation of the UPR is only limited to the neurons, or if the glia as well are undergoing ER stress. It is suspected that glia cells are also undergoing activation of the UPR because previous work in our lab has shown that glial cells only rely on the phospholipase function of SWS and not the PKA regulatory function. These data and the failure of SWS to restore GRP78's elevation to wildtype levels provide strong evidence that the glia cells may also be undergoing ER stress. Having both the neurons and glia responding in different ways to the loss of SWS/NTE function could help to explain some of the variable expressivity detected across patients.

Supplementary Data:

Inflammation also contributes to the sws[1] phenotypes

Recent research has revealed that the immune system not only protects against foreign pathogens, but that it also plays a role in maintaining the health of cells and tissues by recognizing receptors and signals that indicate a cell is distressed. In a way, the function is very similar to the Unfolded Protein Response, cytoprotective up to a point at which apoptosis is initiated. Relish (Rel) is an NF-κβ transcription factor in the Immune Deficiency (Imd) pathway in *Drosophila*, and its associated pathway and subsequent activation is highly similar to the mammalian innate immune pathway of TNFα. Research has demonstrated that the expression of constitutively active Rel is sufficient to induce neurodegeneration in a *Drosophila* model of ataxia-telangiectasia (Petersen et al. 2012). In addition, when ER stress is induced, the antimicrobial peptides (AMP) that are under the control of Rel are detected in the heads of flies. Other experiments also showed that this induction was reliant on peroxiredoxin 4/Jafrac 2, which is known to maintain redox homeostasis levels in the ER and acts as an ER stress sensor (Tenev et al. 2002, Klichko et al. 2015). When UPR is initiated, Jafrac 2 will translocate to the cytosol from the ER to activate proapoptotic pathways, including the Imd pathway through Rel (Tenev et al. 2002, Klichko et al. 2015).

To determine if Rel activation was involved in the locomotor deficits and neurodegeneration of *sws[1]*, an UAS RNAi construct against Rel mRNA was expressed using the Appl-GAL4 driver. Fast phototaxis was used to quantify locomotor deficits at 7 dpe, and the quantification of neurodegeneration was

conducted as before at 14 dpe. Knocking down Rel in the neurons significantly rescued the *sws*^{1} fast phototaxis and neurodegenerative phenotypes indicating that Rel is activated and involved in the *sws*^{1} etiology.

Based on the previous literature and these data, Rel is most likely being activated by the initiation of the UPR through Jafrac 2. While it is clear that inflammation contributes to the neurodegeneration in *sws*^{1}, how much it contributes is yet to be determined. Conducting a qRT-PCR for the AMPs activated by the Toll signaling pathway, while knocking down the expression of Rel may help to elucidate if the other immune pathway's activation could be involved in the *sws*^{1} phenotypes as well.

In addition, there is evidence that expression of constitutively active Rel in glia is also sufficient to induce a gliopathy similar in appearance to what is seen in *sws*^{1}. Further research should determine if knocking down Rel in glia is able to rescue the phenotype, which would lend more evidence that the glia also experience activation of the UPR with a loss of SWS function.

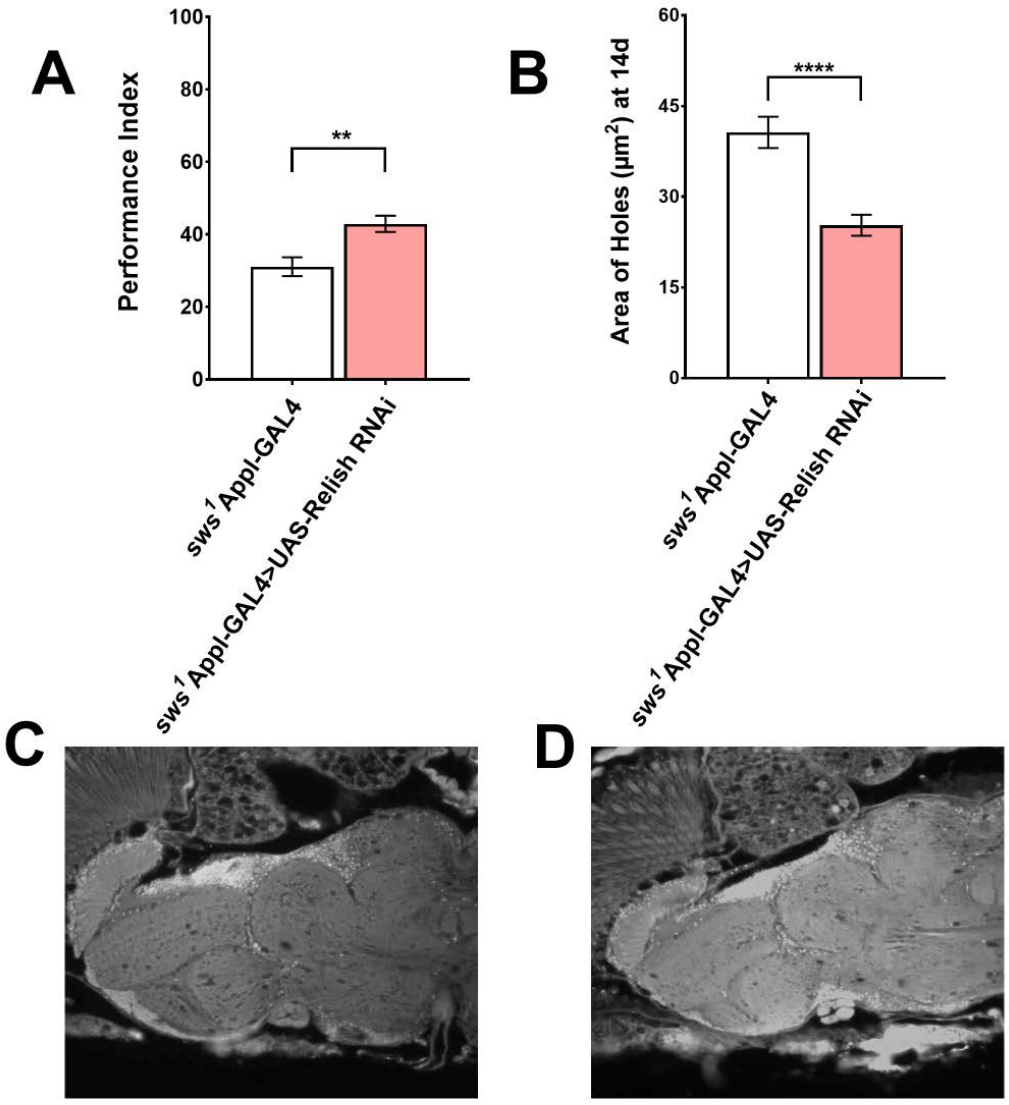

Figure 4-S1: Knocking down Relish rescues *sws[1]*. A. Expressing an RNAi construct against Relish mRNA significantly rescues *sws[1]* fast phototaxis deficits at 7 dpe. **B.** Quantified neurodegeneration showing that expressing Rel RNAi significantly rescues *sws[1]* at 14 dpe. Horizontal sections of **C.** *sws[1]*Appl-GAL4 **D.** *sws[1]*Appl-GAL4>UAS-Relish RNAi taken at 14 dpe. Data represent the mean and SEM of **A.** at least 16 independent trials of 8 or more flies or **B.** at least 18 independent heads for each genotype. The data were analyzed with an unpaired two tailed student t-test (**p<0.01, ****p<0.0001).

Chapter 5

Conclusions and Future Directions

Overview and Summary

NTE, also known as PNPLA6, has been implicated in human diseases since it was discovered to be the target of organophosphates involved in the Jamaica Ginger incident during the Prohibition Era. In recent years, patients with mutations in NTE have been diagnosed with numerous disorders, and a spectrum of symptoms has been described for these diseases, with no genotype-phenotype correlation observed. As science progressed, the location and function of NTE became known, but why the loss of NTE leads to neurodegeneration and other symptoms has not been identified.

In this thesis, the potential mechanisms involved in the etiology and subsequent spectrum of NTE-related disorders is examined using *Drosophila*. *Drosophila* have been used to study the orthologue of NTE, SWS, for years, and experiments in this animal model have led to reciprocal discoveries in mammalian systems. Our lab has previously shown that SWS is capable of regulating Protein Kinase A signaling, and therefore, in Chapter 3, the phenotypes caused by a loss of PKA-C3 were described. While there are many questions left to be answered, using the model developed, what roles the orthologue of PKA-C3, Protein Kinase X (PRKX), has in the nervous system should also be researched further. In Chapter 4, I researched how the loss of SWS function, in particular the phospholipase, resulted in neurodegeneration. While research has shown there is an elevation in lysophosphatidylcholine and phosphatidylcholine with a loss of NTE, why this elevation results in neurodegeneration has not been adequately described before. In this chapter, the mechanism of the Unfolded Protein

Response (UPR) being activated with the loss of NTE was described along with potential therapy options to be further researched.

Chapter 3 Conclusions and Future Directions

Protein Kinase A activity and function has been widely studied in the nervous system, however the unique group of kinases that PKA-C3 and PRKX comprise have been mostly ignored. While it is known that these kinases are expressed in the nervous system, their regulation and targets are unknown. We have previously shown that organophosphate exposure in *Drosophila* and mammalian neuronal cell culture can cause the dysregulation of PKA signaling by disrupting the interaction between SWS/NTE and PKA-C3/PRKX respectively. This study indicates that mutations in NTE could have devastating effects on this unique group's signaling and understanding how loss of these kinases impacts neuronal function is vital for fully understanding the etiology of NTE associated disorders.

In Chapter 3 of this thesis, I examined the loss of PKA-C3 and the impact on coordinated movement in *Drosophila*. With a loss of PKA-C3, significant fast phototaxis and crawling defects were detected, which are not rescued by overexpressing PKA-C1. In addition, when electrophysiology studies were conducted in third instar larva, significant decreases in miniature end plate potential frequency were detected in the PKA-C3 deficiency and RNAi knockdown. These data indicate that PKA-C3 has a role in neuronal function and signaling in *Drosophila* that has never been identified and cannot be compensated for by overexpression of PKA-C1 (Figure 5-1).

However, there are still questions that need to be answered in regards to the targets of PKA-C3 and whether PRKX can rescue the deficiency line. While PKA-C3 deficient larva had defects at the neuromuscular junction, the PKA-C3 rescue experiments still need to be conducted to confirm that the electrophysiology deficits are dependent solely on the loss of PKA-C3. Further studies should also focus on potential targets of PKA-C3, such a as Synapsin. I ran a western that when analyzed indicated that phosphorylation of Synapsin could be decreased in the deficiency line, which could hint at a potential mechanism for the locomotor defects. In addition, with CRISPR/Cas 9 being available in *Drosophila* models, knocking-in PRKX into *Drosophila* would be an ideal way to determine whether PRKX could compensate for the loss of PKA-C3, since it would be under the innate promotor. Additional studies in mammalian systems should be conducted as well to determine further targets of PRKX and whether or not it's activity is regulated by NTE. It is known that both NTE and PRKX are expressed in neurons, and according to the Allen Brain Atlas data, they are both present in Purkinje cells, providing more evidence that NTE could be regulating this signaling cascade. If NTE does regulate the activity of PRKX, then, understanding its role in neurons and signaling is essential for further elucidating the etiology of NTE associated disorders.

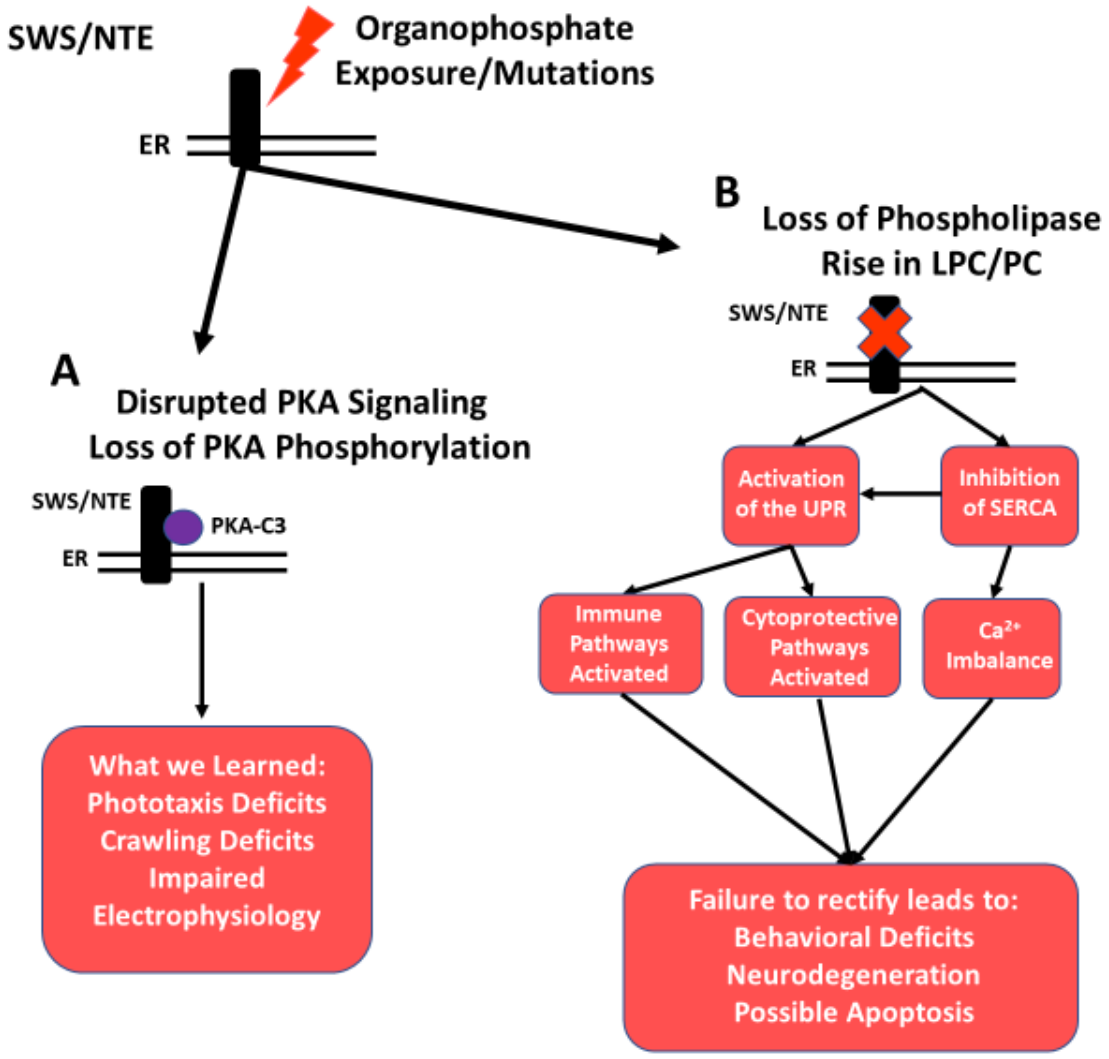

Figure 5-1: Overall Conclusions and Findings A. Chapter 3 showed that a loss of PKA-C3 activity resulted in locomotor defects, which may stem from impaired electrophysiology. Overall, these data indicate that dysregulation of PKA-C3/PRKX signaling could be involved in the etiology of NTE associated disorders. **B.** Chapter 4 provided evidence that the UPR is activated with a loss of SWS function and lipid homeostasis. The data are also consistent with the model that inhibition of SERCA occurs by an increase in PC levels, providing future research opportunities to test the efficacy of SERCA agonists currently in development.

Chapter 4 Conclusions and Future Directions

Loss of SWS/NTE function has been shown to cause an elevation of LPC and PC that fails to be rectified in multiple model systems. However, why this loss of lipid homeostasis leads to neurodegeneration and phenotypes seen in the models has not been described. Recent studies of liver and muscle cells in models of obesity and Duchenne's muscular dystrophy, respectfully, have shown that an increase of PC in the ER can inhibit the function of SERCA, the pump that controls moving Ca^{2+} from the cytosol into the lumen of the ER. Inhibition of this pump has long been known to induce the UPR, which if not alleviated will lead to eventual apoptosis. Thus, I decided to determine if this mechanism could be causing the neurodegeneration when SWS/NTE function is lost.

In Chapter 4 of this thesis, I showed that in *sws*^{1} there is an elevation of GRP78 levels, an ER chaperone, indicating the activation of the UPR. In addition, I also determined that expression of XBP1, a UPR transcription factor, was capable of rescuing the locomotor, neurodegeneration, and part of the lipid imbalance, further indicating that ER stress is occurring. Previous research has revealed that overexpression or activation of SERCA can alleviate the UPR and alter lipid levels. When I overexpressed SERCA in *sws*^{1}, the results were similar. SERCA expression significantly rescued the locomotor, neurodegeneration, and part of the lipid imbalance as well, indicating that inhibition of this pump could be the mechanism by which loss of SWS/NTE leads to phenotypes. To further show there is an imbalance in Ca^{2+} levels, I used the CaLexA system. When expressed in *sws*^{1}, there was consistently a higher level of GFP detected versus controls,

indicating that *sws*^{1} has an inherent higher level of Ca^{2+} in the cytosol, further supporting the model of SERCA inhibition. Finally, I decided to treat the flies with TUDCA, a known attenuator of ER stress. This treatment significantly rescued the locomotor and neurodegeneration phenotypes of the flies, providing evidence that it could be a therapeutic option for patients in the future.

Overall, the evidence presented in this thesis chapter strongly indicates that the UPR is playing a role in the phenotypes of the *sws*^{1} line and continuing to conduct further research on this topic could prove beneficial in finding therapies for patients diagnosed with NTE-associated disorders (Figure 5-1). However, there are still experiments that need to be conducted to further understand how the glia fit into this model and how this research can be used to provide therapies for patients.

In *Drosophila*, it is known that glial cells are also affected by the loss of SWS, but the effects on glia in mammalian systems have been largely ignored. We showed recently that glia function is also affected in a murine glia knockout of NTE, and loss of NTE was sufficient to cause wrapping impairments in non-myelinating Schwann cells, similar to the wrapping issues observed in *Drosophila*. Thus, determining if glial cells are also experiencing ER stress is vital to fully understand the etiology of NTE associated disorders. In this thesis, I showed that expression of SWS in neurons, while capable of lowering the levels of GRP78, was not sufficient to significantly rescue the levels. This result indicates that glia could be undergoing ER stress, since the glia phenotype is not rescued with neuronal expression of SWS.

In addition to discovering if glial cells also undergo ER stress with a loss of SWS/NTE function, mammalian models should be used to determine if agonists of SERCA or other attenuators of ER stress could provide beneficial therapies for patients. Unfortunately, while using *Drosophila* is a good starting point for this research, mammalian systems should be used to determine future therapies due to inherent differences in the UPR pathway and mammalian systems having multiple genes of SERCA. While the major components of the UPR pathways are conserved, there are a few differences as mentioned previously. Potential therapies have been developed to target this protein, and unfortunately due to *Drosophila* not having this protein, experiments studying CHOP need to be conducting using mammalian systems. In addition, *Drosophila* only have one form of SERCA, while mice and humans in particular, have three genes to encode the different forms of the pump. Thus, there might be agonists that can activate the pump that may not work in *Drosophila*.

It is not surprising that the Unfolded Protein Response is playing a role in the etiology of NTE-associated disorders. This response has been implicated to contribute to a number of neurodegenerative diseases, and with SWS/NTE being localized to the ER, it was expected that the loss of the function would disturb this organelle. In addition, knowing this response has been activated, may help to explain why there is a spectrum of symptoms seen in patients. The UPR is a vastly complex signaling cascade that is influenced by signals from multiple organelles, such as the mitochondria. If there are polymorphisms in potential modifying genes within the cascade or in other genes known to influence the response, then, a

genotype-phenotype correlation could never be achieved by identifying the mutations in NTE. This mechanism gives another avenue for researchers to explore that could help to diagnose patients earlier and help determine which therapies may be the best options.

Overall Conclusions

The overall goal of this thesis was to use *Drosophila* to investigate and identify mechanisms for the etiology of NTE-associated disorders, and perhaps gain understanding as to why there is such a spectrum to the symptoms seen in patients. As to the first part of the goal, this thesis provided evidence that dysregulation of an unique kinase and initiation of the UPR could be involved in the etiology of the disorders. While it is clear that the initiation of the UPR is sufficient to cause neurodegeneration, I still believe that dysregulation of PRKX is playing a role in the phenotypes as well, since our PKA-C3 deficient line had locomotor and electrophysiology deficits, as shown in Chapter 3. While there is still research needed to be done, the fact that I found evidence that loss of PKA-C3 can lead to impaired coordinated movement and the elevation of LPC/PC causes the UPR to be activated is a huge step forward in understanding the complete picture in regards to NTE-associated disorders.

Concerning the second part of the goal, I think understanding why there is such a spectrum of symptoms observed in patients may actually require much more research. While compiling the data for this thesis, I realized how many things could be involved and causing the spectrum of symptoms. Knowing that the UPR could be activated, by itself, brings in so many potentials for modifying pathways

that one may never establish a pattern for why one individual is more affected than the other. However, the work I did in this thesis to confirm that the UPR is indeed activated with a loss of SWS function is an excellent starting point to provide therapies to patients, who previously had no options. Many of the attenuators of ER stress, like TUDCA, or treatments using Adeno-associated virus to deliver constructs to manipulate the response are currently being tested in animal models or clinical trials. And, agonists of SERCA are already being developed and tested. With a little more research to confirm my findings in a mammalian system, I think that therapies for the neurodegeneration in these patients could be identified quickly. So, even without the analysis of PRKX and NTE interactions, activation of the UPR as a means to develop treatments should definitely be pursued past this thesis work.

Appendix A

Mutant forms of Neuropathy Target Esterase are capable of rescuing *sws*^{1} to varying degrees

Rationale

NTE is the protein product of the PNPLA6 gene, and recent studies have determined that mutations in PNPLA6 are responsible for several recessive neuronal diseases. Although NTE has only been connected to Oliver-McFarlane, Laurence Moon, and Boucher-Neuhauser syndrome, to name a few, in the last two years over 40 index cases have been identified and it is highly likely that many more patients will be identified in the future. These NTE-associated diseases all display some degree of neuronal dysfunction, but the manifestations and severity are broad. Patients may present with ataxia, weakness in the muscles, spinal cord atrophy, visual impairment or blindness, motor neuron atrophy, and cerebellar atrophy.

Results

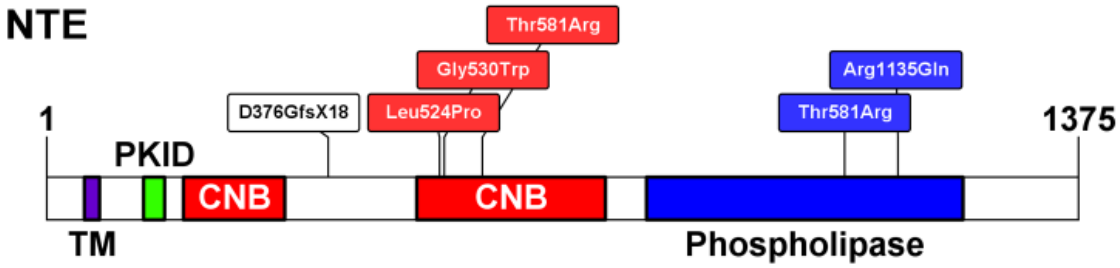

Figure A-1: Schematic of Neuropathy Target Esterase mutations. Cartoon of NTE with all of the mutations made in our laboratory using site directed mutagenesis and cloning techniques. The mutations were selected from patients diagnosed with Gordon Holmes, Boucher-Neuhauser, and Oliver McFarlane syndrome.

To understand how mutations in NTE could be altering its function, we used site-directed mutagenesis to create mutated constructs, and these constructs were then incorporated into the *Drosophila* genome using the p-UASt-attb system. In

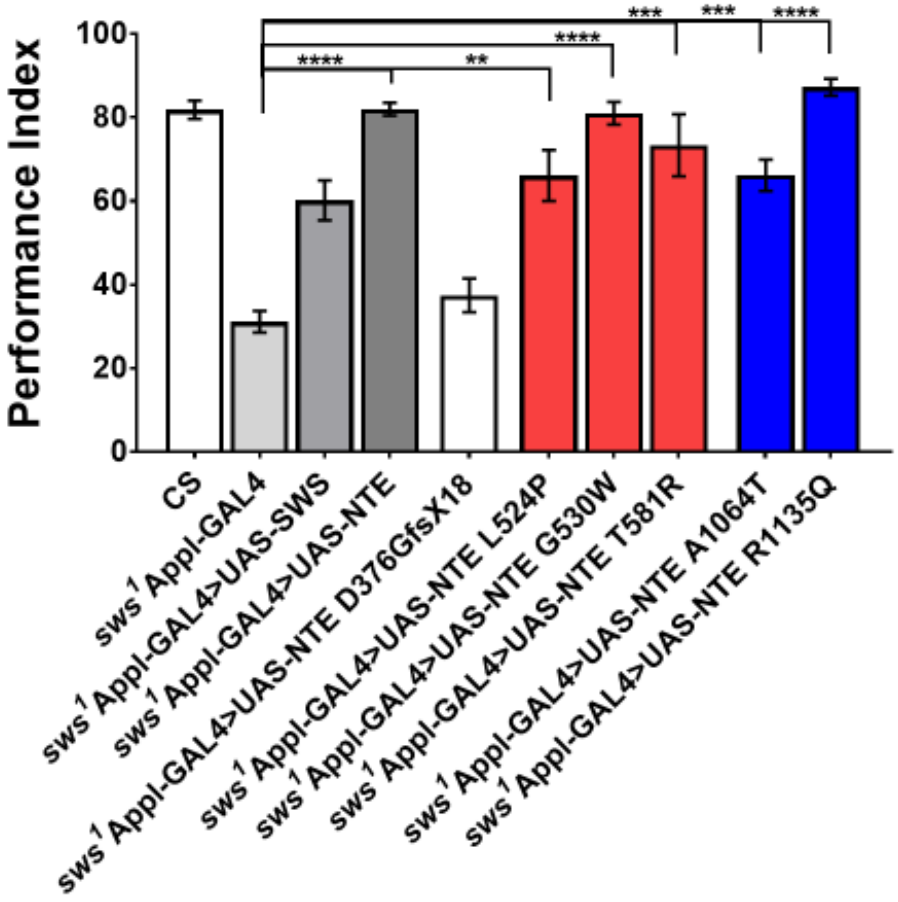

Figure A-2: Expression of most mutated NTE forms in *sws*^{1} is capable of rescuing fast phototaxis deficits. Expression of wildtype NTE was capable of rescuing the fast phototaxis phenotype to wildtype levels. All of the mutated forms of NTE rescued the fast phototaxis phenotype, except the frame shift mutation. However, when compared to the expression of wildtype NTE, NTE G530W was significantly different, indicating that the mutation is affecting the function of NTE. Data represent the mean and SEM of at least 9 independent trials of 10 or more flies. The data were analyzed with a Kruskal-Wallis with a Dunn's multiple comparisons test respectively (*p<0.05, **p<0.01, ***p<0.001, ****p<0.0001).

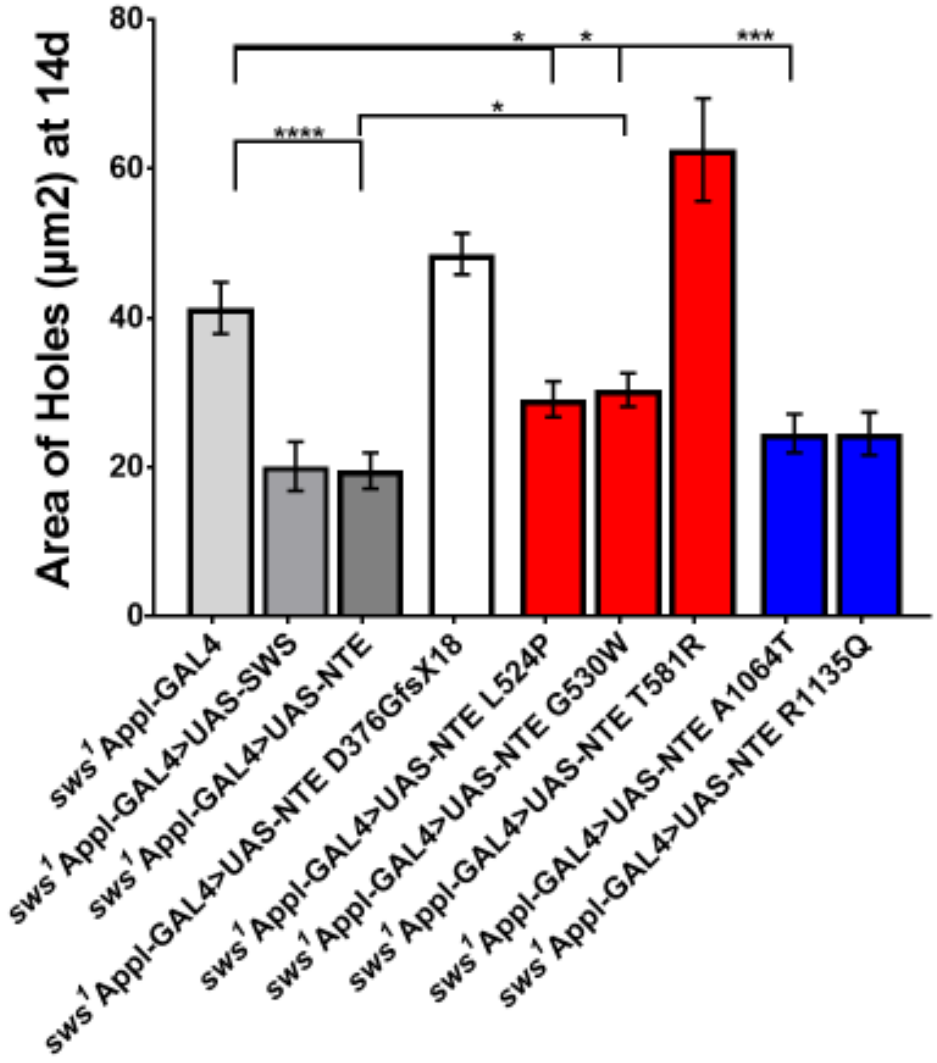

Figure A-3: Expression of most mutated NTE forms in *sws[1]* is capable of rescuing neurodegeneration. Expression of wildtype NTE is capable of rescuing the *sws[1]* neurodegeneration. In addition, expression of mutated forms of NTE are capable of rescuing the neurodegeneration at varying levels, except the frameshift mutation. The NTE T581R and R1135Q mutations have a small sample size; thus, in this assay, no conclusions can be made about their ability to rescue. Data represent the mean and SEM at least 17 independent heads for each genotype. The data were analyzed with a one-way ANOVA test with a Dunnett's multiple comparison test respectively (*p<0.05, **p<0.001, ****p<0.0001).

Figure A-1, all of the mutations made are represented. We then tested the lines by expressing them pan-neuronally with the Appl-GAL4 driver in *sws*^{1} and assessed their efficacy to rescue the fast phototaxis deficits and neurodegeneration. The only NTE mutation that failed to rescue the fast phototaxis assay was the frame shift mutation (NTE D376GfsX18), which results in a protein about one fourth the size of the full length NTE (Figure A-2). In the neurodegenerative assay, the frameshift mutation was again the only construct that failed to rescue the neurodegeneration (Figure A-3). However, when compared to expression of wildtype NTE, NTE G530W was significantly different indicating that the mutant is deficient in some function of NTE. The NTE T581R and R1135Q mutations have only been recently made, and at this point we do not have sufficient sample size to make conclusions about their ability to rescue the *sws*^{1} neurodegenerative phenotype.

Conclusions and Future Directions

Researching how mutations in NTE affect its functions in neurons and glia is essential for understanding the etiology of the disorders. Constructing mutated forms of NTE and using the GAL4/UAS system to express them in *sws*^{1} is a useful tool for figuring out how the mutations in NTE affect its function *in vivo*. Thus, we selected several mutations found in the literature and from collaborators, and we inserted them into the *Drosophila* genome at the same site to obtain comparable expression levels. We then used the Appl-GAL4 driver to express the mutations in neurons and assessed their ability to rescue by utilizing fast phototaxis and neurodegeneration assays. We found that most of the mutations rescued *sws*^{1},

except for the frameshift mutation that expresses a truncated protein one fourth the size of the full length NTE.

One of the reasons why there may not be much of a difference among the mutations could be due to the fact that the Appl-Gal4 driver chosen is one of the strongest in our lab. Thus, the protein levels of the mutated NTE may be high enough to compensate for a mutated NTE that has a lower basal activity.. Choosing a weaker driver may allow for better comparisons of the mutated forms' functions, since the loss of function may not be compensated for by levels of protein. In addition, several other studies of these constructs in neurons should be considered, such as protein localization and PKA regulatory studies. In a previous paper, we showed that with loss of SWS, PKA-C3 was no longer localized to the membrane fraction. It would also be an interesting study to determine if any of the mutations affected the localization of PKA-C3, along with its regulation.

Finally, the mutated constructs should be expressed in glia as well, to assess their ability to rescue *sws*[1]. It is just now coming to be understood that impaired glia cells could also be contributing to the etiology of these disorders. Thus, assessing how the mutated forms rescue the glia phenotype should be another experiment considered in the future as well, since one of the mutated forms may be sufficient to rescue the neuronal phenotype, but fail to rescue the glia.

There are a variety of experiments that remain to be conducted, so that in the future these constructs can be analyzed to fully characterize these mutated forms of NTE.

Appendix B

Expression of a mutant form of SERCA rescues *sws*^{1} due to the phenomenon known as ER stress hormesis

Rationale

In Chapter 4 of this thesis, we showed that activation of the Unfolded Protein Response (UPR), most likely, through inhibition of the Sarco-Endoplasmic Reticulum Ca^{2+}-ATPase (SERCA) contributed to the *sws*^{1} locomotor deficits and neurodegeneration. Many neurodegenerative diseases have been associated with the activation of the UPR, and the current strategy for some of these diseases is to actually induce ER stress or increase the response to strengthen the cytoprotective effects of the UPR pathways. This strategy is known as ER hormesis, whereby a small stress is induced to promote cytoprotective mechanisms that allow the cell to be more resistant to a stronger stress later (Mollereau et al. 2014).

Thus, along with obtaining a GAL4/UAS controlled wildtype SERCA construct, we also obtained a mutated form that is associated with Darier's disease ($SERCA^{S495P}$). This dominant mutation causes ionic leakage from the ER, reducing the ER Ca^{2+} levels, and thus, inducing a mild UPR response, already early on before an ER stress response is detected in the *sws*^{1} mutation (Kaneko et al. 2014). We decided to express this construct in *sws*^{1} to determine what the effects would be on the phenotypes, and if there could be an ER hormesis event.

Results

As was done in Chapter 4, we used negative geotaxis and histological sections to assess the *sws*^{1} locomotor deficits and neurodegeneration, respectively. When we expressed the $SERCA^{S495P}$ construct pan-neuronally using

the Appl-GAL4 driver, we detected a significant improvement in the negative geotaxis assay at 7 dpe when compared to *sws*^{1} alone (Figure B-1).

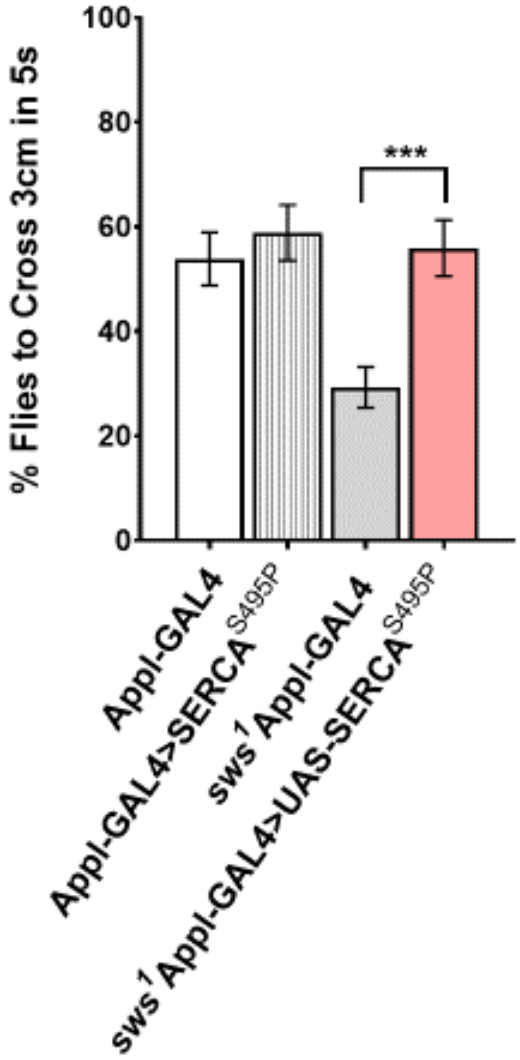

Figure B-1: Expression of the mutated form of SERCA rescues the negative geotaxis deficits of *sws*^{1}. Expression of the SERCA^{S495P} construct significantly rescues the *sws*^{1} locomotor defects. Data represent the mean and SEM of at least 20 independent trials of 8 or more flies for each genotype. The data were analyzed with an ordinary one-way ANOVA with a Dunnett's multiple comparisons test respectively (***p<0.001).

In addition to rescuing the negative geotaxis deficit, expression of the SERCA mutant was sufficient to rescue the neurodegeneration observed in *sws*[1] flies (Figure B-2).

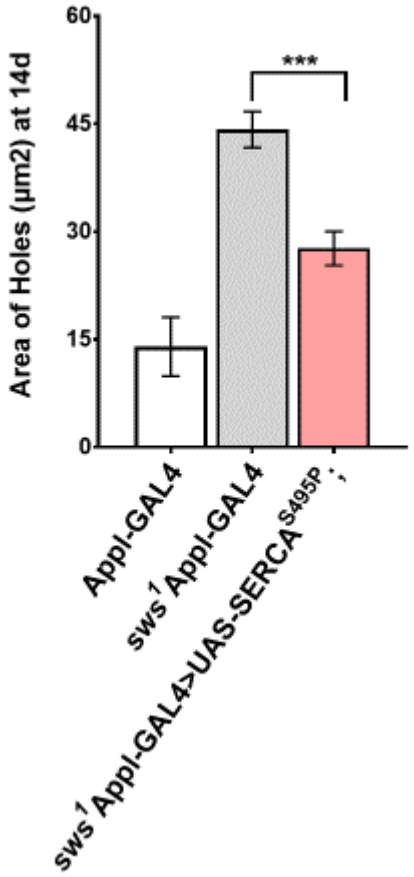

Figure B-2: Expression of the mutated form of SERCA rescues the age-dependent neurodegeneration observed in *sws*[1]. Expression of the SERCA^{S495P} construct significantly rescues the *sws*[1] neurodegeneration. Data represent the mean and SEM of at least 20 independent heads for each genotype. The data were analyzed with an ordinary one-way ANOVA with a Dunnett's multiple comparisons test respectively (***p<0.001).

Conclusions and Future Directions

The UPR is a complex and sometimes contradictory pathway system. In this instance, one would hypothesize that expressing the SERCA mutant would actually cause the *sws*^{1} mutant to have worse phenotypes, but presumably due to ER hormesis, it actually improves the phenotypes. To confirm ER hormesis is occurring, studying whether cytoprotective factors such as autophagy genes or chaperones are elevated should be the next step. Another experiment that could be conducted would be to induce the UPR pathway through another mechanism to see if *sws*^{1} phenotypes are again diminished.

While the locomotor and neurodegeneration are improved at the selected time points, activation of the UPR pathways is like a double-edged sword. If too much stress is occurring, then eventually, the cell will shift and activate apoptosis. In this case, expressing SERCA^{S495P} may help at these relatively early timepoints, but there could be a drastic enhancement if the flies were aged more, which may be masked by only studying early time points. Conducting survival studies would be an excellent way of determining if the cytoprotective effects of ER hormesis continue as the flies age or if there is a certain point where the apoptotic effects are initiated.

Studying ER hormesis in *sws*^{1} could provide clues as to why there is such a spectrum of symptoms observed in patients diagnosed with Neuropathy Target Esterase (NTE) disorders. Crossing this SERCA line to commercial deficiency lines, each of which has a deletion of a different region of the chromosomes, to detect potential modifiers could be a way to predict if inducers of ER hormesis

could influence the loss of SWS phenotypes. Identifying these genes could then be translated to mammalian systems to determine if this phenomenon is contributing to the spectrum of disorders associated with mutations in NTE. Some of the patients have had their exome sequenced, and it could be interesting to reexamine the sequence data to determine if there may be mutations in the identified genes.

Appendix C

Overactivation of the innate immunity pathways leads to neurodegeneration

Rationale

As we age, changes occur in the strength and regulation of our immune system. Although the function of the immune system to protect against pathogens is diminished with age, innate immune gene expression is upregulated in the brain. But, what causes this upregulation in the brain is unclear. In *Drosophila*, it has been shown that an upregulation of the innate immune system through loss of a regulator leads to neurodegeneration in older flies (Cao et al. 2013). Due to connections between the circadian clock and immune genes in the periphery, we wanted to investigate if expression of innate immunity factors in the brain might also be regulated by the circadian clock.

Results

To address this function of the circadian clock, we first decided to express innate immune genes using the TIM-GAL4 driver to determine whether expression in clock-containing cells was sufficient to cause neurodegeneration. When the Antimicrobial Peptides (AMPs) were expressed using the TIM-GAL4 driver, neurodegeneration was readily detectable around 45 days of age, indicating that overactivation of the innate immune pathways in clock-containing cells is sufficient to induce neurodegeneration (Figure C-1).

We next decided to overexpress the Relish (Rel) construct and a RNAi against Rel mRNA using the TIM-GAL4 driver again to determine if neurodegeneration was induced as the flies aged. Rel is the NF-κβ that is cleaved to activate the expression of the Immune Deficiency (Imd) pathway with its respective AMPs. Thus, we wished to see if expression of this upstream

transcription factor was sufficient to induce neurodegeneration. There was a significant increase in neurodegeneration when Rel was overexpressed, but the expression of the RNAi did not significantly differ from the control (Figure C-2). These data indicate that overexpression of Relish is sufficient to induce neurodegeneration.

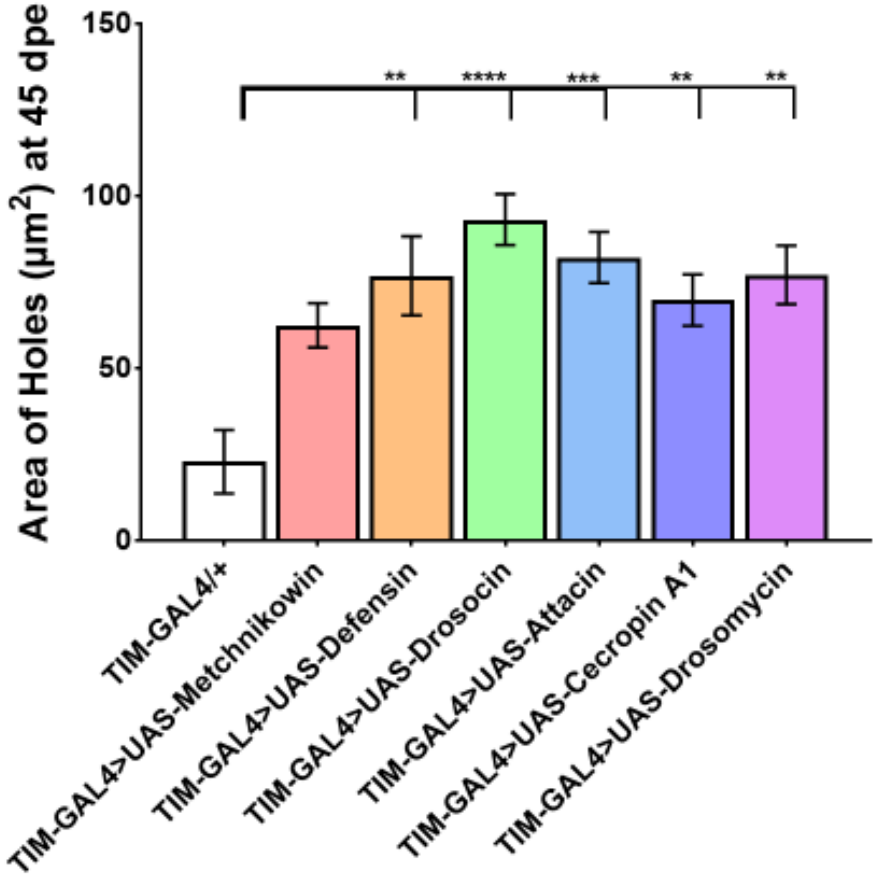

Figure C-1: Expression of AMPs induces neurodegeneration. Expression of the AMPs using the TIM-GAL4 driver significantly induces neurodegeneration in fly brains at 45 dpe. Data represent the mean and SEM of at least 8 independent heads for each genotype. The data were analyzed with an ordinary one-way ANOVA with a Dunnett's multiple comparisons test respectively (**p<0.01, ***p<0.001, ****p<0.0001).

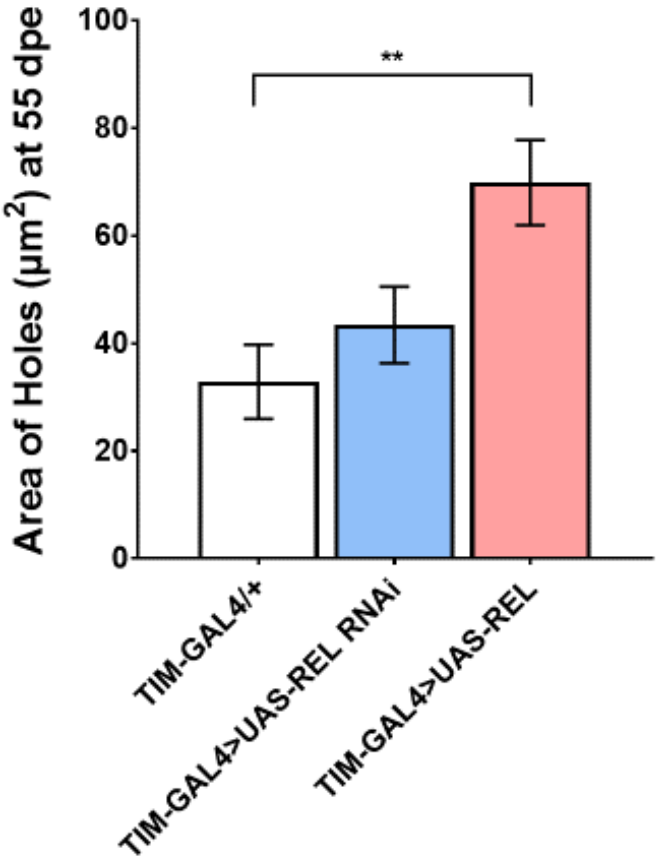

Figure C-2: Overexpression of Relish induces neurodegeneration. Overexpression of Rel using the TIM-GAL4 driver significantly induces neurodegeneration in fly brains at 55 dpe. Expression of the RNAi against the Rel mRNA was not significantly different from the control (the driver alone). Data represent the mean and SEM of at least 8 independent heads for each genotype. The data were analyzed with an ordinary one-way ANOVA with a Dunnett's multiple comparisons test respectively (**p<0.01).

Finally, we wanted to investigate if AMP expression is elevated in fly brains as they age and when the circadian clock is disrupted. For the circadian clock experiments, we used flies that had a mutation in the core clock gene *period* (*per*), which we have previously shown to have age dependent neurodegeneration as well (Krishnan et al. 2009). Heads of young (5d) and old (25d) control Canton S

(CS) and *per* null flies were collected and used for RT-qPCR. We showed that there is a significant elevation in the mRNA levels of the AMPs when 5d old CS were compared to aged CS (25dpe), corroborating previous results in the literature (Figure C-3 A). We also showed that there was a significant elevation of AMPs expression in *per* null fly heads compared to aged match controls at 5dpe and 25dpe, indicating the circadian clock is somehow regulating the innate immune response of *Drosophila* (Figure C-3 B, C).

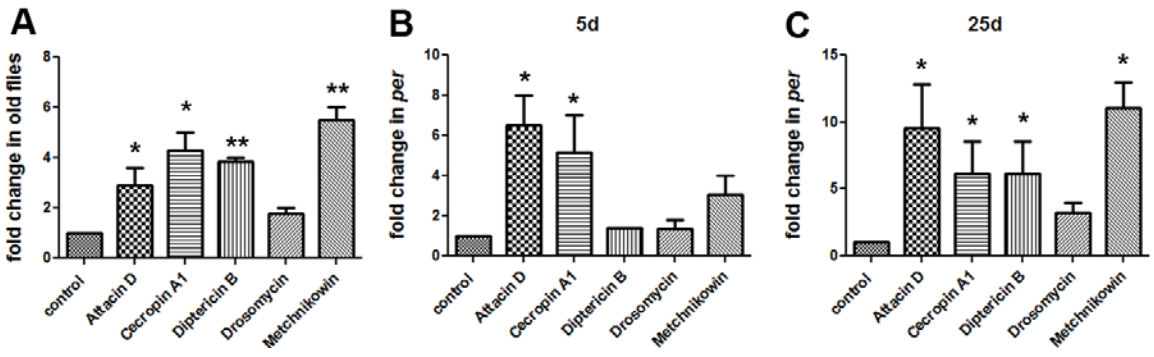

Figure C-3: Aging flies and loss of the circadian clock induce elevated expression of innate immune genes. A. A qRT-PCR analysis showed a significant elevation in the expression of AMPs in the heads of aged CS flies when compared to younger flies. **B.** A qRT-PCR analysis also showed significant elevation of AMP expression in the heads of *per* null flies at 5dpe. **C.** This phenomenon is still detected when aged *per* null fly heads were compared to aged CS. Data represent the mean and SEM of at least 3 independent batches of fly heads. The data were analyzed with an ordinary one-way ANOVA with a Dunnett's multiple comparisons test respectively (*p<0.05).

Conclusions and Future Directions

As we age, changes occur in the strength and regulation of our circadian clock and immune system. Loss of the circadian clock has been shown to cause early aging symptoms in many animal models, including *Drosophila melanogaster*. In the *period* (*per*) null mutant, we previously showed that the loss of the circadian clock leads to neurodegeneration in fly brains. Work conducted by a collaborator identified Rel, as a possible connection between the circadian clock and the innate immune system. They conducted RT-qPCR across multiple time points, and they detected that the Rel mRNA cycled in a circadian fashion. Thus, we suspect that there could potentially be a link between the weakening of the circadian clock and upregulation of the innate immune system as the flies age.

The data presented here indicate that activation of the innate immune pathways is sufficient to induce neurodegeneration, which lends credence to the neurodegeneration overserved in the *per* null fly being caused by overactivation of the innate immune response. Especially, since we've shown expression of AMPs are significantly elevated in the heads of young and old *per* null flies when compared to age matched controls. More studies need to be conducted to research the connection between the circadian clock and the innate immune pathways of *Drosophila* to better understand how the two are connected, which could provide insight into how the mammalian systems could be connected as well.

Additional Material

Mass histology to quantify neurodegeneration in *Drosophila*

Sunderhaus, Elizabeth R. and Kretzschmar, Doris

Oregon Institute of Occupational Health Sciences, Oregon Health & Sciences University, Portland, OR, USA

e-mail: Doris Kretzschmar: kretzsch@ohsu.edu, Corresponding author

Elizabeth R. Sunderhaus: sunderha@ohsu.edu

Keywords: Neuroscience, degenerative diseases, vacuoles, histology, paraffin sections, *Drosophila*, adult nervous system

Short abstract:

Drosophila is widely used as a model system to study neurodegeneration. This protocol describes a method by which degeneration, as determined by vacuole formation in the brain, can be quantified. It also minimizes effects due to the experimental procedure by processing and sectioning control and experimental flies as one sample.

Long Abstract:

Progressive neurodegenerative diseases like Alzheimer's disease or Parkinson's disease are an increasing threat to human health worldwide. Although mammalian models have provided important insights into the underlying mechanisms of pathogenicity, the complexity of mammalian systems together with their high costs are limiting their use. Therefore, the simple but well-established *Drosophila* model provides an alternative for investigating the molecular pathways that are affected in these diseases. Besides behavioral deficits, neurodegenerative diseases are characterized by histological phenotypes such as neuronal death and axonopathy. To quantify neuronal degeneration and to determine how it is affected by genetic and environmental factors, we use a histological approach that is based on measuring the vacuoles in adult fly heads. To minimize the effects of systematic error and to directly compare sections from control and experimental flies in one preparation, we use the "collar" method for paraffin sections. Neurodegeneration is then assessed by measuring the size and/or number of vacuoles that have developed in the fly brain. This can either be done by focusing on a specific region of interest or by analyzing the entire brain by obtaining serial sections that span the complete head. Therefore, this method allows one to measure not only severe degeneration but also relatively mild phenotypes that are only detectable in a few sections, as occurs during normal aging.

Introduction

With the increase in life expectancy, neurodegenerative diseases like Alzheimer's or Parkinson's have become an increasing health threat for the general population. According to the National Institutes of Health, 115 million people worldwide are predicted to be affected by dementia in 2050. Although significant progress has been made in identifying genes and risk factors involved in at least some of these diseases, for many of them, the underlying molecular mechanisms are still unknown or not well understood.

Simple invertebrate model organisms like *Caenorhabditis elegans* and *Drosophila melanogaster* offer a variety of experimental advantages to study the mechanisms of neurodegenerative diseases, including a short life cycle, large number of progeny, and the availability of well-established and sometimes unique genetic and molecular methods[1-12]. Furthermore, these organisms are amenable to unbiased interaction screens that can identify factors contributing to these diseases by their aggravating or ameliorating effects on neurodegenerative phenotypes.

Analyzing such genetic interactions and assessing aging effects requires quantitative protocols to detect neurodegeneration and to measure its severity. This assessment can be done relatively easily when measuring behavioral aspects in *Drosophila*, such as olfactory learning, negative geotaxis, or fast phototaxis, which provide a numeric performance value[13-21]. It is also possible to determine the effects on neuronal survival by counting neurons. However, this is only possible when focusing on a specific population that is clearly identifiable, like the

dopaminergic neurons that are affected in Parkinson's disease, and even then, the results have been controversial[22-24].

The protocol described here uses the collar method to perform paraffin serial sections, a method that was originally developed by Heisenberg and Böhl, who used it to isolate anatomical brain mutants in *Drosophila*[25]. The use of the collar method has subsequently been adapted, including in cryosections, vibratome sections, and plastic sections[26-28]. Here, this method is employed to obtain serial sections of the entire fly head, which can then be used to measure the vacuoles that develop in flies with neurodegenerative phenotypes[16,21,29-32]. These measurements can be done in specific brain areas or can cover the entire brain; the latter approach allows one to identify even weak degenerative phenotypes, as observed during aging. Finally, when using the collars, up to 20 flies can be processed as one preparation, which is not only less time-consuming, but also allows for the analysis of control and experimental flies in the same preparation, minimizing artifacts due to slight changes in the preparation.

Protocol:

1. Fixing the Head on Collars and Embedding in Paraffin

Note: All of the steps in the fixation process should be done in a fume hood. Methylbenzoate, while not posing a health risk, has a highly distinct odor, which can be overwhelming if not handled in a fume hood.

1.1 Before anesthetizing the flies, make up 50 mL of Carnoy solution by adding 15 mL of chloroform and 5 mL of glacial acetic acid to 30 mL of 99% ethanol (do not mix the chloroform and acetic acid). Pour it in a glass container with a flat bottom, such as a crystalizing dish, to ensure that the collars can lay flat and are completely covered by the solution.

1.2 Anesthetize the flies with CO_2 or ether.

1.3 Thread flies (up to 20 with most collars) by their necks into the collars using forceps. Remember to align all of the heads in the same orientation, as seen in Figure 1A, and be gentle to ensure that no damage occurs to the head or eyes.

1.4 Include *sine oculis* flies (arrows, Figure 1A) at random positions so that the order of the flies can be easily identified in the sections. In addition, if the experimental flies have a light or white eye color, thread some red-eyed flies, such as wild type, between them to ensure that sufficient pigment is present to stain the slide. Record the order of the flies on a protocol sheet together with the collar number if using more than one collar.

1.5 Once a collar has been finished, place it in the prepared Carnoy solution for 3.5-4 h.

1.6 Dump out the Carnoy solution into the appropriate disposal canister and begin the ethanol washes. Make sure to pour slowly so as not to disturb the placement of the collars in the container.

1.7 Wash the collars for 30 min in 99% ethanol twice.

1.8 Wash the collars in 100% ethanol for 1 h. Be sure to change the washes on time to prevent over-dehydration.

1.9 Put the collars in methylbenzoate overnight at room temperature. Seal the container with parafilm to prevent the evaporation of the methyl benzoate.

1.10 Pour the methylbenzoate into the proper disposable container in the fume hood. Add a previously-prepared mixture of 1:1 low melting point (56-57 °C) paraffin wax and methylbenzoate. From this point on, the collars need to be kept in an incubator at 65 °C to make sure that the paraffin does not harden.

1.11 Pour out the methylbenzoate and paraffin mixture into the proper disposable container, and pour molten pure paraffin wax, kept at 65 °C, onto the collars.

1.12 Change the paraffin after 30 min and repeat this at least five times. At least 6 to 8 washes should be performed.

1.13 Once the washes are complete, place the collars into a rubber ice cube tray with slots approximately the size of the collars. Pour molten paraffin over them until completely covered and allow it to harden overnight (try to avoid air bubbles).

1.14 Remove the paraffin blocks containing the collars from the ice cube tray. Separate the paraffin block from the collar using a razor blade, gently breaking off the collar. The heads will be in the paraffin block while the bodies will stay in the collar. The blocks can be kept at room temperature.

1.15 To clean the collars, soak them in a deparaffinization agent at 65 °C to remove the paraffin, clean with light scrubbing, and wash in ethanol before reusing.

2. Sectioning and Mounting

2.1 Warm a heating plate to 50 °C. Place the object holders (or metal mounting blocks) and razor blades on the plate and let them warm up.

2.2 Depending on the desired orientation for sectioning, attach the paraffin block either with the heads towards the side (for horizontal sections) or facing upwards (for frontal sections) to a heated mounting block (briefly melting the block at the contact side). Remove the block from the heating plate and allow it to cool for at least 10 min to ensure that the paraffin is hardened enough for a proper seal onto the mounting block. Keep the row of heads aligned in parallel with the surface of the block as much as possible to prevent uneven sections.

2.3 Take a razor blade and trim the excess paraffin away from the fly heads so that only a small row with the embedded heads remains (the razor blade can be warmed up for easier trimming). Make sure not to trim too much so that the paraffin does not break during sectioning (more trimming can be done during sectioning).

2.4 Place the mounting block into the object holder of the microtome and ensure that the alignment of the row of heads is as parallel as possible to the edge of the blade.

2.5 Prepare microscope slides by covering them with a thin layer of poly-lysine solution and let them dry for 5 min. Cover them with water shortly before use.

2.6 Cut 7-µm sections and transfer the ribbon of sections to the slide floating on the water.

Note: To obtain the entire brain for horizontal sections, we collect the ribbon from when starting to cut into the eye until the head has been completely cut (cutting from the proboscis into the brain). More than one slide may be needed for the entire head.

2.7 Place the slide on a heat plate at 37 °C and allow the ribbon to expand for about 1 min.

2.8 Remove excess water (by pouring it off or using a tissue) and dry the slides overnight.

2.9 Remove the paraffin wax from the slide by placing the slides in a tall, vertical slide-staining jar filled with a deparaffinization agent (completely covering the sections). Perform three washes for 30 min to 1 h each.

2.10 Remove the slide from the final wash. Place two drops of embedding media onto the slide and cover it with a large coverslip.

3. Photographing and Analyzing the Sections

3.1 Allow the prepared slides to dry for 1-2 days. Then, examine them on a fluorescence microscope under blue light.

3.2 Use a lower magnification to determine the orientation of the flies and to find the region of interest if focusing on a specific region.

Note: For the *sws* flies (see Figure 2), we find the section that contains the great commissure and take an image (usually at 40X magnification). When analyzing the entire brain (as in Figure 3), we scroll through all the sections from a head and either photograph the section with the most severe phenotype or all sections that show vacuoles.

3.3 For a double-blind analysis, take and number images without knowing the genotype and record the collar number and position of the head in the row to identify them later.

3.4 Once the images have been taken, analyze them using an imaging software.

3.5 Count the number of vacuoles per section or per head. To measure the vacuole size, open the images in a software program and select the vacuoles with a selection tool. Determine the amount of pixels in the selected vacuoles.

3.6 For conversion to μm^2, take a photo of a stage micrometer calibration slide at the magnification used for acquiring photos. Determine the amount of pixels in 100 μm^2 to calculate a conversion factor.

3.7 Convert the total pixel number into μm^2 by dividing the number of pixels by the conversion factor calculated in the above step.

Representative Results:

Using the described method results in serial sections stained by the eye pigment[33] that encompass the entire fly head. A part of this is shown in **Figure 1B**, where the sections from an individual head are shown from top to bottom. The sections from different flies are seen left to right in this example. To facilitate orientation and identification of the flies, an eyeless fly (*sine oculis*) is inserted as a marker at position three (arrow, **Figure 1B**).

To quantify neurodegeneration, we measure the formation of vacuoles that can be detected in these sections. Vacuoles are defined as round, dark spots that are within the green fluorescent neuropil (arrowheads in **Figure 2** and **3**) or cortex and that are visible in at least two consecutive sections of the fly brain. Quantifying neurodegeneration by measuring vacuoles can either be done by focusing on a specific brain region or by analyzing the entire brain. Limiting the analysis to a specific region of the brain is useful in cases where a mutation only affects a specific region, like the olfactory lobes in the *futsch*^{olk} mutant[34], but it can also be used when there is severe degeneration in all or many regions of the brain. An example for the latter is the *swiss-cheese (sws)* mutant (**Figure 2**), where measuring all vacuoles would be too time consuming. We therefore took only one image and, to ensure that the measurements were always done at the same level, we took all images at the level of the great commissure (gc, **Figure 2A**), which is only contained in one or two sections. Whereas we did not detect vacuole formation in 1-day-old *sws*^{1} flies (data not shown), a loss-of-function allele[35], some vacuoles were detectable in 7-day-old *sws*^{1} flies (arrowheads, **Figure 2A**). Aging

the flies to 14 days (**Figure 2B**) and 21 days (**Figure 2C**) further increased this phenotype, showing its progressive nature. Counting the number of vacuoles in the deutocerebral neuropil (dn) using the described method confirmed a significant increase in the number of vacuoles with age. Also, the combined area encompassed by vacuoles was significantly increased with aging (**Figure 2D**).

However, not all mutants show such a severe phenotype as *sws*, and in those cases, differences in degeneration are difficult to determine when focusing on a small area. Similarly, the degeneration that occurs during aging is quite mild (**Figure 3A-C**) and therefore, we analyzed the entire brain when quantifying this phenotype. Determining the sum of all vacuoles in the brain revealed a significant increase with age, and this was also the case when measuring the combined area of these vacuoles (**Figure 3D**).

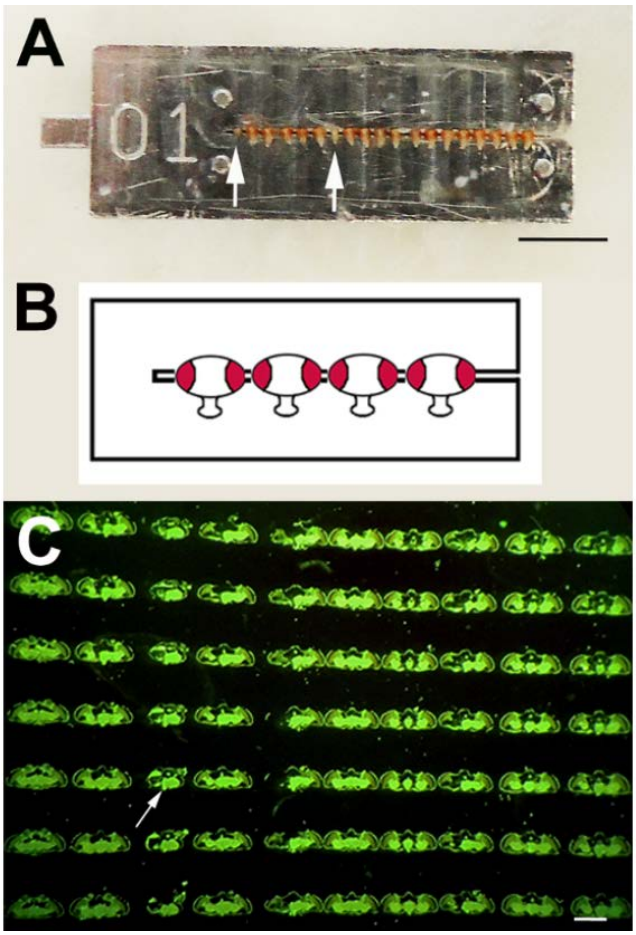

Figure 1. Paraffin serial sections.

A) Using the collar method, experimental and control flies can be processed as one sample by threading them onto one collar. Eyeless *sine oculis* flies are inserted for orientation (arrows). **B)** Schematic showing the orientation of the fly heads in the collar. **C)** In this image, sections from different fly heads are oriented left to right on the slide. From top to bottom on the slide, serial sections from the same fly head can be seen. In this case, a *sine oculis* fly was inserted at position three (arrow). The sections are stained by the fluorescent eye pigment that washes over the sections after cutting. Scale bar in A = 5 mm and in C = 0.5 mm.

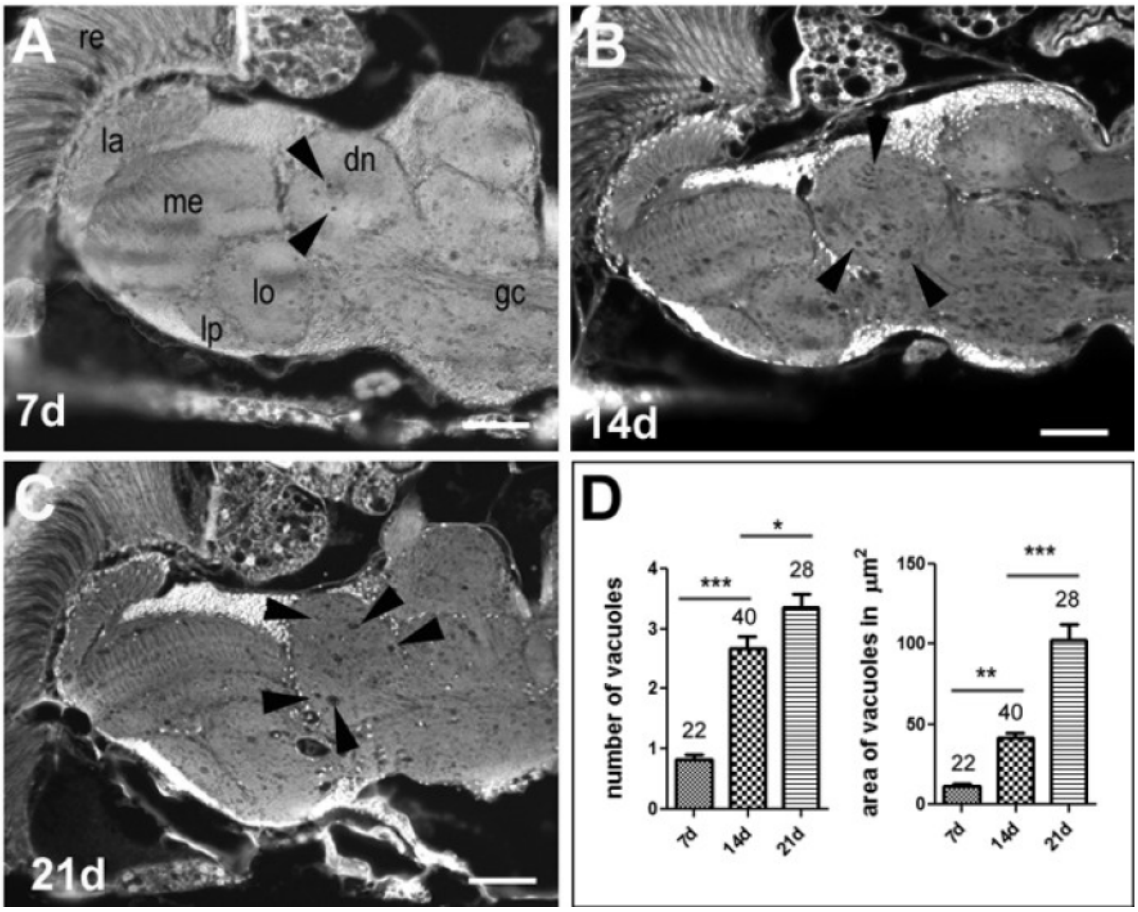

Figure 2. Progressive neurodegeneration in the *swiss-cheese* mutant.

Paraffin head section from 7-day- **(A)**, 14-day- **(B)** and 21-day- **(C)** old *sws*^{1} flies. The arrowheads point to vacuoles that have developed with aging. The age-related degeneration is quantified by counting the number of vacuoles and measuring their combined area **(D)**. The SEM and number of analyzed flies is indicated. The scale bar = 25 µm. ***p < 0.001.

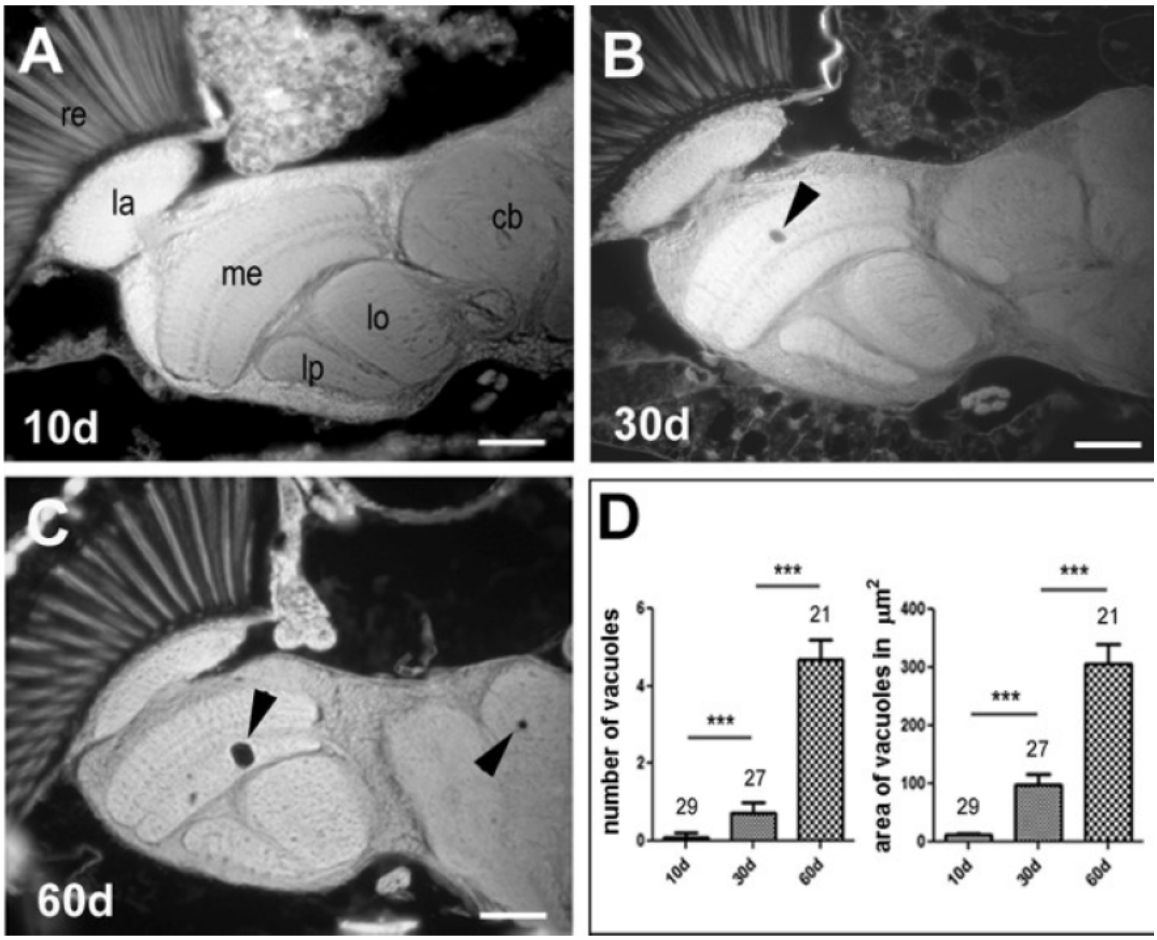

Figure 3. Neurodegeneration occurs with age.

Paraffin head section from 10-day- **(A)**, 30-day- **(B)** and 60-day- **(C)** old wild-type flies. The arrowheads point to vacuoles that have developed in aged flies. The age-related degeneration is quantified by counting the number of vacuoles and measuring their combined area **(D)**. The SEM and number of analyzed flies is indicated. The scale bar = 25 µm. ***p < 0.001.

Discussion:

The described method provides a means to quantify neurodegeneration in the brain of *Drosophila*. While other methods, like counting a specific cell type, can be used to identify neurodegeneration, the advantage of this method is that it can be applied more generally. Counting cells requires that these cells can be reliably identified using either a specific antibody or the expression of a cell-specific marker, which is not always available. Furthermore, it has been shown that dramatically different results can be obtained with that method[24], presumably due to the conditions used for labelling and for detection. Another method to detect degenerating cells is the use of cell death markers, like anti-activated caspase 3. However, this only identifies cells actively undergoing cell death, and after the cells have died, they are no longer detectable. Another advantage of the method proposed here is that no staining is required due to the autofluorescence caused by the eye pigment, which saves time and minimizes artifacts caused by changes in the staining conditions. It is important to note that, when using this method, the flies' eyes have enough pigment to stain the slide. If the eye color is too light, adding some wild-type flies to the collar would be advisable to ensure sufficient and even staining across the slide. An additional advantage of this method is that multiple areas can be examined, even in the same head. Although we do not show the data, we have used these sections to examine neurodegeneration in the retina and glial cell loss in the lamina cortex[30,36]. As described here, this method provides horizontal sections, but by turning the paraffin block by 90° when melting it onto the object holder, one can also obtain frontal sections. Thus, this method is a

versatile procedure that allows for the timely and efficient measurement of neurodegeneration in the fly brain. Because the formation of vacuoles has been observed in many fly models of human neurodegenerative diseases, including models for Alzheimer's disease, Parkinson's disease, amyotrophic lateral sclerosis, and diseases caused by polyglutamine-repeats[16,37-40], this method can be used to quantify neurodegenerative phenotypes in a variety of disease models.

Overall, this protocol is simple and easily completed once the initial setup of the equipment is carried out. Some notes to keep in mind are to carefully time the ethanol washes to avoid over-dehydration of the heads, to carefully trim the paraffin blocks so as not to lose sections or heads, and to not over-expand the ribbon on the water when the slide is on the heat block. If the ribbon is allowed to expand too far, tearing of the fly heads can result and the order of the heads in the ribbon can be lost. In addition, being blind to the genotype while doing the analyses is essential to avoid bias. This is best achieved by having one person preparing the slides and keeping the records while another person is taking the pictures and doing the measurements. One of the limitations of this method is that degeneration of only a few cells will be very difficult to detect. In that case, a specific stain of the affected cell population would be more informative. In addition, this method does not allow one to distinguish between different kinds of cell death, which requires more specific methods, such as a TUNEL staining to determine apoptotic cell death. Lastly, this method cannot differentiate between cell death and axonal degeneration, which would also be detectable as vacuoles in the neuropil.

As shown in our results, this method can be used to address degeneration in specific brain areas or in the entire brain. In our experience, it is useful to analyze only a specific area when the phenotype is quite strong, even when all brain regions are affected. This significantly reduces the work load and does not affect the outcome. We originally analyzed several areas in the *sws* mutant and observed very similar results in the progression of the phenotype when comparing only one area and when analyzing all areas (data not shown). However, it should be noted that a clearly-identifiable region should be chosen to avoid artifacts due to the analysis of different areas or areas at different levels.

In contrast, in cases where the phenotype is relatively mild, it is better to analyze the entire brain, because the likelihood of finding vacuoles in a specific region is low. For example, this is the case when determining age-related neurodegeneration, as shown in Figure 3, which results in only 4-5 vacuoles in the entire brain in 60-day-old flies. When counting vacuoles in the entire brain, one has to take into account that small vacuoles will only show up in one section, whereas larger ones will extend over several sections. Concerning the latter, the close proximity of adjacent sections when using this method (Figure 1) provides another advantage, because it is relatively easily to determine whether the same vacuole is present in several sections.

In conclusion, this protocol can prove useful for studying many *Drosophila* models of different neurodegenerative diseases. Identifying interacting proteins that ameliorate or aggravate the degenerative phenotype can provide crucial insights about the underlying mechanisms that cause or

modify diseases such as Alzheimer's and Parkinson's. In this publication, we use this method to detect degeneration that is progressive, where the animals develop normally but show increasing degeneration during aging. Additionally, this method can also be adapted to determine degeneration that is caused by developmental defects, which should already be present in newly-eclosed flies.

Acknowledgements:

This work was supported by grants to D.K. from the Medical Research Foundation of Oregon and from NIH/NINDS (NS047663). E.S. was supported by a training grant from the NIH (T32AG023477).

Disclosures:

The authors have nothing to disclose.

References:

1 Alexander, A. G., Marfil, V. & Li, C. Use of Caenorhabditis elegans as a model to study Alzheimer's disease and other neurodegenerative diseases. *Front Genet* **5**, 279, doi:10.3389/fgene.2014.00279 (2014).

2 Bonini, N. M. & Fortini, M. E. Human neurodegenerative disease modeling using *Drosophila*. *Annu Rev Neurosci* **26**, 627-656 (2003).

3 Calahorro, F. & Ruiz-Rubio, M. Caenorhabditis elegans as an experimental tool for the study of complex neurological diseases: Parkinson's disease, Alzheimer's disease and autism spectrum disorder. *Invert Neurosci* **11**, 73-83, doi:10.1007/s10158-011-0126-1 (2011).

4 Chen, X., Barclay, J. W., Burgoyne, R. D. & Morgan, A. Using C. elegans to discover therapeutic compounds for ageing-associated neurodegenerative diseases. **9**, 65, doi:10.1186/s13065-015-0143-y (2015).

5 Gama Sosa, M. A., De Gasperi, R. & Elder, G. A. Modeling human neurodegenerative diseases in transgenic systems. *Hum Genet* **131**, 535-563, doi:10.1007/s00439-011-1119-1 (2012).

6 Jaiswal, M., Sandoval, H., Zhang, K., Bayat, V. & Bellen, H. J. Probing mechanisms that underlie human neurodegenerative diseases in *Drosophila*. *Annu Rev Genet* **46**, 371-396, doi:10.1146/annurev-genet-110711-155456 (2012).

7 Konsolaki, M. Fruitful research: drug target discovery for neurodegenerative diseases in *Drosophila*. *Expert Opin Drug Discov* **8**, 1503-1513, doi:10.1517/17460441.2013.849691 (2013).

8 Kretzschmar, D. Neurodegenerative mutants in *Drosophila*: a means to identify genes and mechanisms involved in human diseases? *Invert Neurosci* **5**, 97-109, doi:10.1007/s10158-005-0005-8 (2005).

9 Kretzschmar, D. Swiss cheese et allii, some of the first neurodegenerative mutants isolated in *Drosophila*. *J Neurogenet* **23**, 34-41, doi:10.1080/01677060802471635 (2009).

10 Li, J. & Le, W. Modeling neurodegenerative diseases in Caenorhabditis elegans. *Exp Neurol* **250**, 94-103, doi:10.1016/j.expneurol.2013.09.024 (2013).

11 Prussing, K., Voigt, A. & Schulz, J. B. *Drosophila* melanogaster as a model organism for Alzheimer's disease. *Mol Neurodegener* **8**, 35, doi:10.1186/1750-1326-8-35 (2013).

12 Wentzell, J. & Kretzschmar, D. Alzheimer's disease and tauopathy studies in flies and worms. *Neurobiol Dis* **40**, 21-28 (2010).

13 Ali, Y. O., Escala, W., Ruan, K. & Zhai, R. G. Assaying locomotor, learning, and memory deficits in *Drosophila* models of neurodegeneration. *J Vis Exp*, doi:10.3791/2504 (2011).

14 Barone, M. C. & Bohmann, D. Assessing neurodegenerative phenotypes in *Drosophila* dopaminergic neurons by climbing assays and whole brain immunostaining. *J Vis Exp*, e50339, doi:10.3791/50339 (2013).

15 Dutta, S., Rieche, F., Eckl, N., Duch, C. & Kretzschmar, D. Glial expression of Swiss-cheese (SWS), the *Drosophila* orthologue of Neuropathy Target Esterase, is required for neuronal ensheathment and function. *Dis Model Mech*, doi:10.1242/dmm.022236 (2015).

16 Iijima, K. *et al.* Abeta42 mutants with different aggregation profiles induce distinct pathologies in *Drosophila*. *PLoS One* **3**, e1703 (2008).

17 Krishnan, N. *et al.* Loss of circadian clock accelerates aging in neurodegeneration-prone mutants. *Neurobiol Dis* **45**, 1129-1135, doi:10.1016/j.nbd.2011.12.034 (2012).

18 Liu, H. *et al.* Automated rapid iterative negative geotaxis assay and its use in a genetic screen for modifiers of Abeta(42)-induced locomotor decline in *Drosophila*. *Neurosci Bull* **31**, 541-549, doi:10.1007/s12264-014-1526-0 (2015).

19 Papanikolopoulou, K. & Skoulakis, E. M. Temporally distinct phosphorylations differentiate Tau-dependent learning deficits and premature mortality in *Drosophila*. *Hum Mol Genet* **24**, 2065-2077, doi:10.1093/hmg/ddu726 (2015).

20 Ping, Y. *et al.* Linking abeta42-induced hyperexcitability to neurodegeneration, learning and motor deficits, and a shorter lifespan in an Alzheimer's model. *PLoS Genet* **11**, e1005025, doi:10.1371/journal.pgen.1005025 (2015).

21 Sujkowski, A., Rainier, S., Fink, J. K. & Wessells, R. J. Delayed Induction of Human NTE (PNPLA6) Rescues Neurodegeneration and Mobility

Defects of *Drosophila* swiss cheese (sws) Mutants. *PLoS One* **10**, e0145356, doi:10.1371/journal.pone.0145356 (2015).

22 Barone, M. C., Sykiotis, G. P. & Bohmann, D. Genetic activation of Nrf2 signaling is sufficient to ameliorate neurodegenerative phenotypes in a *Drosophila* model of Parkinson's disease. *Dis Model Mech* **4**, 701-707, doi:10.1242/dmm.007575 (2011).

23 Coulom, H. & Birman, S. Chronic exposure to rotenone models sporadic Parkinson's disease in *Drosophila* melanogaster. *J Neurosci* **24**, 10993-10998, doi:10.1523/jneurosci.2993-04.2004 (2004).

24 Navarro, J. A. *et al.* Analysis of dopaminergic neuronal dysfunction in genetic and toxin-induced models of Parkinson's disease in *Drosophila*. *J Neurochem* **131**, 369-382, doi:10.1111/jnc.12818 (2014).

25 Heisenberg, M. & Böhl, K. in *Zeitschrift für Naturforschung C* Vol. 34 143 (1979).

26 Han, P. L., Meller, V. & Davis, R. L. The *Drosophila* brain revisited by enhancer detection. *J Neurobiol* **31**, 88-102, doi:10.1002/(SICI)1097-4695(199609)31:1<88::AID-NEU8>3.0.CO;2-B (1996).

27 Lin, C. W. *et al.* Automated in situ brain imaging for mapping the *Drosophila* connectome. *J Neurogenet* **29**, 157-168, doi:10.3109/01677063.2015.1078801 (2015).

28 Strausfeld, N. J., Sinakevitch, I. & Vilinsky, I. The mushroom bodies of *Drosophila* melanogaster: an immunocytological and golgi study of Kenyon

cell organization in the calyces and lobes. *Microsc Res Tech* **62**, 151-169, doi:10.1002/jemt.10368 (2003).

29 Bettencourt da Cruz, A., Wentzell, J. & Kretzschmar, D. Swiss Cheese, a protein involved in progressive neurodegeneration, acts as a noncanonical regulatory subunit for PKA-C3. *J Neurosci* **28**, 10885-10892, doi:10.1523/jneurosci.3015-08.2008 (2008).

30 Bolkan, B. J. & Kretzschmar, D. Loss of Tau results in defects in photoreceptor development and progressive neuronal degeneration in *Drosophila*. *Dev Neurobiol* **74**, 1210-1225, doi:10.1002/dneu.22199 (2014).

31 Cook, M., Mani, P., Wentzell, J. S. & Kretzschmar, D. Increased RhoA prenylation in the loechrig (loe) mutant leads to progressive neurodegeneration. *PLoS One* **7**, e44440, doi:10.1371/journal.pone.0044440 (2012).

32 Wittmann, C. W. *et al.* Tauopathy in *Drosophila*: neurodegeneration without neurofibrillary tangles. *Science* **293**, 711-714 (2001).

33 Rasmuson, B., Green, M. M. & Ewertson, G. QUALITATIVE AND QUANTITATIVE ANALYSES OF EYE PIGMENTS AND PTERIDINES IN BACK-MUTATIONS OF THE MUTANT wa IN *DROSOPHILA* MELANOGASTER. *Hereditas* **46**, 635-650, doi:10.1111/j.1601-5223.1960.tb03106.x (1960).

34 Bettencourt da Cruz, A. *et al.* Disruption of the MAP1B-related protein FUTSCH leads to changes in the neuronal cytoskeleton, axonal transport

defects, and progressive neurodegeneration in *Drosophila*. *Mol Biol Cell* **16**, 2433-2442 (2005).

35 Kretzschmar, D., Hasan, G., Sharma, S., Heisenberg, M. & Benzer, S. The swiss cheese mutant causes glial hyperwrapping and brain degeneration in *Drosophila*. *J Neurosci* **17**, 7425-7432. (1997).

36 Dutta, S., Rieche, F., Eckl, N., Duch, C. & Kretzschmar, D. Glial expression of Swiss cheese (SWS), the *Drosophila* orthologue of neuropathy target esterase (NTE), is required for neuronal ensheathment and function. *Dis Model Mech* **9**, 283-294, doi:10.1242/dmm.022236 (2016).

37 Davis, M. Y. *et al.* Glucocerebrosidase Deficiency in *Drosophila* Results in alpha-Synuclein-Independent Protein Aggregation and Neurodegeneration. *PLoS Genet* **12**, e1005944, doi:10.1371/journal.pgen.1005944 (2016).

38 Dias-Santagata, D., Fulga, T. A., Duttaroy, A. & Feany, M. B. Oxidative stress mediates tau-induced neurodegeneration in *Drosophila*. *J Clin Invest* **117**, 236-245, doi:10.1172/JCI28769 (2007).

39 Kretzschmar, D. *et al.* Glial and neuronal expression of polyglutamine proteins induce behavioral changes and aggregate formation in *Drosophila*. *Glia* **49**, 59-72, doi:10.1002/glia.20098 (2005).

40 Li, Y. *et al.* A *Drosophila* model for TDP-43 proteinopathy. *Proc Natl Acad Sci U S A* **107**, 3169-3174, doi:10.1073/pnas.0913602107 (2010).

NTE/PNPLA6 is expressed in mature Schwann cells and is required for glial ensheathment of Remak fibers

Janis McFerrin[1], Bruce L. Patton[1], Elizabeth R. Sunderhaus[1, 2], and Doris Kretzschmar[1, 2]

[1]Oregon Institute of Occupational Health Sciences, [2]Molecular and Medical Genetics, Oregon Health & Science University, 3181 SW Sam Jackson Park Road, Portland, OR 97239, USA

Running title: NTE/PNPLA6 function in Schwann cells

Corresponding author: Doris Kretzschmar, Oregon Institute of Occupational Health Sciences, 3181, Oregon Health & Science University, SW Sam Jackson Park Road, Portland, OR 97239, Tel: +1-503-494-0243; fax: +1-503-494-6831. E-mail kretzsch@ohsu.edu

**ERS contributed to this publication by conducting experiments to finish edits requested by the editors, in particular a Western on page 169, and providing edits to the written document.

Main Points

- NTE/PNPLA6 is expressed in Schwann cells in the sciatic nerve after the pro-myelin stage, and highly expressed in non-myelinating Schwann cells

-NTE/PNPLA6 expression is upregulated after axonal injury

-Loss of NTE/PNPLA6 causes incomplete glial ensheathment of Remak fibers

Key words: non-myelinating Schwann cells, neuropathy, spastic paraplegia, nerve injury, *Drosophila* SWS

Abstract

Neuropathy Target Esterase (NTE) or patatin-like phospholipase domain containing 6 (PNPLA6) was first linked with a neuropathy occurring after organophosphate poisoning and was later also found to cause complex syndromes when mutated, which can include mental retardation, spastic paraplegia, ataxia, and blindness. NTE/PNPLA6 is widely expressed in neurons but experiments with its *Drosophila* orthologue Swiss-Cheese (SWS) suggested that it may also have glial functions. Investigating whether NTE/PNPLA6 is expressed in glia, we found that NTE/PNPLA6 is expressed by Schwann cells in the sciatic nerve of adult mice with the most prominent expression in non-myelinating Schwann cells. Within Schwann cells, NTE/PNPLA6 is enriched at the Schmidt-Lanterman incisures and around the nucleus. When analyzing postnatal expression patterns, we did not detect NTE/PNPLA6 in promyelinating Schwann cells, while weak expression was detectable at post-natal day 5 in Schwann cells and increased with their maturation. Interestingly, NTE/PNPLA6 levels were upregulated after nerve crush and localized to ovoids forming along the nerve fibers. Using a GFAP-based knock-out of NTE/PNPLA6, we detected an incomplete ensheathment of Remak fibers whereas myelination did not appear to be affected. These results suggest that NTE/PNPLA6 is involved in the maturation of non-myelinating Schwann cells during development and de-/remyelination after neuronal injury. Since Schwann cells play an important role in maintaining axonal viability and function, it is therefore likely that changes in Schwann cells contribute to the locomotor deficits and neuropathy observed in patients carrying mutations in NTE.

Introduction

Neuropathy Target Esterase (NTE), also called patatin-like phospholipase domain containing 6 (PNPLA6) belongs to a family of phospholipases that are conserved from flies to humans (Lush et al., 1998). Mutations in NTE have been shown to cause a spectrum of diseases that include NTE-related motor neuron disorder or Spastic Paraplegia type 39, a condition that starts in childhood and is characterized by progressive weakness of the upper and lower limbs (Rainier et al. 2008). More recently isolated mutations have been associated with Boucher-Neuhäuser and Gordon-Holmes syndrome, complex disorders that can include hypogonadism, cerebellar atrophy, ataxia, and cognitive impairment (Deik et al. 2014; Synofzik et al. 2014a; Synofzik et al. 2014b; Topaloglu et al. 2014). Furthermore, NTE mutations can lead to Oliver-McFarlane and Laurence-Moon syndrome, which are characterized by retinal degeneration with choroidal atrophy, and in the case of Laurence-Moon syndrome also include progressive spinocerebellar ataxia and spastic paraplegia (Hufnagel et al. 2015; Kmoch et al. 2015). Locomotion problems and ataxia are also observed by environmentally induced changes in NTE activity caused by its interaction with organophosphates that are found in pesticides and nerve gases (Emerick et al. 2012; Glynn 2007; Pope et al. 1993). This phenomenon was first observed in the 1930s, when thousands of people were paralyzed after consuming a beverage (Jamaica Ginger) that contained the organophosphorus compound, tri-ortho-cresyl phosphate (TOCP) (Parascandola 1995). TOCP and other organophosphates bind to and interfere with the phospholipase activity of NTE, over time leading to a neuropathy

that was consequently named Organophosphate-Induced Delayed Neuropathy (OPIDN) (Johnson 1969).

Defects in motor coordination and neuronal degeneration are also detectable after the loss of NTE in the mouse brain (Akassoglou et al. 2004). A complete knock-out of NTE in mice is lethal around day 9 postcoitum with the embryos showing impaired vasculogenesis and placental defects (Moser et al. 2004). The earliest expression of NTE was found in the mesonephric duct followed by expression in the cranial and dorsal root ganglia (Moser et al. 2000). Around day 13 postcoitum, NTE mRNA is also detectable in the spinal ganglia, as well as the epithelium of the respiratory system and the gut. Postnatally, NTE is widely expressed in the brain but becomes more restricted with age, with prominent expression in large neurons in the cortex, olfactory bulb, thalamus, hypothalamus, pons, and medulla oblongata (Glynn et al. 1998; Moser et al. 2000). Similarly, the *Drosophila* ortholog of NTE, Swiss-Cheese (SWS), is expressed in most or all neurons in younger animals but becomes more restricted during aging (Muhlig-Versen et al. 2005). SWS shares the highly conserved phospholipase domain with NTE that also contains the organophosphate binding site (Glynn 2013; Muhlig-Versen et al. 2005; Quistad et al. 2003). As in vertebrates, organophosphate treatment of *Drosophila* induces neuronal degeneration and locomotion deficits and similar phenotypes occur in flies carrying mutations in SWS (Kretzschmar et al. 1997; Wentzell et al. 2014). In addition, the functional conservation of NTE and SWS was confirmed by the finding that expression of mouse NTE in sws mutant flies can completely restore the wild type phenotype (Muhlig-Versen et al. 2005).

In addition to neurons, SWS was found to be expressed in glia (Muhlig-Versen et al. 2005) and sws mutant flies showed defects in glial wrapping of neurons and glial cell death (Kretzschmar et al. 1997). A glial-specific knockdown approach revealed that SWS is required in ensheathing glia in flies (Dutta et al. 2016), a glial subtype that belongs to the neuropil glia which enwraps axons and that has therefore been described to be similar to oligodendrocytes in vertebrates (Freeman and Doherty 2006). In addition, glial-specific SWS knockdown flies showed severe locomotion deficits and changes in synaptic transmission (Dutta et al. 2016), revealing that the loss of SWS in glia impairs neuronal function and contributes to the behavioural phenotypes of the sws mutant. Although glial expression of NTE has not previously been described in vertebrates, NTE-activity has been detected in both mammalian neurons and glial cells (Glynn 2006; Glynn 2007). Furthermore, the glial phenotype in sws mutants and knockdown flies can also be rescued by the expression of mouse NTE (Dutta et al. 2015; Muhlig-Versen et al. 2005), further indicating that this protein family may serve evolutionarily conserved functions in glial cells. Here we demonstrate that NTE is expressed in Schwann cells within the sciatic nerves of mice, particularly in non-myelinating Schwann cells, and that its loss induces defects in the glial wrapping of Remak fibers.

Materials and Methods

ANIMALS

Mice were maintained and handled according to the guidelines established by the National Institutes of Health and approved by the Oregon Health and Science University's Institutional Animal Care and Use Committee. All mice were housed in PIV caging on a 12/12-hour light/dark cycle and provided with food and water ad libidum. C57BL/6J mice were used as wild type mice. NTEflox/flox mice were previously described by (Akassoglou et al. 2004) and kindly provided by M. Chao, Skirball Institute, New York University School of Medicine. Mice carrying Tamoxifen (TAM)-inducible GFAP-cre carrying mice were kindly provided by our colleague G. Mandel (Vollum Institute, OHSU) and are described in (Lioy et al. 2011). Both lines were backcrossed five generations to C57BL/6J before crossing them to obtain heterozygous Tam-GFAP-cre; NTEflox mice, which were then crossed with each other. The genotypes of the progeny were identified by PCR analyses of tail-tip DNA, using the following sense (-S) and antisense (-AS) primers: GFAP-cre-S: 5′-CCTGGAAAATGCTTCTGTCCG -3′; -AS: 5′-CAGGGTGTTATAAGCAATCCC -3′. NTE-S: 5′-GCTTAAGGGCACCTGCCAGC -3′; -AS: 5′-GGTCTTGTAGCCTGCAGTCC -3′. PCR was performed with an annealing temperature of 50°C with 35 cycles. Axonal injury was induced by repeated crushes of one sciatic nerve with forceps using anesthetized 4-6-week-old mice as described in (Patton et al. 1999) while the uninjured nerve was used as a matched control.

SCHWANN CELL CULTURES

Primary Schwann cell cultures were established from the sciatic nerves of neonatal C57BL/6J mice as described in (Sherman et al. 2000). Cells were initially grown on poly-l-lysine–coated tissue culture plastic (Sigma-Aldrich) in DMEM supplemented with 10% FBS, 5 ng/ml recombinant human (rh)-GGF2, and 2 µM forskolin (Calbiochem-Novabiochem), and then switched to a serum-free defined medium (N2) for an additional 24 h.

HISTOLOGY

For resin sections, animals were sacrificed and perfused with 3% (wt/vol) paraformaldehyde (PFA), 1% (vol/vol) glutaraldehyde, in PBS. Dissected nerves were then incubated overnight at 4°C in 4% PFA, 4% glutaraldehyde in 0.1 M cacodylate and 1-mm pieces were post-fixed 1 h in 1% OsO4, dehydrated through ethanol, and embedded in Epon. Semithin sections (1 µm) were stained with toluidine blue (1% in alcohol) and imaged by digital color photomicroscopy. Ultrathin sections (50 nm) were stained with uranyl acetate and analyzed using an FEI Tecnai G2 transmission electron microscope.

IMMUNOHISTOCHEMISTRY

Immunohistochemistry was performed as described in (Miner et al. 1997), using 8–10-µm cryostat sections cut from OCT-embedded unfixed tissue that had been snap frozen in 2-methylbutane at −150°C. Sections were fixed for 20 min in 2% PFA, incubated with 100 mM glycine in PBS for 10 min and blocked in PBS with 5% BSA and 0.5% Triton X-100. Primary antibodies were diluted in PBS containing

5% (wt/vol) BSA and applied overnight. Anti-peripherin (8G2) was obtained from Sigma and was used at 1:1000, anti-GFAP (AB5541) from EMD Millipore and was used at 1:500, anti-L1 from the Developmental Studies Hybridoma Bank (created by the NICHD of the NIH and maintained at The University of Iowa, Department of Biology, Iowa City) and was used at 1:200, anti-MAG from Santa Cruz Biotechnology (A11) and was used at 1:200, and anti-CD44 (5GA) was kindly provided by L. Sherman (OHSU) and used at 1:200 (Sleeman et al. 1996) and anti-MBP (EMD Millipore) was provided by F. Robinson (OHSU), and was used at 1:200. Rhodamine-Phalloidin was obtained from Thermo Fisher Scientific. A rabbit antiserum against NTE (Chang et al. 2005) was kindly provided by Y.J. Wu (Chinese Academy of Science, Beijing, China) and used at 1:500, while anti-NTE from Abcam (ab110391) was used at 1:200. Bound antibodies were then detected with the following species-specific fluorescent-labeled secondary antibodies (1 h incubation, used at 1:1000): FITC-conjugated anti-mouse (Boehringer Mannheim), FITC-conjugated anti-rat (EMD Millipore), and Cy3-conjugated anti-rabbit (Molecular Probes, Thermoscientific). DAPI (Sigma) was used to visualize nuclei.

ANALYZING MYELINATION AND GLIAL WRAPPING OF REMAK FIBERS

The g-ratio was determined on photographs of semithin sections stained with toluidine blue as a means of measuring myelin thickness. Quantification of the ensheathment of Remak fibers was performed on electron microscopic sections by determining the percentage of fibers that were not completely wrapped by glial sheaths in each Remak bundle. Statistics were conducted using GraphPad Prism and Student’s t-tests.

WESTERN BLOTS

Western Blots were performed as described in (Carmine-Simmen et al., 2009). 20 µg of protein was loaded on a 10% SDS gels and blotted onto PVDF transfer membranes (ThermoScientifc). Anti-NTE was used at 1:1000 and anti-GADPH (Sigma) at 1:2000 was used for a loading control. All antibodies were diluted in TBST supplemented with 5% milk powder and incubated overnight at 4ºC. Bands were visualized using horseradish peroxidase-conjugated secondary antibodies (Jackson ImmunoResearch) at 1:1000 at room temperature for 2 hours and the SuperSignal West Pico or Femto chemiluminiscent substrate (ThermoScientific).

Results

NTE IS EXPRESSED IN SCHWANN CELLS

Mutations in NTE cause a variety of symptoms, whereby locomotion deficits are the most common phenotype. Similarly, the delayed neuropathy caused by the inhibition of NTE by organophosphates is also characterized by movement problems, especially affecting the lower limbs. We therefore investigated whether NTE might play a role in the peripheral nervous system, particularly in Schwann cells, focusing on the sciatic nerve. Using an anti-NTE antisera kindly provided by Y-J. Wu (Chinese Academy of Science), we could readily detect NTE in immunolabeled frozen sections of sciatic nerves prepared from adult mice at post-natal day (PND) 42 (Fig. 1A, arrowheads). Notably, some of the immunostaining was detectable in close proximity to DAPI-positive nuclei (Fig. 1B), suggesting its expression in glial cell bodies. A similar pattern was also seen when using a commercially available anti-NTE (data not shown). To verify this observation, we

co-immunolabeled the sections with anti-GFAP, which is highly expressed by astrocytes in the CNS but is also expressed by non-myelinating and immature Schwann cells within the peripheral nervous system (Jessen and Mirsky 2005; Jessen et al. 1990). Although some cells were only positive for NTE (arrow in Fig. 1B), many of the NTE staining co-localized with this glial marker (arrowheads, Fig. 1A', B''). Since these sections were derived from adult animals, this pattern of immunoreactivity suggests that NTE is abundantly expressed by non-myelinating Schwann cells.

To verify this observation, we also co-immunolabeled sciatic nerve sections with anti-CD44 and antiperipherin. Whereas anti-peripherin is a marker for unmyelinated axons (Lariviere et al. 2002; Yuan et al. 2012), anti-CD44 labels non-myelinating Schwann cells in the adult sciatic nerve (Gorlewicz et al. 2009; Sherman et al. 2000). As shown in figure 2, NTE was detected in close proximity to peripherin (arrowheads, 2A-A'') and co-localized with CD44 (Fig. 2B-B''). The co-localization of NTE with CD44 was even more apparent at higher magnification (Fig. 2E, E' shows the cell indicated by the arrow in 2B). By analyzing sections from the tibial nerve, we again detected prominent expression of NTE in non-myelinating Schwann cells (white arrows, Fig. 2C) and weaker expression in the cytoplasm of myelinating Schwann cells, detectable as discontinuous rings (red arrowheads, Fig. 2C). Consistent with previous reports of NTE expression in neurons, we also found weak expression in axons (red arrows, Fig. 2C). Lastly, we confirmed the expression of NTE in Schwann cells by performing

immunohistochemistry with anti-NTE antibodies on cultured primary Schwann cells (Fig. 2D).

NTE IS ENRICHED AT SCHMIDT-LANTERMAN INCISURES

Schwann cells form distinct compartments along the axon, including the nodes of Ranvier, Cajal bands, and Schmidt-Lanterman incisures (Ghabriel and Allt 1979; Ghabriel and Allt 1980; Salzer 2003; Salzer et al. 2008; Ushiki and Ide 1987). To determine whether NTE is localized to any of these compartments, we prepared teased fibers from adult (PND42) sciatic nerves. Cajal bands and Schmidt-Lanterman incisures (SLIs) are cytoplasmic channels that are actin-rich (Gupta et al. 2012; Jung et al. 2011; Salzer 2003) and can therefore be stained with Phalloidin. As shown in figure 3, NTE co-localized with Phalloidin in SLIs (arrowheads, Fig. 3A, A', B, B') and it could be found in close proximity to nuclei (arrows, Fig. 3B, B''), consistent with findings in neurons that NTE localizes to the endoplasmic reticulum (Li et al. 2003). At higher magnification, weaker NTE staining could also be detected in Cajal bands (figure 3C, arrows). As described below (see Fig. 7A), we subsequently confirmed the enrichment of NTE in SLIs by co-labelling with another marker for this compartment, myelin-associated glycoprotein (MAG) (Trapp 1990).

NTE IS NOT EXPRESSED IN IMMATURE OR PROMYELINATING SCHWANN CELLS

Schwann cell precursors are produced from the neural crest and develop into immature Schwann cells during embryonic development, surrounding bundles of closely associated axons (Jessen and Mirsky 1997; Jessen and Mirsky 2005;

Monk et al. 2015; Woodhoo and Sommer 2008). Radial sorting of axons occurs around birth, whereby large diameter axons are separated by Schwann cells that differentiate and form myelin. The remaining small caliber axons are ensheathed in small groups by the differentiating non-myelinating Schwann cells, thereby forming the Remak bundles, a process that is completed around PND10. To investigate whether the expression of NTE is developmentally regulated and correlates with the differentiation of Schwann cells, we immunohistochemically stained sciatic nerve sections derived from different postnatal stages with anti-NTE. Sections were also co-stained with anti-L1, a cell adhesion molecule expressed in Schwann cell precursors, immature Schwann cells, and mature non-myelinating Schwann cells (Mirsky and Jessen 2009; Stewart et al. 1995). As shown in figure 4A, NTE was absent from early postnatal nerves (PND0), whereas weak immunopositive staining was detectable at PND5 (Fig. 4B, B'). At PND10, NTE was readily detectable in L1-positive cells (Fig. 4C, C'), correlating with the presence of mature non-myelinating Schwann cells. However, its levels were still lower than observed in the adult sciatic nerve. A similar result was obtained when co-staining sciatic nerves from PND0, PND5 and PND8 with peripherin (Supp. Fig. 1). Although the onset of NTE staining around PND5 suggested that it is not expressed in immature or promyelinating Schwann cells, we addressed this further by using antibodies against MAG and myelin basic protein (MBP), whose expression starts in the promyelination stage (Martini and Schachner 1986; Martini and Schachner 1997; Schachner and Bartsch 2000). As expected, both MAG and MBP were detectable at PND3, but we did not observe any NTE staining at this

age (Fig. 5A, Supp. Fig. 2A). Confirming our earlier studies, weak NTE expression was detectable at PND5 (Fig. 5B) and increased levels were detected at PND14, at which stage much of the NTE staining co-localized with MAG and MBP (Fig. 5C, Supp. Fig. 2B, C). These results confirm that NTE is not expressed in promyelinating Schwann cells but that it is expressed later during the maturation of myelinating and non-myelinating Schwann cells.

NTE IS UPREGULATED AFTER PERIPHERAL NERVE INJURY

Many proteins expressed during the development of Schwann cells (including L1, peripherin, and GFAP), are also induced after neuronal injury and axonal re-growth of peripheral nerves, a process that requires the de-differentiation and proliferation of Schwann cells (Berg et al. 2013; Jessen et al. 1990; Martini 1994; Neuberger and Cornbrooks 1989; Triolo et al. 2006). In addition, it has been shown that the SLIs play an important role in demyelination after injury and during Wallerian degeneration, due the fragmentation of myelin occurring adjacent to SLIs (Berger and Gupta 2006; Ghabriel and Allt 1979; Jung et al. 2011; Klein et al. 2014). We therefore investigated whether we could detect changes in the levels or localization of NTE after injury. Performing immunohistochemistry on sciatic nerves of adult mice harvested four days after unilateral crush lesions indeed revealed an upregulation of NTE as well as GFAP (Fig. 6A), compared to their expression levels in matched uninjured nerves (Fig. 6C). Eleven days after the injury, the levels of NTE begin to decrease, coinciding with the decrease in GFAP levels (Fig. 6E). Similarly, we detected an upregulation of NTE four days after injury in Western blots (Supp. Fig. 3). Our immunohistochemical analysis also revealed

a prominent ring-shaped pattern of staining (arrowheads in Fig. 6A, B), which though weaker, could still be detected after eleven days (Fig. 6E, F). To determine whether this pattern could be due to an upregulation of NTE in the SLIs, we again used teased fiber preparations from nerves obtained four days after crush. As noted above, we found that NTE was enriched in Schmidt-Lanterman incisures in uninjured control fibers, where it colocalized with MAG (Fig. 7A). In contrast, NTE expression was widespread along the damaged fibers, localizing to ovoids (arrowheads, Fig. 7B). Co-staining these preparations with MAG suggested that most of the NTE staining does not co-localize with MAG (arrows, Fig. 7B). At a higher magnification, we could detect MAG staining adjacent to both sides of weakly stained NTE-positive ovoids (Fig. 7C, green arrows). In the case of the ovoid with higher NTE expression levels, NTE and MAG co-localized at the margins of the ovoid (Fig. 7C, white arrows), whereas MAG is absent in the case of the ovoid with the highest NTE expression levels (Fig. 7C, arrowhead). Together, these results reveal that NTE changes it subcellular localization after injury and shows a dynamic co-localization pattern with MAG.

THE CONDITIONAL GLIAL KNOCK-OUT OF NTE RESULTS IN INCOMPLETE WRAPPING OF REMAK FIBERS

The expression of NTE during early postnatal stages and its induction after nerve injury suggest that NTE may play a role in the maturation of Schwann cells. As mentioned above, a complete knock-out of NTE is lethal during embryonic development (Moser et al. 2004), while a nestin-cre mediated conditional knock-out of NTE has been shown to result in neuronal degeneration in the CNS

(Akassoglou et al. 2004). To specifically assess the glial function of NTE, we crossed Tamoxifen (TAM)-inducible GFAP-cre carrying mice (Lioy et al. 2011) with NTE-flox mice (Akassoglou et al. 2004). Due to GFAP being expressed in non-myelinating and immature Schwann cells (Jessen and Mirsky 2005; Jessen et al. 1990) and our evidence that NTE co-localizes with GFAP in Schwann cells (Fig. 1), this strategy should specifically delete NTE in peripheral glia. GFAP-cre was induced by daily neonatal administration of TAM through maternal lactation starting at PND0 for three weeks. Performing sciatic nerve sections at PND14 from the conditional knock-out animals revealed a strong downregulation of NTE levels in the NTE(fl/fl);Cre+ mice (Fig. 8B, D) when compared to their TAM-treated NTE(+/+);Cre+ siblings (Fig. 8A, C). As expected, the levels of GFAP (Fig. 8A, B) and CD44 (Fig. 8C, D) were not altered in the conditional NTE knock-out.

Next, we analyzed sciatic nerve sections from four-month-old conditional knock-out mice at the light and electron microscopic level to determine whether these mice show defects in myelination or Remak bundle formation. A comparison of toluidine-blue-stained sections from TAM-treated NTE(fl/fl);Cre+ mice (Fig. 9A) with treated NTE(+/+);Cre+ siblings (Fig. 9B) did not reveal defects in myelination, nor was the g-ratio significantly different (Fig. 9C). Furthermore, we did not detect defects in myelination in electron microscopic images (data not shown). Together, this result suggests that the conditional knock-out of NTE had no consequences for the differentiation of myelinating Schwann cells. In contrast, we did observe effects on non-myelinating Schwann cells in our electron microscopic studies. Whereas the Remak fibers in four-month-old control mice (TAM treated

NTE(+/+);Cre+ siblings) were almost always completely ensheathed by non-myelinating Schwann cells (Fig. 10A, C), many of these fibers were incompletely wrapped in TAM-treated NTE(fl/fl);Cre+ animals (arrowheads, Fig. 10B, D). In addition, some of the axons in the conditional knock-out animals looked shrunken and more electron dense, indicating that these fibers were undergoing degeneration (arrows, Fig. 10B, D). Quantifying this glial wrapping phenotype by determining the percentage of incompletely wrapped axons in a Remak bundle, we found that on average, 12% of axons showed mostly small gaps in their glial sheaths in NTE(+/+), whereas this number increased to 55% in the conditional knock-out animals (Fig. 10E). This result shows that the loss of NTE does affect the maturation of non-myelinating Schwann cells and the formation of Remak bundles, corresponding to the higher expression levels of NTE in this Schwann cell population.

DISCUSSION

NTE was previously shown to be expressed in neurons (Glynn et al. 1998; Moser et al. 2000), but experiments with cultured astrocytes suggested that its activity is also present in glia (Glynn 2007; Glynn 2012). A role for NTE in glia was also suggested from studies in *Drosophila*, which demonstrated the presence of SWS (the fly orthologue of NTE) in CNS glia and showed that expression of mouse NTE in *Drosophila* glia could rescue the glial defects seen in sws mutant flies (Muhlig-Versen et al. 2005). Focusing on the sciatic nerve, we verified that NTE is present in axons, but we could also detect its expression in Schwann cells. The levels of NTE were highest in non-myelinated Schwann cells, although lower levels

could be detected in myelinating Schwann cells, with an enrichment at Schmidt-Lanterman incisures and around the nucleus. The latter observation is in agreement with the localization of NTE to the endoplasmic reticulum, as has been described in neurons (Li et al. 2003; Zaccheo et al. 2004). Furthermore, NTE expression was detectable in primary Schwann cell cultures lacking neurons.

By analyzing the developmental profile of NTE expression, we found that it was absent during early postnatal stages of Schwann cell differentiation. Around birth, the peripheral nerves go through a stage of axonal sorting, in which immature Schwann cells either associate with large axons and differentiate into mature myelinating Schwann cells or with the small Remak fibers, which are enwrapped by Schwann cells but are not myelinated (Feltri et al. 2015; Kaplan et al. 2009). This process requires a close interaction between neurons and Schwann cells and is regulated by several signaling pathways, including axonal signaling via Neuregulin 1 and ErbB receptors, as well as extracellular matrix signaling via laminin and β1 integrin and dystroglycan receptors (Berti et al. 2011; Birchmeier and Nave 2008; Monk et al. 2015; Nave and Salzer 2006; Newbern and Birchmeier 2010; Taveggia et al. 2005; Woodhoo and Sommer 2008). After this sorting phase, the Schwann cells differentiate into mature cells that form myelin sheaths (around large axons) or enwrap Remak fibers, which also requires signaling between the axons and glial populations (Fricker et al. 2009; Raphael et al. 2011; Yu et al. 2009). NTE was not detectable at PND0 and its levels were still quite low at PND5, suggesting that it is not expressed in immature or promyelinating Schwann cells. This was confirmed by co-immunolabeling with anti-MAG and anti BMP. In

contrast, NTE levels increased a few days after birth (PND8), suggesting a role late in Schwann cell maturation. When we examined GFAP-Cre mediated conditional NTE knock-out animals, we could not detect effects on axonal sorting or myelination, indicating that NTE is not required for the differentiation of myelinating Schwann cells. However, we did find that non-myelinating Schwann cells failed to completely enwrap Remak fibers, which correlated with the higher expression levels in these cells, showing that NTE is required for the maturation of non-myelinating Schwann cells.

Inhibition of NTE by organophosphates induces a neuropathy that shows the characteristic signs of Wallerian degeneration (Abou-Donia 2003; Dyer et al. 1992; Emerick et al. 2012). We therefore also investigated whether we could detect changes in NTE after neuronal injury caused by nerve crush. Indeed, we found not only an increase in NTE levels following injury but also a strong accumulation of NTE in ovoids distributed along the fibers. Surprisingly, it appeared that NTE was excluded from the SLIs after injury, although it was enriched in SLIs in uninjured fibers and SLIs have been shown to play an important role in demyelination responses after injury or disease (Jung et al. 2011; Klein et al. 2014). During Wallerian degeneration, the myelin sheath becomes fragmented and forms ovoids similar to the ones we observed with NTE immunolabeling, a process that occurs near the SLIs (Ghabriel and Allt 1979; Jung et al. 2011). The similarity of the NTE-positive ovoids with the ovoids observed during myelin fragmentation indicates that NTE may play a role in demyelination responses after injury. NTE is a phospholipase that hydrolyzes phosphatidylcholine and lysophosphatidylcholine

(LPC) by degrading it to glycerophosphocholine (Quistad et al. 2003; van Tienhoven et al. 2002). Of note is that LPC synthesis is also upregulated after injury and is a well-known demyelinating agent (Ghasemlou et al. 2007; Velasco et al. 2016). It is therefore possible that NTE plays a role in the changes that occur in Schwann cell membranes during demyelination and/or remyelination.

Problems with motor coordination and paralysis are prominent symptoms of NTE-related diseases. Likewise, a nestin-Cre induced NTE knock-out resulted in hindlimb dysfunction and behavioral deficits in Rotarod tests (Akassoglou et al. 2004; Read et al. 2009). However, due to Nestin being expressed in the early development of the peripheral and central nervous system (Michalczyk and Ziman 2005), these experiments did not distinguish the roles of NTE in the CNS versus the PNS, nor did they discriminate between its potential functions in glia versus neurons. Although the loss of neuronal NTE most likely contributes to disease progression, the maintenance of axonal viability is strongly dependent on their associated glial cell partners, and defects in Schwann cells have been shown to cause peripheral neuropathies like Charcot-Marie-Tooth (Berger et al. 2006). In addition, our previous studies in *Drosophila* showed that a glial-specific knockdown not only caused incomplete glial wrapping of axons but also induced severe locomotion defects and changes in neuronal function (Dutta et al. 2015), suggesting that glial loss of NTE contributes to the pathogenesis of NTE-related diseases. Lastly, given the role of disrupted Remak bundles in neuropathic pain (Koltzenburg and Scadding 2001), the defects in Remak bundle formation that we detected in the conditional knock-out mice indicates that NTE could also play a

role in the neuropathic pain responses that can accompany peripheral neuropathies.

ACKNOWLEDGEMENT

Thanks are due to the OHSU imaging facility, which was supported by the NIH P30NS061800 grant and provided support for the electron microscopic studies. We are also grateful for valuable input from Fred Robinson and Charles Allen, both OHSU. This work was supported by a grant (NS047663) to D.K. from the National Institute of Health.

FIGURES

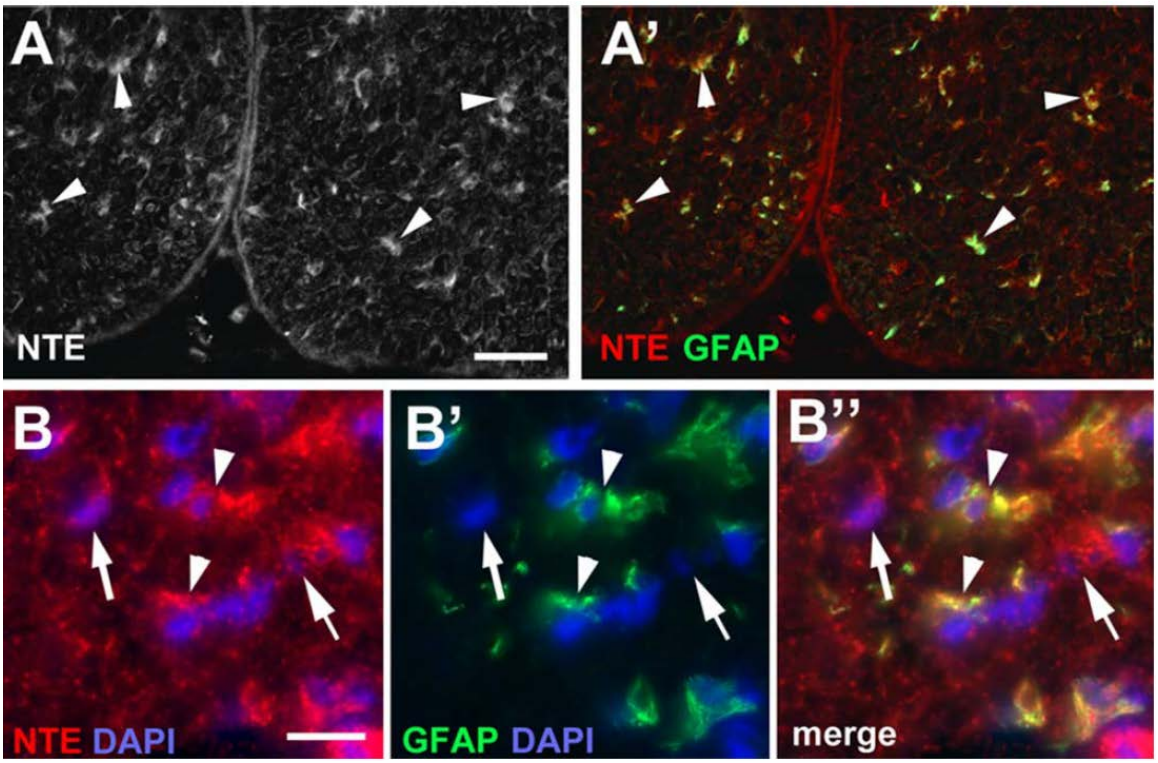

Figure 1: NTE is detectable in glia in the adult (PND42) sciatic nerve. (A) Using anti-NTE, immunopositive staining is found in the sciatic nerve (arrowheads) and co-localizes with GFAP (A'). (B-B'') NTE is detectable in the cell cytoplasm of GFAP-positive cells (arrowheads) and in some non-GFAP positive cells (arrows). NTE is shown in red, GFAP in green, and DAPI in blue. Scale bar in A=30 µm, in B=10 µm.

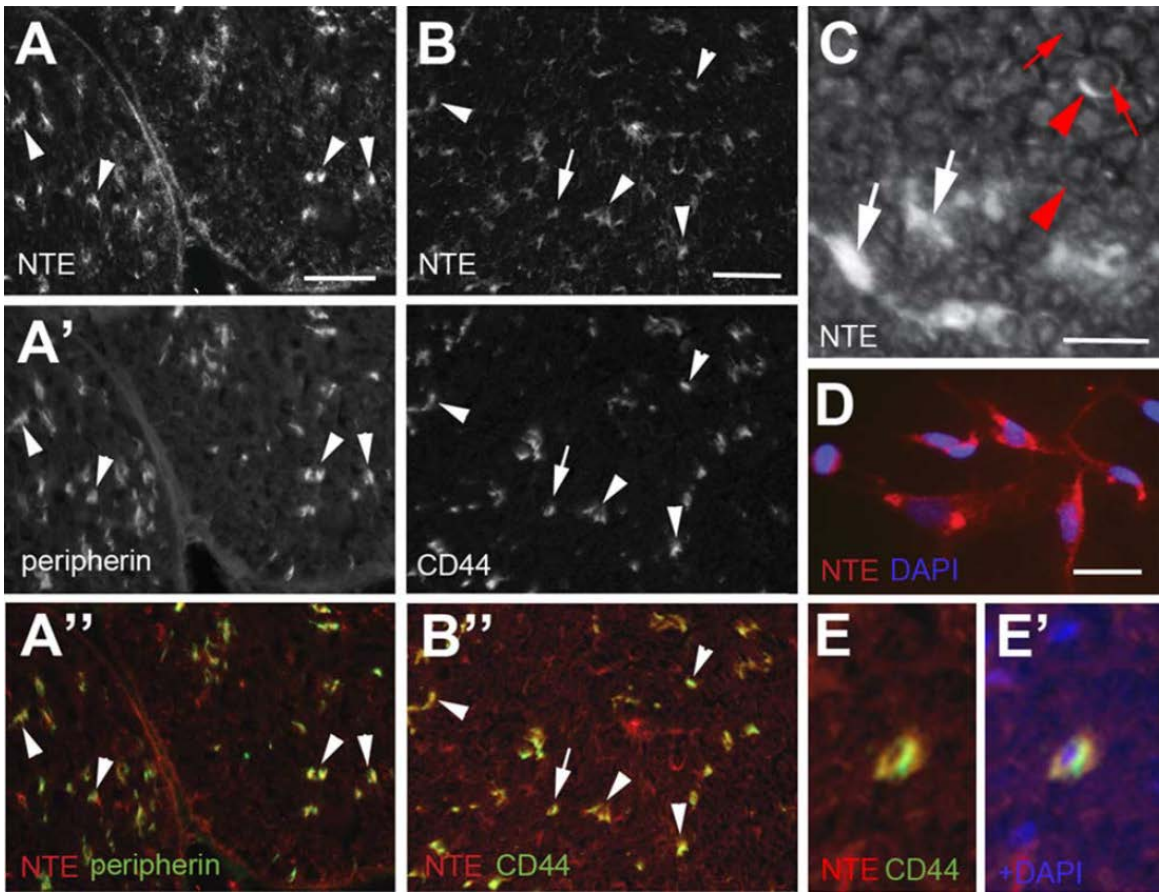

Figure 2: NTE is highly expressed in non-myelinating Schwann cells. (A-A'') NTE is found in close proximity to peripherin (arrowheads), a marker for unmyelinated axons. (B-B'') NTE also co-localizes with CD44, which is expressed in adult non-myelinating Schwann cells. (C) In tibial nerve sections, strong staining is found in non-myelinating Schwann cells (white arrows) while weaker staining can be detected in axons (red arrows) and in the cytoplasm of myelinating Schwann cells (red arrowheads). (D) NTE is expressed in cultured Schwann cells. (E, E') Higher magnification view showing co-localization of NTE and CD44 in the neuron labeled with an arrow in B. NTE is shown in red, peripherin and CD44 in green and DAPI in blue. Sections were derived from mice at PND42. Scale bar in A, B=50 µm, in C, D=10 µm.

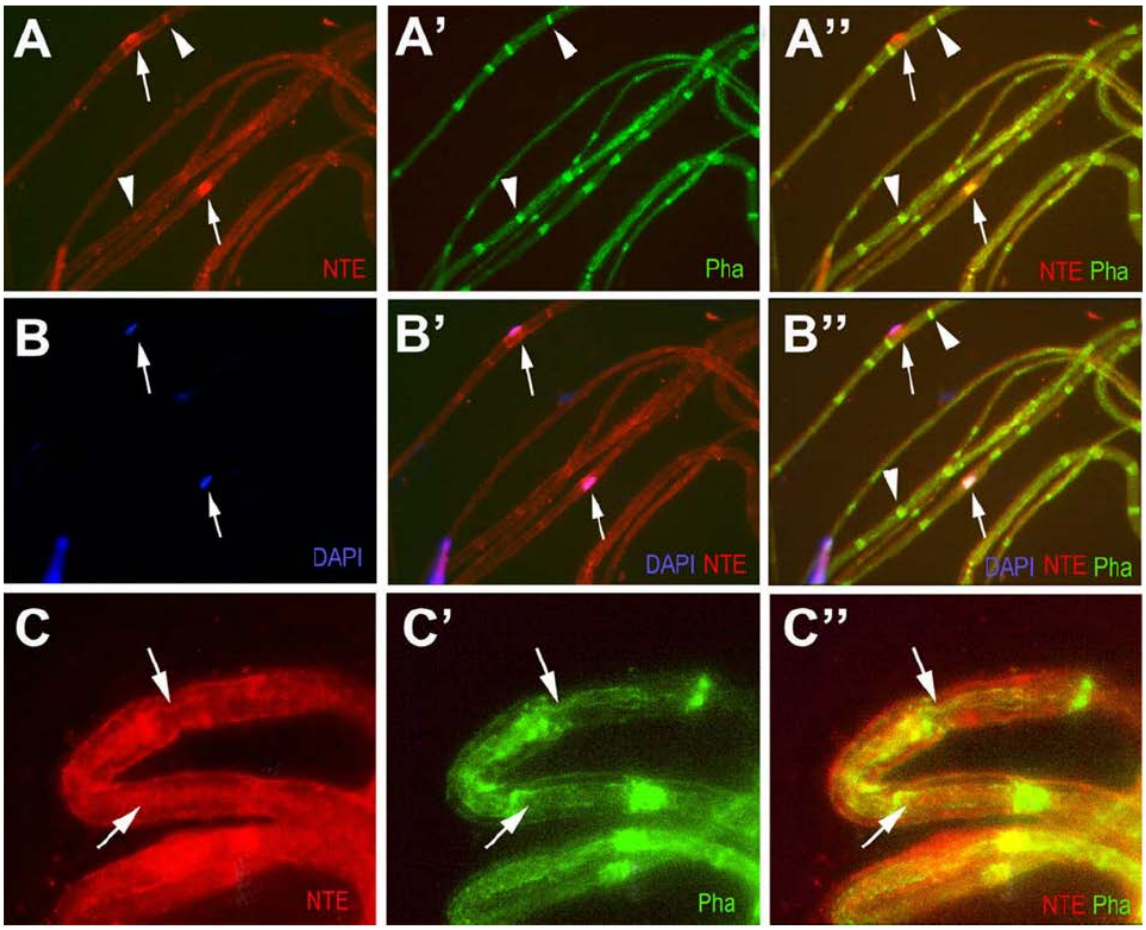

Figure 3: NTE is enriched in Schmidt-Lanterman incisures and around the nucleus. (A-A'') NTE co-localizes with Phalloidin (Pha) in Schmidt-Lanterman incisures (arrowheads). (B-B'') Higher levels of NTE can also be found adjacent to nuclei labeled by DAPI (arrows). (C-C'') Higher magnification view showing co-localization of NTE and Phalloidin in Cajal bands (arrows). NTE in red, Phalloidin in green and DAPI in blue. Teased fibers were obtained at PND42.

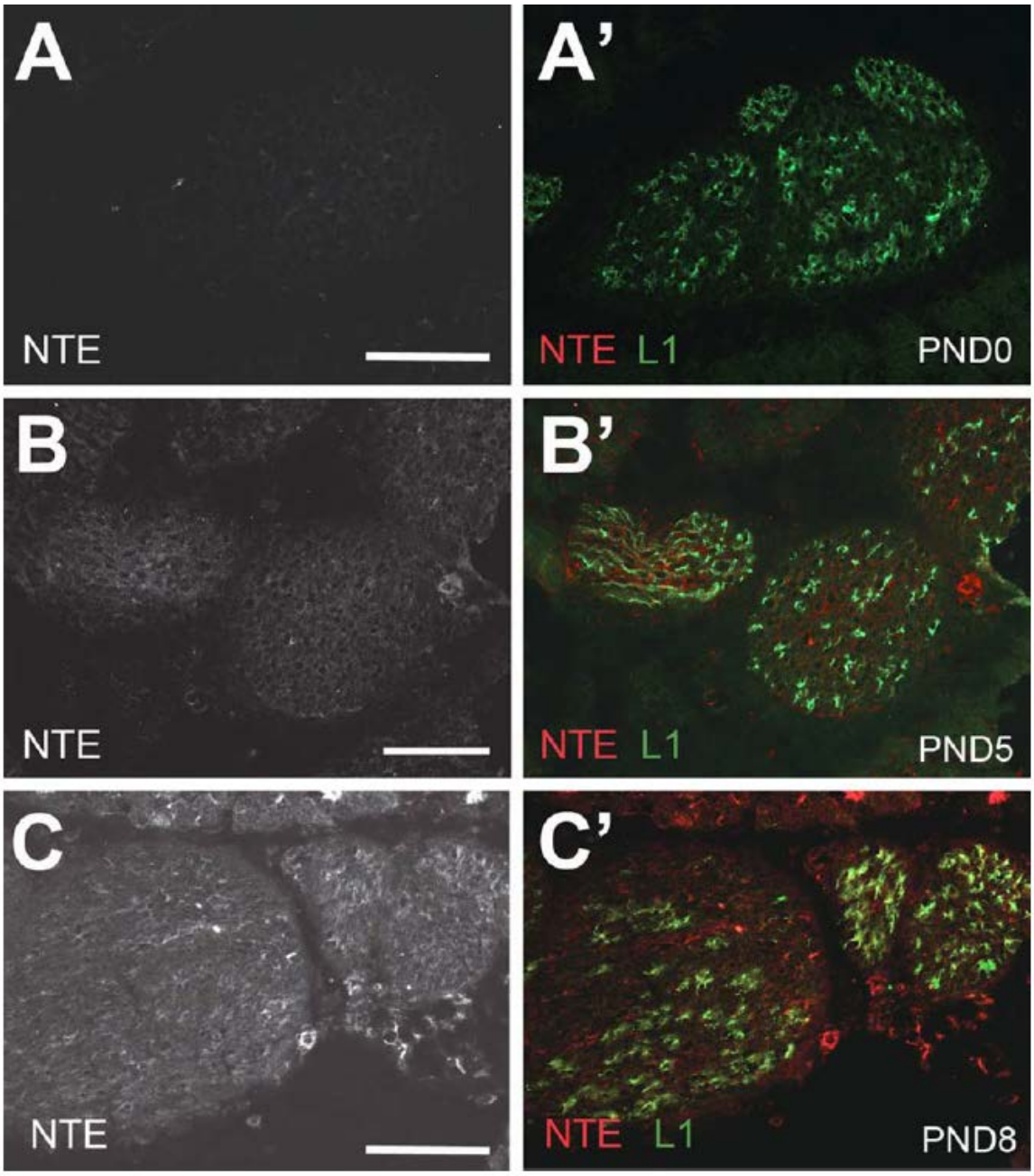

Figure 4: Developmental expression pattern of NTE. (A, A') At PND0, NTE is not detectable in the sciatic nerve. (B, B') NTE is first apparent at PND5 and its level increase with further aging (C, C', PND8), whereas L1 is detectable at all ages. L1 in green, NTE in red. Scale bar=100 µm.

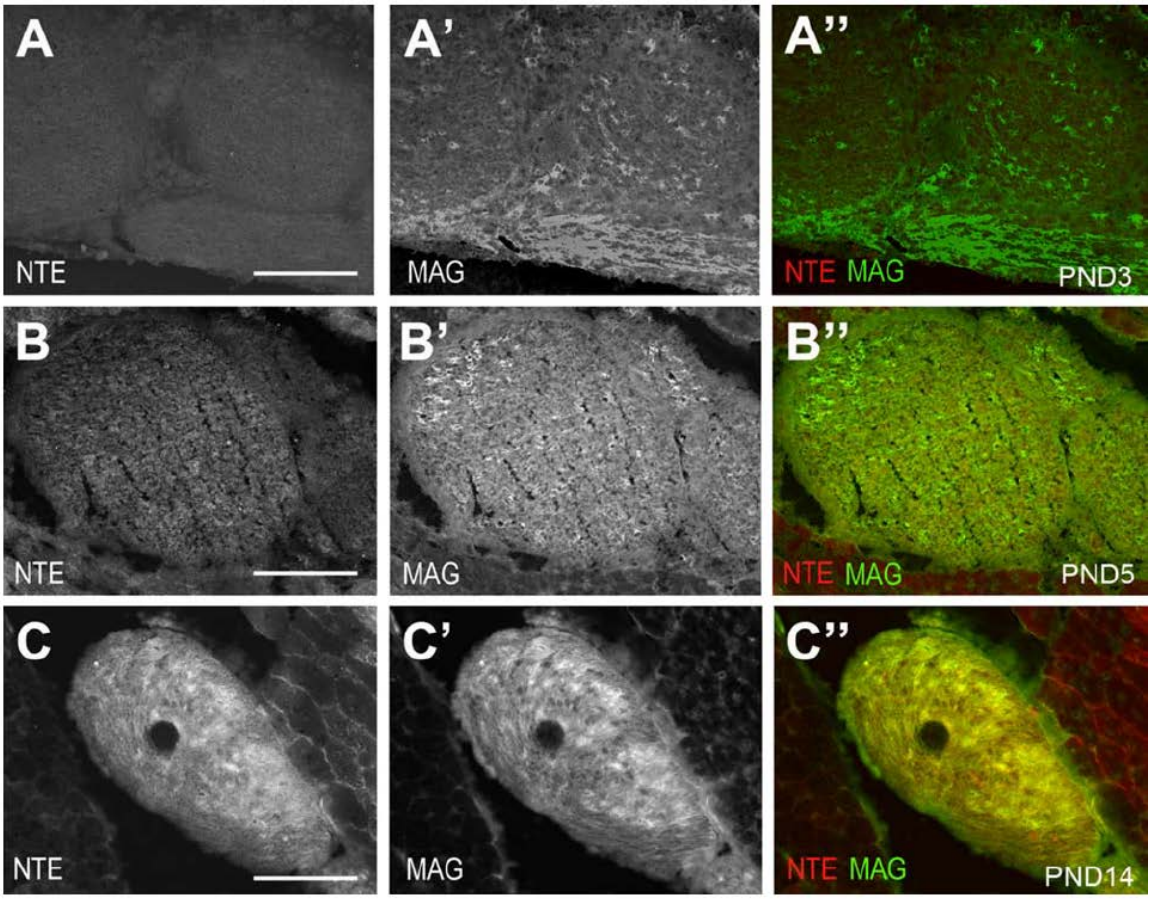

Figure 5: NTE is not expressed in immature or promyelinating Schwann cells. (A-A'') At PND0, some cells are MAG-positive in the sciatic nerve whereas NTE is not detectable. NTE is detectable at PND5 (B-B'') and PND14 (C-C''), together with MAG. MAG in green, NTE in red. Scale bar=100, µm.

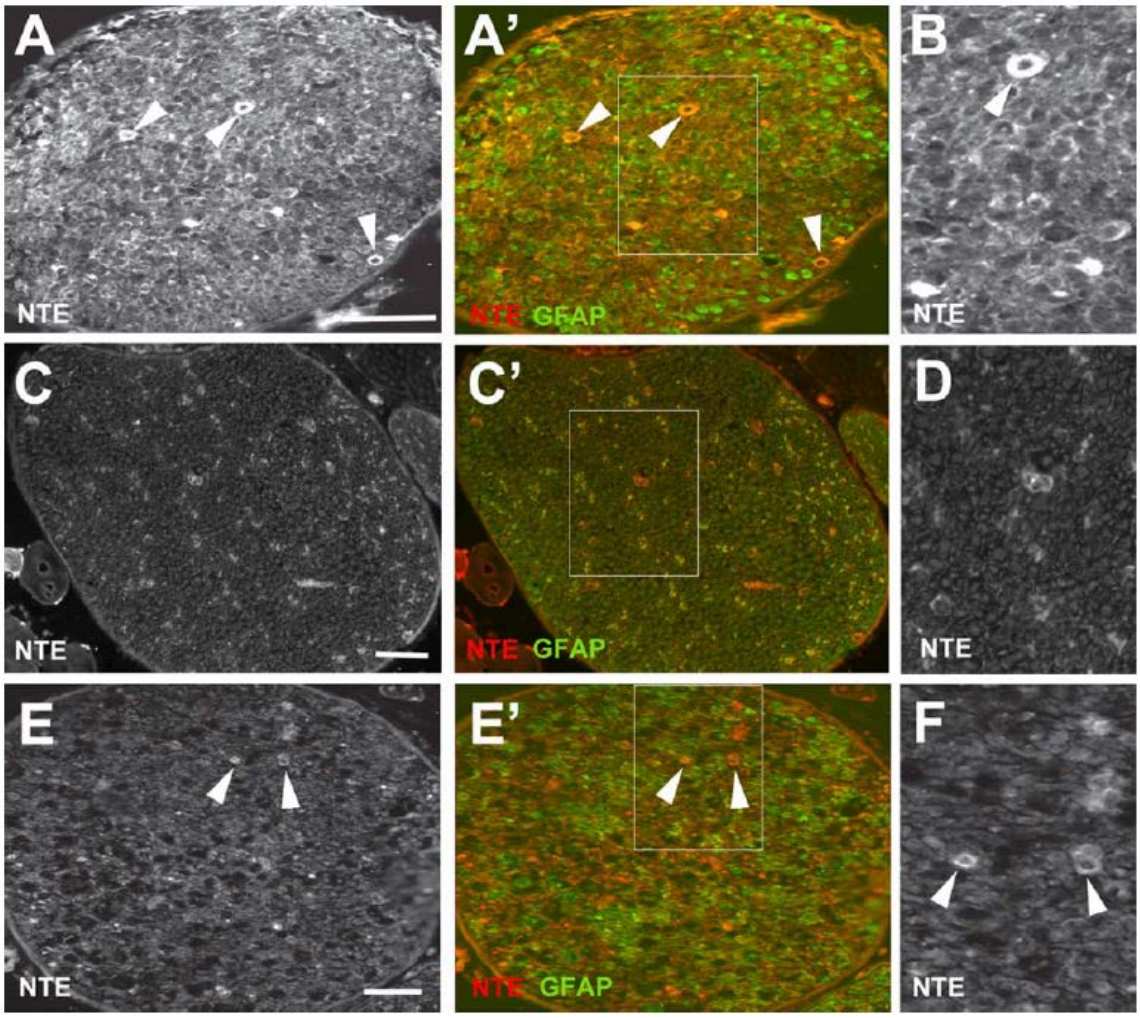

Figure 6: NTE is upregulated after axotomy. (A, A') 4d after nerve crush, NTE levels are increased in the nerve with strong staining detectable in some ring-shaped structures (arrowheads). (B) Magnified view of the boxed region in A'. (C, C') NTE staining in the uninjured sciatic nerve 4d after nerve crush. (D) Magnified view of the boxed region in C'. (E, E') 11d after nerve injury, an increase in NTE levels is still detectable, including in the ring-shaped structures (arrowheads) but the NTE levels have decreased compared to 4d post-injury. (F) Magnified view of the boxed region in E'.NTE in red, GFAP in green. The nerve crush was performed at PND28. Scale bar=50 µm.

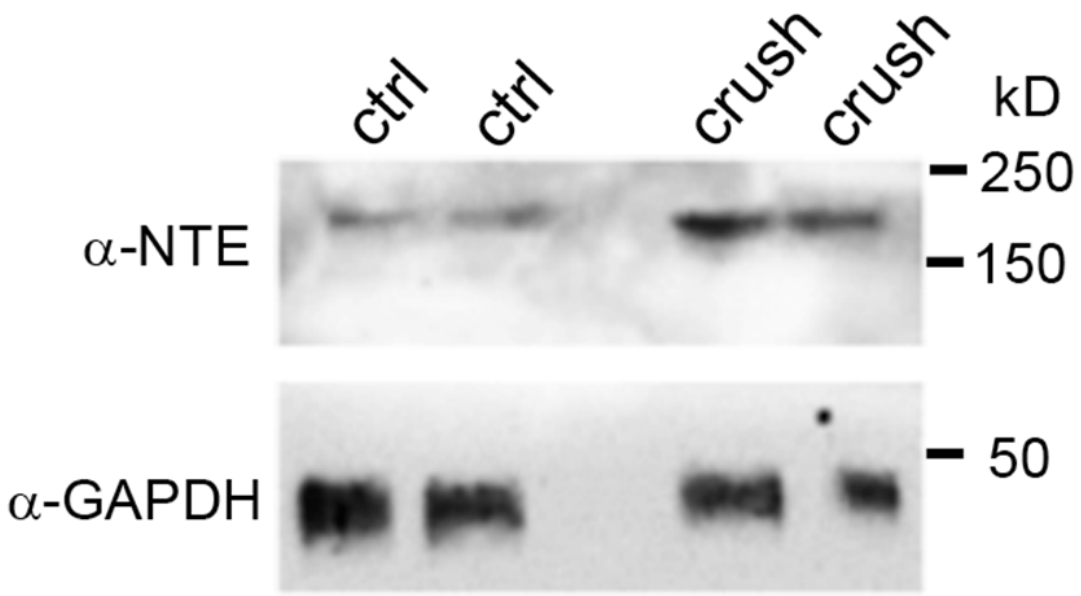

Supplementary Figure 3: NTE is upregulated after nerve crush. Western blot showing that NTE levels are increased after nerve crush (crush) compared to the control (ctrl). Anti-GADPH was used as a loading control.

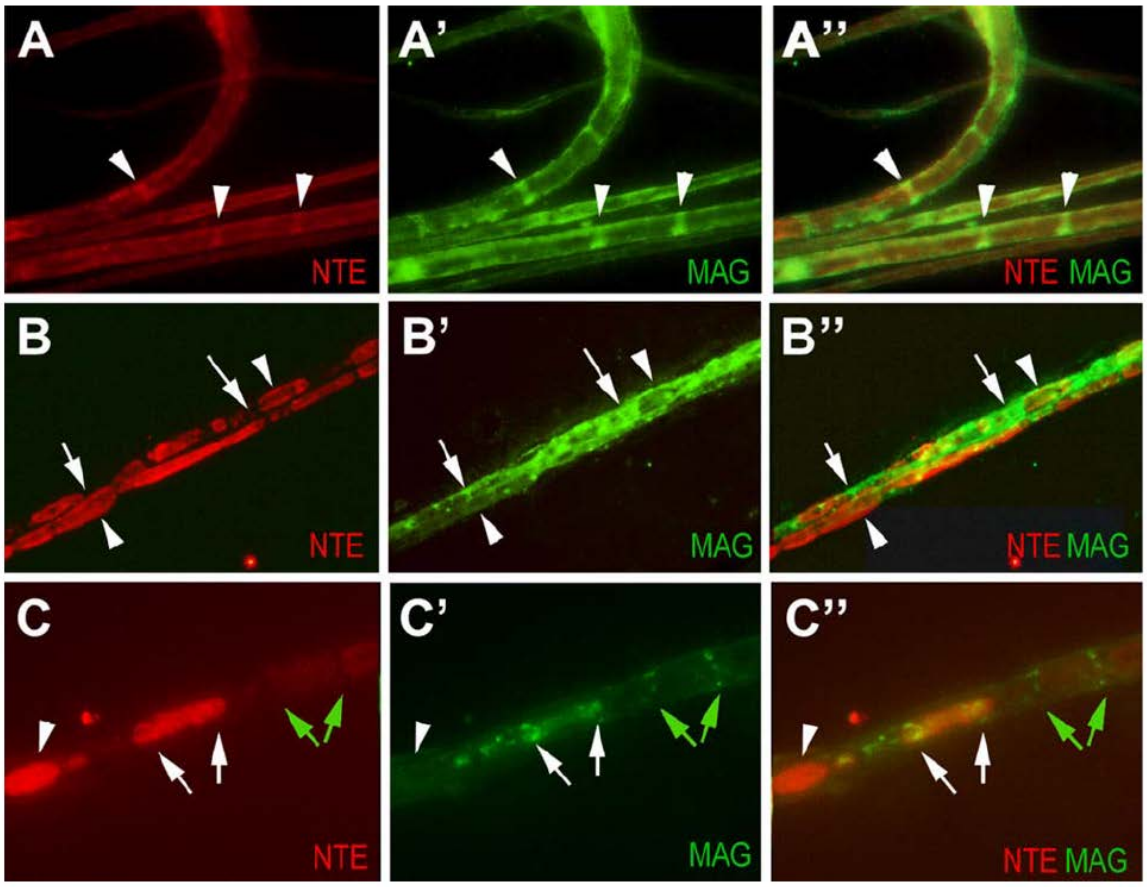

Figure 7: NTE staining is found in ovoids along the nerve after injury. (A-A'') NTE is enriched in Schmidt-Lanterman incisures (arrowheads), co-localizing with MAG in the uninjured nerve. (B-B''). On the crushed side, strong NTE staining is detectable in ovoids along the nerve (arrowheads). NTE staining only co-localize with MAG (arrows) at the margins of ovoids. (C-C'') Magnification showing that MAG-positive incisures are adjacent to weakly stained NTE-positive ovoids (green arrows). Another ovoid that contains higher levels of NTE shows MAG-positive staining at the distal and proximal end of the ovoid (white arrows). The ovoid with the highest levels of NTE does not co-stain for MAG, nor is it delimited by MAG staining (arrowhead). The crush was performed at PND42. NTE in red, MAG in green.

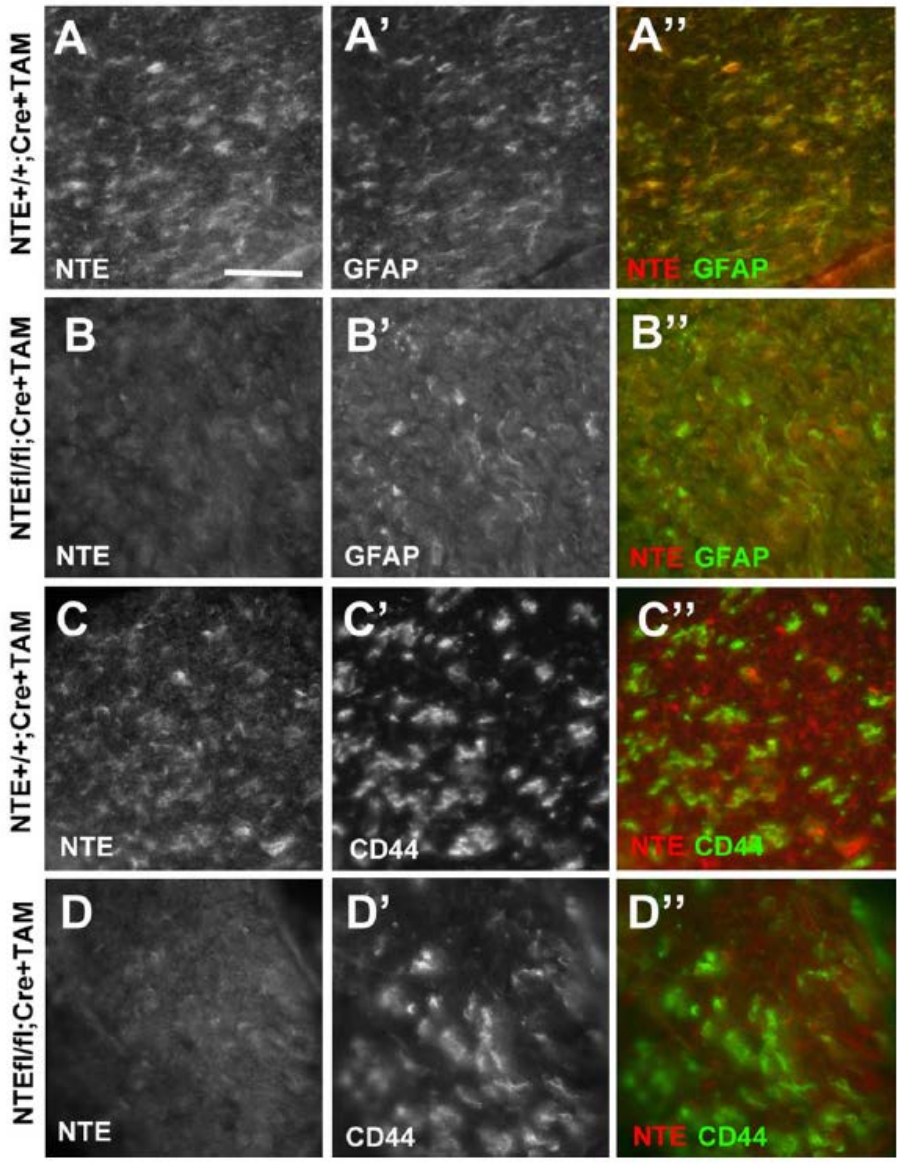

Figure 8: The conditional knock-out reduces NTE levels. NTE levels are reduced in sciatic nerves of NTE(fl/fl);Cre+ mice (B, D) compared to their NTE(+/+);Cre+ siblings (A, C). The levels of the Schwann cell markers GFAP (A, B) and CD44 (C, D) are not affected by the conditional NTE knock-out. Sections were obtained at PND14. All animals were treated with TAM. NTE in red, GFAP and CD44 in green. Scale bar=30µm.

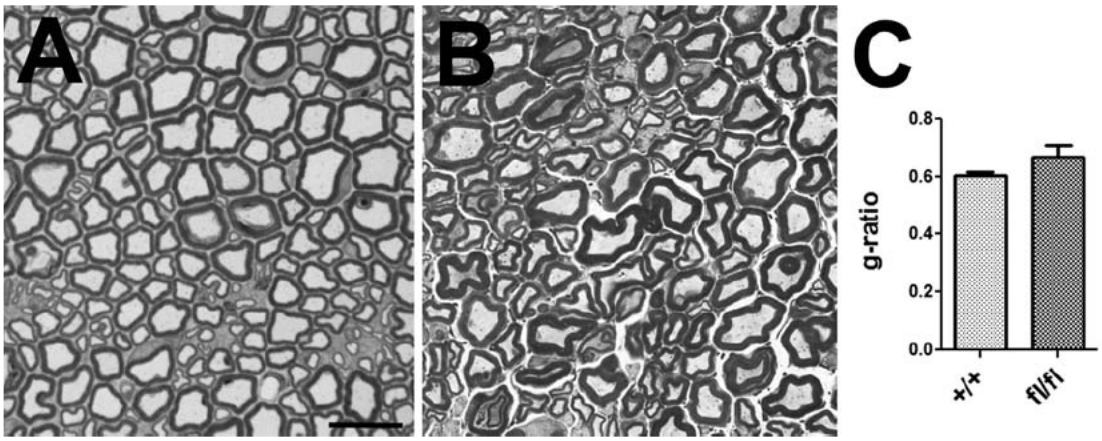

Figure 9: Glial loss of NTE does not affect myelination. Toluidine-blue stained sciatic nerve sections from TAM treated NTE(+/+);Cre+ (A) and NTE(fl/fl);Cre+ mice (B). (C) Determining the g-ratio did not reveal a significant difference between the conditional knock-out animals and controls. Two mice were used per genotype. 200 axons from each genotype were analyzed in C. Histogram represents means ± SEM. Scale bar=5µm.

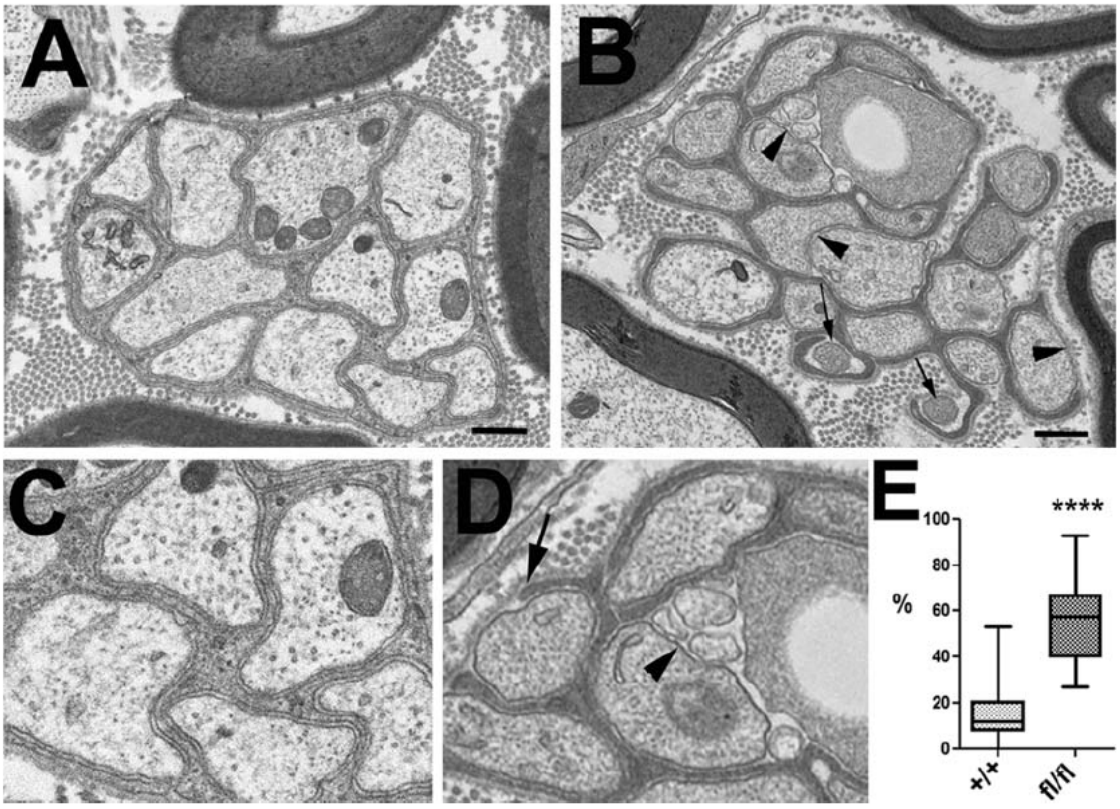

Figure 10: The conditional NTE knock-out results in incomplete glial wrapping of Remak fibers. (A, C) Electron microscopic image from a Remak bundle in a TAM treated NTE(+/+);Cre+ mouse. (B, D) Remak bundle in a TAM-treated NTE(fl/fl);Cre+ mouse. The arrowheads point to areas where the glial sheath is missing, arrows point to electron dense, shrunken axons. (D) Quantification showing the percentage of axons in a Remak bundle that are not completely wrapped by glia. The horizontal line represents the medians, boxes denote the 25% and 75% quartiles, and whiskers express 10% and 90% quantiles. Twenty Remak bundles were analyzed per genotype, with two mice used for each experiment. Scale bar=500 nm. ***p<0.0001 (Student's t-test).

References

Abou-Donia MB. 2003. Organophosphorus ester-induced chronic neurotoxicity. Arch Environ Health 58(8):484-97.

Akassoglou K, Malester B, Xu J, Tessarollo L, Rosenbluth J, Chao MV. 2004. Brain-specific deletion of neuropathy target esterase/swisscheese results in neurodegeneration. Proc Natl Acad Sci U S A 101(14):5075-80.

Berg A, Zelano J, Pekna M, Wilhelmsson U, Pekny M, Cullheim S. 2013. Axonal regeneration after sciatic nerve lesion is delayed but complete in GFAP- and vimentin-deficient mice. PLoS One 8(11):e79395.

Berger BL, Gupta R. 2006. Demyelination secondary to chronic nerve compression injury alters Schmidt-Lanterman incisures. J Anat 209(1):111-8.

Berger P, Niemann A, Suter U. 2006. Schwann cells and the pathogenesis of inherited motor and sensory neuropathies (Charcot-Marie-Tooth disease). Glia 54(4):243-257.

Berti C, Bartesaghi L, Ghidinelli M, Zambroni D, Figlia G, Chen ZL, Quattrini A, Wrabetz L, Feltri ML. 2011. Non-redundant function of dystroglycan and beta1 integrins in radial sorting of axons. Development 138(18):4025-37.

Birchmeier C, Nave KA. 2008. Neuregulin-1, a key axonal signal that drives Schwann cell growth and differentiation. Glia 56(14):1491-7.

Chang P-A, Chen R, Wu Y-J. 2005. Reduction of neuropathy target esterase does not affect neuronal differentiation, but moderate expression induces neuronal differentiation in human neuroblastoma (SK-N-SH) cell line. Molecular Brain Research 141(1):30-38.

Deik A, Johannes B, Rucker JC, Sanchez E, Brodie SE, Deegan E, Landy K, Kajiwara Y, Scelsa S, Saunders-Pullman R and others. 2014. Compound heterozygous PNPLA6 mutations cause Boucher-Neuhauser syndrome with late-onset ataxia. J Neurol 261(12):2411-23.

Dutta S, Rieche F, Eckl N, Duch C, Kretzschmar D. 2015. Glial expression of Swiss-cheese (SWS), the *Drosophila* orthologue of Neuropathy Target Esterase, is required for neuronal ensheathment and function. Dis Model Mech.

Dutta S, Rieche F, Eckl N, Duch C, Kretzschmar D. 2016. Glial expression of Swiss cheese (SWS), the *Drosophila* orthologue of neuropathy target esterase (NTE), is required for neuronal ensheathment and function. Dis Model Mech 9(3):283-94.

Dyer KR, Jortner BS, Shell LG, Ehrich M. 1992. Comparative dose-response studies of organophosphorus ester-induced delayed neuropathy in rats and hens administered mipafox. Neurotoxicology 13(4):745-55.

Emerick GL, DeOliveira GH, dos Santos AC, Ehrich M. 2012. Mechanisms for consideration for intervention in the development of organophosphorus-induced delayed neuropathy. Chem Biol Interact 199(3):177-84.

Feltri ML, Poitelon Y, Previtali SC. 2015. How Schwann Cells Sort Axons: New Concepts. Neuroscientist.

Freeman MR, Doherty J. 2006. Glial cell biology in *Drosophila* and vertebrates. Trends Neurosci 29(2):82-90.

Fricker FR, Zhu N, Tsantoulas C, Abrahamsen B, Nassar MA, Thakur M, Garratt AN, Birchmeier C, McMahon SB, Wood JN and others. 2009. Sensory axon-derived neuregulin-1 is required for axoglial signaling and normal sensory function but not for long-term axon maintenance. J Neurosci 29(24):7667-78.

Ghabriel MN, Allt G. 1979. The role of Schmidt-Lanterman incisures in Wallerian degeneration. Acta Neuropathologica 48(2):83-93.

Ghabriel MN, Allt G. 1980. Schmidt-Lanterman Incisures. I. A quantitative teased fibre study of remyelinating peripheral nerve fibres. Acta Neuropathol 52(2):85-95.

Ghasemlou N, Jeong SY, Lacroix S, David S. 2007. T cells contribute to lysophosphatidylcholine-induced macrophage activation and demyelination in the CNS. Glia 55(3):294-302.

Glynn P. 2006. A mechanism for organophosphate-induced delayed neuropathy. Toxicol Lett 162(1):94-7.

Glynn P. 2007. Axonal degeneration and neuropathy target esterase. Arh Hig Rada Toksikol 58(3):355-8.

Glynn P. 2012. Neuronal phospholipid deacylation is essential for axonal and synaptic integrity. Biochim Biophys Acta.

Glynn P. 2013. Neuronal phospholipid deacylation is essential for axonal and synaptic integrity. Biochim Biophys Acta 1831(3):633-41.

Glynn P, Holton JL, Nolan CC, Read DJ, Brown L, Hubbard A, Cavanagh JB. 1998. Neuropathy target esterase: immunolocalization to neuronal cell bodies and axons. Neuroscience 83(1):295-302.

Gorlewicz A, Wlodarczyk J, Wilczek E, Gawlak M, Cabaj A, Majczynski H, Nestorowicz K, Herbik MA, Grieb P, Slawinska U and others. 2009. CD44 is expressed in non-myelinating Schwann cells of the adult rat, and may play a role in neurodegeneration-induced glial plasticity at the neuromuscular junction. Neurobiology of Disease 34(2):245-258.

Gupta R, Nassiri N, Hazel A, Bathen M, Mozaffar T. 2012. Chronic nerve compression alters Schwann cell myelin architecture in a murine model. Muscle & nerve 45(2):231-241.

Hufnagel RB, Arno G, Hein ND, Hersheson J, Prasad M, Anderson Y, Krueger LA, Gregory LC, Stoetzel C, Jaworek TJ and others. 2015. Neuropathy target esterase impairments cause Oliver-McFarlane and Laurence-Moon syndromes. J Med Genet 52(2):85-94.

Jessen KR, Mirsky R. 1997. Embryonic Schwann cell development: the biology of Schwann cell precursors and early Schwann cells. Journal of Anatomy 191(Pt 4):501-505.

Jessen KR, Mirsky R. 2005. The origin and development of glial cells in peripheral nerves. Nat Rev Neurosci 6(9):671-682.

Jessen KR, Morgan L, Stewart HJ, Mirsky R. 1990. Three markers of adult non-myelin-forming Schwann cells, 217c(Ran-1), A5E3 and GFAP: development and regulation by neuron-Schwann cell interactions. Development 109(1):91-103.

Johnson MK. 1969. The delayed neurotoxic effect of some organophosphorus compounds: identification of the phosphorylation site as an esterase. T Biochem J 114:711-714.

Jung J, Cai W, Lee HK, Pellegatta M, Shin YK, Jang SY, Suh DJ, Wrabetz L, Feltri ML, Park HT. 2011. Actin polymerization is essential for myelin sheath fragmentation during Wallerian degeneration. The Journal of neuroscience: the official journal of the Society for Neuroscience 31(6):2009-2015.

Kaplan S, Odaci E, Unal B, Sahin B, Fornaro M. 2009. Chapter 2: Development of the peripheral nerve. Int Rev Neurobiol 87:9-26.

Klein D, Groh J, Wettmarshausen J, Martini R. 2014. Nonuniform molecular features of myelinating Schwann cells in models for CMT1: Distinct disease patterns are associated with NCAM and c-Jun upregulation. Glia 62(5):736-750.

Kmoch S, Majewski J, Ramamurthy V, Cao S, Fahiminiya S, Ren H, MacDonald IM, Lopez I, Sun V, Keser V and others. 2015. Mutations in PNPLA6 are linked to photoreceptor degeneration and various forms of childhood blindness. Nat Commun 6:5614.

Koltzenburg M, Scadding J. 2001. Neuropathic pain. Curr Opin Neurol 14(5):641-7.

Kretzschmar D, Hasan G, Sharma S, Heisenberg M, Benzer S. 1997. The swiss cheese mutant causes glial hyperwrapping and brain degeneration in *Drosophila*. J Neurosci 17(19):7425-32.

Lariviere RC, Nguyen MD, Ribeiro-da-Silva A, Julien JP. 2002. Reduced number of unmyelinated sensory axons in peripherin null mice. J Neurochem 81(3):525-32.

Li Y, Dinsdale D, Glynn P. 2003. Protein domains, catalytic activity, and subcellular distribution of neuropathy target esterase in Mammalian cells. J Biol Chem 278(10):8820-5.

Lioy DT, Garg SK, Monaghan CE, Raber J, Foust KD, Kaspar BK, Hirrlinger PG, Kirchhoff F, Bissonnette JM, Ballas N and others. 2011. A role for glia in the progression of Rett's syndrome. Nature 475(7357):497-500.

Martini R. 1994. Expression and functional roles of neural cell surface molecules and extracellular matrix components during development and regeneration of peripheral nerves. J Neurocytol 23(1):1-28.

Martini R, Schachner M. 1986. Immunoelectron microscopic localization of neural cell adhesion molecules (L1, N-CAM, and MAG) and their shared carbohydrate epitope and myelin basic protein in developing sciatic nerve. J Cell Biol 103(6 Pt 1):2439-48.

Martini R, Schachner M. 1997. Molecular bases of myelin formation as revealed by investigations on mice deficient in glial cell surface molecules. Glia 19(4):298-310.

Michalczyk K, Ziman M. 2005. Nestin structure and predicted function in cellular cytoskeletal organization. Histol Histopathol 20(2):665-71.

Miner JH, Patton BL, Lentz SI, Gilbert DJ, Snider WD, Jenkins NA, Copeland NG, Sanes JR. 1997. The Laminin α Chains: Expression, Developmental Transitions, and Chromosomal Locations of α1-5, Identification of Heterotrimeric Laminins 8–11, and Cloning of a Novel α3 Isoform. The Journal of Cell Biology 137(3):685-701.

Mirsky R, Jessen KR. 2009. Schwann Cell Development A2 - Squire, Larry R. Encyclopedia of Neuroscience. Oxford: Academic Press. p 463-473.

Monk KR, Feltri ML, Taveggia C. 2015. New insights on Schwann cell development. Glia 63(8):1376-93.

Moser M, Li Y, Vaupel K, Kretzschmar D, Kluge R, Glynn P, Buettner R. 2004. Placental failure and impaired vasculogenesis result in embryonic lethality for neuropathy target esterase-deficient mice. Mol Cell Biol 24(4):1667-79.

Moser M, Stempfl T, Li Y, Glynn P, Buttner R, Kretzschmar D. 2000. Cloning and expression of the murine sws/NTE gene. Mech Dev 90(2):279-82.

Muhlig-Versen M, da Cruz AB, Tschape JA, Moser M, Buttner R, Athenstaedt K, Glynn P, Kretzschmar D. 2005. Loss of Swiss cheese/neuropathy target esterase activity causes disruption of phosphatidylcholine homeostasis and neuronal and glial death in adult *Drosophila*. J Neurosci 25(11):2865-73.

Nave KA, Salzer JL. 2006. Axonal regulation of myelination by neuregulin 1. Curr Opin Neurobiol 16(5):492-500.

Neuberger TJ, Cornbrooks CJ. 1989. Transient modulation of Schwann cell antigens after peripheral nerve transection and subsequent regeneration. J Neurocytol 18(5):695-710.

Newbern J, Birchmeier C. 2010. Nrg1/ErbB signaling networks in Schwann cell development and myelination. Semin Cell Dev Biol 21(9):922-8.

Parascandola J. 1995. The Public Health Service and Jamaica ginger paralysis in the 1930s. Public Health Reports 110(3):361-363.

Patton BL, Connoll AM, Martin PT, Cunningham JM, Mehta S, Pestronk A, Miner JH, Sanes JR. 1999. Distribution of ten laminin chains in dystrophic and regenerating muscles. Neuromuscul Disord 9(6-7):423-33.

Pope CN, Tanaka D, Jr., Padilla S. 1993. The role of neurotoxic esterase (NTE) in the prevention and potentiation of organophosphorus-induced delayed neurotoxicity (OPIDN). Chem Biol Interact 87(1-3):395-406.

Quistad GB, Barlow C, Winrow CJ, Sparks SE, Casida JE. 2003. Evidence that mouse brain neuropathy target esterase is a lysophospholipase. Proc Natl Acad Sci U S A 100(13):7983-7.

Rainier S, Bui M, Mark E, Thomas D, Tokarz D, Ming L, Delaney C, Richardson RJ, Albers JW, Matsunami N and others. 2008. Neuropathy target esterase gene mutations cause motor neuron disease. Am J Hum Genet 82(3):780-5.

Raphael AR, Lyons DA, Talbot WS. 2011. ErbB signaling has a role in radial sorting independent of Schwann cell number. Glia 59(7):1047-55.

Read DJ, Li Y, Chao MV, Cavanagh JB, Glynn P. 2009. Neuropathy target esterase is required for adult vertebrate axon maintenance. J Neurosci 29(37):11594-600.

Salzer JL. 2003. Polarized domains of myelinated axons. Neuron 40(2):297-318.

Salzer JL, Brophy PJ, Peles E. 2008. Molecular domains of myelinated axons in the peripheral nervous system. Glia 56(14):1532-1540.

Schachner M, Bartsch U. 2000. Multiple functions of the myelin-associated glycoprotein MAG (siglec-4a) in formation and maintenance of myelin. Glia 29(2):154-165.

Sherman LS, Rizvi TA, Karyala S, Ratner N. 2000. Cd44 Enhances Neuregulin Signaling by Schwann Cells. The Journal of Cell Biology 150(5):1071-1084.

Sleeman JP, Arming S, Moll JF, Hekele A, Rudy W, Sherman LS, Kreil G, Ponta H, Herrlich P. 1996. Hyaluronate-independent Metastatic Behavior of CD44 Variant-expressing Pancreatic Carcinoma Cells. Cancer Research 56(13):3134-3141.

Stewart HJS, Rougon G, Dong Z, Dean C, Jessen KR, Mirsky R. 1995. TGF-βs upregulate NCAM and L1 expression in cultured Schwann cells, suppress cyclic AMP–induced expression of O4 and galactocerebroside, and are widely expressed in cells of the Schwann cell lineage in vivo. Glia 15(4):419-436.

Synofzik M, Gonzalez MA, Lourenco CM, Coutelier M, Haack TB, Rebelo A, Hannequin D, Strom TM, Prokisch H, Kernstock C and others. 2014a. PNPLA6

mutations cause Boucher-Neuhauser and Gordon Holmes syndromes as part of a broad neurodegenerative spectrum. Brain 137(Pt 1):69-77.

Synofzik M, Kernstock C, Haack TB, Schols L. 2014b. Ataxia meets chorioretinal dystrophy and hypogonadism: Boucher-Neuhauser syndrome due to PNPLA6 mutations. J Neurol Neurosurg Psychiatry.

Taveggia C, Zanazzi G, Petrylak A, Yano H, Rosenbluth J, Einheber S, Xu X, Esper RM, Loeb JA, Shrager P and others. 2005. Neuregulin-1 type III determines the ensheathment fate of axons. Neuron 47(5):681-94.

Topaloglu AK, Lomniczi A, Kretzschmar D, Dissen GA, Kotan LD, McArdle CA, Koc AF, Hamel BC, Guclu M, Papatya ED and others. 2014. Loss-of-function mutations in PNPLA6 encoding neuropathy target esterase underlie pubertal failure and neurological deficits in Gordon Holmes syndrome. J Clin Endocrinol Metab 99(10):E2067-75.

Trapp BD. 1990. Myelin-associated glycoprotein. Location and potential functions. Ann N Y Acad Sci 605:29-43.

Triolo D, Dina G, Lorenzetti I, Malaguti M, Morana P, Del Carro U, Comi G, Messing A, Quattrini A, Previtali SC. 2006. Loss of glial fibrillary acidic protein (GFAP) impairs Schwann cell proliferation and delays nerve regeneration after damage. J Cell Sci 119(Pt 19):3981-93.

Ushiki T, Ide C. 1987. Scanning electron microscopic studies of the myelinated nerve fibres of the mouse sciatic nerve with special reference to the Schwann cell cytoplasmic network external to the myelin sheath. J Neurocytol 16(6):737-47.

van Tienhoven M, Atkins J, Li Y, Glynn P. 2002. Human neuropathy target esterase catalyzes hydrolysis of membrane lipids. J Biol Chem 277(23):20942-8.

Velasco M, O'Sullivan C, Sheridan GK. 2016. Lysophosphatidic acid receptors (LPARs): Potential targets for the treatment of neuropathic pain. Neuropharmacology.

Wentzell JS, Cassar M, Kretzschmar D. 2014. Organophosphate-induced changes in the PKA regulatory function of Swiss Cheese/NTE lead to behavioral deficits and neurodegeneration. PLoS One 9(2):e87526.

Woodhoo A, Sommer L. 2008. Development of the Schwann cell lineage: from the neural crest to the myelinated nerve. Glia 56(14):1481-90.

Yu WM, Yu H, Chen ZL, Strickland S. 2009. Disruption of laminin in the peripheral nervous system impedes nonmyelinating Schwann cell development and impairs nociceptive sensory function. Glia 57(8):850-9.

Yuan A, Sasaki T, Kumar A, Peterhoff CM, Rao MV, Liem RK, Julien J-P, Nixon RA. 2012. Peripherin Is a Subunit of Peripheral Nerve Neurofilaments: Implications for Differential Vulnerability of CNS and PNS Axons. The Journal of Neuroscience 32(25):8501-8508.

Zaccheo O, Dinsdale D, Meacock PA, Glynn P. 2004. Neuropathy target esterase and its yeast homologue degrade phosphatidylcholine to glycerophosphocholine in living cells. J Biol Chem.

References

Abe, T., Lu, X., Jiang, Y., Boccone, C.E., Qian, S., Vattem, K.M., Wek, R.C., Walsh, J.P., 2003. Site-directed mutagenesis of the active site of diacylglycerol kinase alpha: calcium and phosphatidylserine stimulate enzyme activity via distinct mechanisms. Biochem. J. 375, 673–80. Https://doi.org/10.1042/BJ20031052

Akassoglou, K., Malester, B., Xu, J., Tessarollo, L., Rosenbluth, J., Chao, M. V, 2004. Brain-specific deletion of neuropathy target esterase/swiss cheese results in neurodegeneration. Proc. Natl. Acad. Sci. U. S. A. 101, 5075–80. Https://doi.org/10.1073/pnas.0401030101

Atkins, J., Glynn, P., 2000. Membrane association of and critical residues in the catalytic domain of human neuropathy target esterase. J. Biol. Chem. 275, 24477–83. Https://doi.org/10.1074/jbc.M002921200

Baum, D., 2003. Jake Leg Annals of Epidemiology. New Yorker 79, 50.

Beebe, S.J., 1994. The camp-dependent protein kinases and camp signal transduction. Semin. Cancer Biol. 5, 285–294.

Benzer, S., 1967. BEHAVIORAL MUTANTS OF *Drosophila* ISOLATED BY COUNTERCURRENT DISTRIBUTION. Proc. Natl. Acad. Sci. 58, 1112–1119. Https://doi.org/10.1073/pnas.58.3.1112

Bettencourt da Cruz, A., Wentzell, J., Kretzschmar, D., 2008. Swiss Cheese, a protein involved in progressive neurodegeneration, acts as a noncanonical regulatory subunit for PKA-C3. J. Neurosci. 28, 10885–92. Https://doi.org/10.1523/JNEUROSCI.3015-08.2008

Blaschke, R.J., Monaghan, a P., Bock, D., Rappold, G. A, 2000. A novel murine PKA-related protein kinase involved in neuronal differentiation. Genomics 64, 187–94. Https://doi.org/10.1006/geno.2000.6116

Cao, Y., Chtarbanova, S., Petersen, A.J., Ganetzky, B., 2013. Dnr1 mutations cause neurodegeneration in *Drosophila* by activating the innate immune response in the brain. Proc. Natl. Acad. Sci. U. S. A. 110, E1752-60. Https://doi.org/10.1073/pnas.1306220110/-/dcsupplemental.www.pnas.org/cgi/doi/10.1073/pnas.1306220110

Carter, B., 1930. Jake Leg Blues.

Cassar, M., Issa, A.R., Riemensperger, T., Petitgas, C., Rival, T., Coulom, H., Iché-Torres, M., Han, K.A., Birman, S., 2015. A dopamine receptor contributes to paraquat-induced neurotoxicity in *Drosophila*. Hum. Mol. Genet. 24, 197–212. Https://doi.org/10.1093/hmg/ddu430

Cavanagh, J.B., 1954. THE TOXIC EFFECTS OF TRI-ORTHO-CRESYL PHOSPHATE ON THE NERVOUS SYSTEM.

Debattisti, V., Pendin, D., Ziviani, E., Daga, A., Scorrano, L., 2014. Reduction of endoplasmic reticulum stress attenuates the defects caused by *Drosophila* mitofusin depletion. J. Cell Biol. 204, 303–312. Https://doi.org/10.1083/jcb.201306121

Deik, A., Johannes, B., Rucker, J.C., Sanchez, E., Brodie, S.E., Deegan, E., Landy, K., Kajiwara, Y., Scelsa, S., Saunders-Pullman, R., Paisan-Ruiz, C., 2014. Compound heterozygous PNPLA6 mutations cause Boucher-Neuhauser syndrome with late-onset ataxia. J. Neurol. 261, 2411–2423. Https://doi.org/10.1007/s00415-014-7516-3

Dutta, S., Rieche, F., Eckl, N., Duch, C., Kretzschmar, D., 2016. Glial expression of Swiss cheese (SWS), the *Drosophila* orthologue of neuropathy target esterase (NTE), is required for neuronal ensheathment and function. Dis. Model. Mech. 9, 283 LP-294.

Elia, A.E., Lalli, S., Monsurrï, M.R., Sagnelli, A., Taiello, A.C., Reggiori, B., La Bella, V., Tedeschi, G., Albanese, A., 2016. Tauroursodeoxycholic acid in the treatment of patients with amyotrophic lateral sclerosis. Eur. J. Neurol. 23, 45–52. https://doi.org/10.1111/ene.12664

Fu, S., Yang, L., Li, P., Hofmann, O., Dicker, L., Hide, W., Lin, X., Watkins, S.M., Ivanov, A.R., Hotamisligil, G.S., 2011. Aberrant lipid metabolism disrupts calcium homeostasis causing liver endoplasmic reticulum stress in obesity. Nature 473, 528–531. Https://doi.org/10.1038/nature09968

Gailey, D.A., Jackson, F.R., Siegel, R.W., 1982. Male courtship in *Drosophila*: The conditioned response to immature males and its genetic control. Genetics 102, 771–782.

Glynn, P., 2000. Neural development and neurodegeneration: two faces of neuropathy target esterase. Prog. Neurobiol. 61, 61–74.

Glynn, P., Holton, J.L., Nolan, C.C., Read, D.J., Brown, L., Hubbard, A., Cavanagh, J.B., 1998. Neuropathy target esterase: Immunolocalization to neuronal cell bodies and axons. Neuroscience 83, 295–302. Https://doi.org/https://doi.org/10.1016/S0306-4522(97)00388-6

Golic, K.G., Golic, M.M., 1996. Engineering the *Drosophila* genome: chromosome rearrangements by design. Genetics 144, 1693–1711.

Götz, K.G., 1980. Visual Guidance in *Drosophila*, in: Siddiqi, O., Babu, P., Hall, L.M., Hall, J.C. (Eds.), Development and Neurobiology of *Drosophila*. Basic Life Sciences, Springer, Boston, MA.

Gramates, L.S., Marygold, S.J., Dos Santos, G., Urbano, J.M., Antonazzo, G., Matthews, B.B., Rey, A.J., Tabone, C.J., Crosby, M.A., Emmert, D.B., Falls, K., Goodman, J.L., Hu, Y., Ponting, L., Schroeder, A.J., Strelets, V.B., Thurmond, J., Zhou, P., Perrimon, N., Gelbart, S.R., Extavour, C., Broll, K., Zytkovicz, M., Brown, N.H., Attrill, H., Costa, M., Fexova, S., Jones, T., Larkin, A., Millburn, G.H., Staudt, N., Kaufman, T., Grumbling, G.B., Cripps, R., Werner-Washburne, M., Baker, P., 2017. Flybase at 25: Looking to the future. Nucleic Acids Res. 45, D663–D671. Https://doi.org/10.1093/nar/gkw1016

Hanks, S.K., Hunter, T., 1995. The eukaryotic protein kinase superfamily: kinase (catalytic) domain structure and classification. FASEB J. 9, 576–596.

Hetz, C., Mollereau, B., 2014. Disturbance of endoplasmic reticulum proteostasis in neurodegenerative diseases. Nat. Rev. Neurosci. 15, 233.

Hou, N.S., Gutschmidt, A., Choi, D.Y., Pather, K., Shi, X., Watts, J.L., Hoppe, T., Taubert, S., 2014. Activation of the endoplasmic reticulum unfolded protein response by lipid disequilibrium without disturbed proteostasis in vivo. Proc. Natl. Acad. Sci. U. S. A. 111, E2271-80. Https://doi.org/10.1073/pnas.1318262111

Huang, S., Li, Q., Alberts, I., Li, X., 2016. PRKX, a Novel cAMP-Dependent Protein Kinase Member, Plays an Important Role in Development. J. Cell. Biochem. 117, 566–573. Https://doi.org/10.1002/jcb.25304

Inoue, H., Yoshioka, T., 1997. Purification of a regulatory subunit of type II camp-dependent protein kinase from *Drosophila* heads. Biochem. Biophys. Res. Commun. 235, 223–226. Https://doi.org/10.1006/bbrc.1997.6764

Jiang, H., Lkhagva, A., Chae, H., Simo, L., Jung, S., Yoon, Y., Lee, N., Seong, J.Y., Park, Y., Kim, Y., 2013. Natalisin, a tachykinin-like signaling system, regulates sexual activity and fecundity in insects. Https://doi.org/10.1073/pnas.1310676110/-/dcsupplemental.www.pnas.org/cgi/doi/10.1073/pnas.1310676110

Johnson, M.K., 1974. The primary biochemical lesion leading to the delayed neurotoxic effects of some organophosphorus esters. J. Neurochem. 785–789. Https://doi.org/10.1111/j.1471-4159.1974.tb04404.x

Johnson, M.K., 1992. 10 - Molecular events in delayed neuropathy: experimental aspects of neuropathy target esterase, Clinical and Experimental Toxicology of Organophosphates and Carbamates. Butterworth-Heinemann Ltd. Https://doi.org/http://dx.doi.org/10.1016/B978-0-7506-0271-6.50016-4

JOHNSON, M.K., 1982. THE TARGET FOR INITIATION OF DELAYED NEUROTOXICITY BY ORGANOPHOSPHORUS ESTERS: BIOCHEMICAL STUDIES AND TOXICOLOGICAL APPLICATIONS. Rev. Biochem. Toxicol. 4, 141–212.

Kalderon, D., Rubin, G.M., 1988. Isolation and characterization of *Drosophila* camp-dependent protein kinase genes. Genes Dev. 2, 1539–1556.

Kaneko, M., Desai, B.S., Cook, B., 2014. Ionic leakage underlies a gain-of-function effect of dominant disease mutations affecting diverse P-type ATPases. Nat. Genet. 46, 144–151. Https://doi.org/10.1038/ng.2850

Kang, S., Dahl, R., Hsieh, W., Shin, A., Zsebo, K.M., Buettner, C., Hajjar, R.J., Lebeche, D., 2016. Small molecular allosteric activator of the sarco/endoplasmic reticulum Ca2+-ATPase (SERCA) attenuates diabetes and metabolic disorders. J. Biol. Chem. 291, 5185–5198. Https://doi.org/10.1074/jbc.M115.705012

Kienesberger, P.C., Oberer, M., Lass, A., Zechner, R., 2009. Mammalian patatin domain containing proteins: a family with diverse lipolytic activities involved in multiple biological functions. J. Lipid Res. 50, S63–S68. Https://doi.org/10.1194/jlr.R800082-JLR200

Klichko, V.I., Orr, W.C., Radyuk, S.N., 2016. The role of peroxiredoxin 4 in inflammatory response and aging. Biochim. Biophys. Acta - Mol. Basis Dis. 1862, 265–273. Https://doi.org/10.1016/j.bbadis.2015.12.008

Klink, A., Schiebel, K., Winkelmann, M., Rao, E., Horsthemke, B., Ludecke, H.J., Claussen, U., Scherer, G., Rappold, G., 1995. The human protein kinase gene PKX1 on Xp22.3 displays Xp/Yp homology and is a site of chromosomal instability. Hum. Mol. Genet. 4, 869–878.

Kmoch, S., Majewski, J., Ramamurthy, V., Cao, S., Fahiminiya, S., Ren, H., macdonald, I.M., Lopez, I., Sun, V., Keser, V., Khan, a., Stránecký, V., Hartmannová, H., Přistoupilová, a., Hodaňová, K., Piherová, L., Kuchař, L., Baxová, a., Chen, R., Barsottini, O.G.P., Pyle, a., Griffin, H., Splitt, M., Sallum, J., Tolmie, J.L., Sampson, J.R., Chinnery, P., Boycott, K., mackenzie, A., Brudno, M., Bulman, D., Dyment, D., Banin, E., Sharon, D., Dutta, S., Grebler, R., Helfrich-Foerster, C., Pedroso, J.L., Kretzschmar, D., Cayouette, M., Koenekoop, R.K., 2015. Mutations in PNPLA6 are linked to photoreceptor degeneration and various forms of childhood blindness. Nat. Commun. 6, 5614. https://doi.org/10.1038/ncomms6614

Koh, K., Kobayashi, F., Miwa, M., Shindo, K., Isozaki, E., Ishiura, H., Tsuji, S., Takiyama, Y., 2015. Novel mutations in the PNPLA6 gene in Boucher-Neuhauser syndrome. J. Hum. Genet. 60, 217–220. Https://doi.org/10.1038/jhg.2015.3

Kretzschmar, D., Hasan, G., Sharma, S., Heisenberg, M., Benzer, S., 1997. The swiss cheese mutant causes glial hyperwrapping and brain degeneration in *Drosophila*. J. Neurosci. 17, 7425–32.

Krishnan, N., Kretzschmar, D., Rakshit, K., Chow, E., Giebultowicz, J.M., 2009. The circadian clock gene period extends health span in aging <italic>*Drosophila* melanogaster</italic>. Aging (Albany. NY). 1, 937–948. Https://doi.org/10.18632/aging.100103

Lagace, T.A., Ridgway, N.D., 2013. The role of phospholipids in the biological activity and structure of the endoplasmic reticulum. Biochim. Biophys. Acta - Mol. Cell Res. 1833, 2499–2510. Https://doi.org/https://doi.org/10.1016/j.bbamcr.2013.05.018

Lane, M.E., Kalderon, D., 1994. RNA localization along the anteroposterior axis of the *Drosophila* oocyte requires PKA-mediated signal transduction to direct normal microtubule organization. Genes Dev. 8, 2986–2995.

Langdahl, J.H., Frederiksen, A.L., Nguyen, N., Brusgaard, K., Juhl, C.B., 2017. Boucher Neuhauser Syndrome - A rare cause of inherited hypogonadotropic hypogonadism. A case of two adult siblings with two novel mutations in PNPLA6. Eur. J. Med. Genet. 60, 105–109. Https://doi.org/10.1016/j.ejmg.2016.11.003

Li, W., Yu, Z.X., Kotin, R.M., 2005. Profiles of PRKX expression in developmental mouse embryo and human tissues. J. Histochem. Cytochem. 53, 1003–1009. Https://doi.org/10.1369/jhc.4A6568.2005

Lush, M.J., Li, Y., Read, D.J., Willis, a C., Glynn, P., 1998. Neuropathy target esterase and a homologous *Drosophila* neurodegeneration-associated mutant protein contain a novel domain conserved from bacteria to man. Biochem. J. 332 (Pt 1, 1–4. Https://doi.org/10.1074/jbc.M605790200

Mayford, M., Abel, T., Kandel, E.R., 1995. Transgenic approaches to cognition. Curr. Opin. Neurobiol. 5, 141–148.

Mei, Y., Thompson, M.D., Cohen, R.A., Tong, X., 2013. Endoplasmic Reticulum Stress and Related Pathological Processes. J. Pharmacol. Biomed. Anal. 1, 1000107.

Meléndez, A., Li, W., Kalderon, D., Melendez, A., Li, W., Kalderon, D., 1995. Activity, expression and function of a second *Drosophila* protein kinase A catalytic subunit gene. Genetics 141, 1507–20.

Mollereau, B., Manié, S., Napoletano, F., 2014. Getting the better of ER stress. J. Cell Commun. Signal. 8, 311–321. Https://doi.org/10.1007/s12079-014-0251-9

Morgan, J.P., Penovich, P., 1978. Jamaica ginger paralysis. Forty-seven-year follow-up. Arch. Neurol. 35, 530–532.

Moser, M., Li, Y., Vaupel, K., Kretzschmar, D., Kluge, R., Glynn, P., Buettner, R., 2004. Placental failure and impaired vasculogenesis result in embryonic lethality for neuropathy target esterase-deficient mice. Mol. Cell. Biol. 24, 1667–1679. Https://doi.org/10.1128/MCB.24.4.1667-1679.2004

Moser, M., Stempfl, T., Li, Y., Glynn, P., Büttner, R., Kretzschmar, D., 2000. Cloning and expression of the murine sws/NTE gene. Mech. Dev. 90, 279–282. Https://doi.org/https://doi.org/10.1016/S0925-4773(99)00239-7

Mühlig-Versen, M., da Cruz, A.B., Tschäpe, J.-A., Moser, M., Büttner, R., Athenstaedt, K., Glynn, P., Kretzschmar, D., 2005. Loss of Swiss cheese/neuropathy target esterase activity causes disruption of phosphatidylcholine homeostasis and neuronal and glial death in adult *Drosophila*. J. Neurosci. 25, 2865–73. Https://doi.org/10.1523/JNEUROSCI.5097-04.2005

Nichols, C.D., Becnel, J., Pandey, U.B., 2012. Methods to Assay *Drosophila* Behavior. J. Vis. Exp. 3–7. Https://doi.org/10.3791/3795

Pan, D., Rubin, G.M., 1995. Camp-dependent protein kinase and hedgehog act antagonistically in regulating decapentaplegic transcription in *Drosophila* imaginal discs. Cell 80, 543–552.

Paran, C.W., Zou, K., Ferrara, P.J., Song, H., Turk, J., Funai, K., 2015. Lipogenesis mitigates dysregulated sarcoplasmic reticulum calcium uptake in muscular dystrophy. Biochim. Biophys. Acta - Mol. Cell Biol. Lipids 1851, 1530–1538. Https://doi.org/https://doi.org/10.1016/j.bbalip.2015.09.001

Paschen, W., Mengesdorf, T., 2005. Endoplasmic reticulum stress response and neurodegeneration. Cell Calcium 38, 409–415. Https://doi.org/https://doi.org/10.1016/j.ceca.2005.06.019

Petersen, A.J., Katzenberger, R.J., Wassarman, D. A, 2013. The innate immune response transcription factor relish is necessary for neurodegeneration in a *Drosophila* model of ataxia-telangiectasia. Genetics 194, 133–42. Https://doi.org/10.1534/genetics.113.150854

Pfaffl, M.W., 2001. A new mathematical model for relative quantification in real-time RT-PCR. Nucleic Acids Res. 29, 45e–45. Https://doi.org/10.1093/nar/29.9.e45

Quistad, G.B., Barlow, C., Winrow, C.J., Sparks, S.E., Casida, J.E., 2003. Evidence that mouse brain neuropathy target esterase is a lysophospholipase. Proc. Natl. Acad. Sci. U. S. A. 100, 7983–7. Https://doi.org/10.1073/pnas.1232473100

Rainier, S., Albers, J.W., Dyck, P.J., Eldevik, O.P., Wilcock, S., Richardson, R.J., Fink, J.K., 2011. Motor neuron disease due to neuropathy target esterase gene mutation: clinical features of the index families. Muscle Nerve 43, 19–25. Https://doi.org/10.1002/mus.21777

Read, D.J., Li, Y., Chao, M. V, Cavanagh, J.B., Glynn, P., 2009. Neuropathy target esterase is required for adult vertebrate axon maintenance. J. Neurosci. 29, 11594–600. Https://doi.org/10.1523/JNEUROSCI.3007-09.2009

Rodrigues, C.M.P., Solá, S., Sharpe, J.C., Moura, J.J.G., Steer, C.J., 2003. Tauroursodeoxycholic acid prevents Bax-induced membrane perturbation and cytochrome c release in isolated mitochondria. Biochemistry 42, 3070–3080. Https://doi.org/10.1021/bi026979d

Roman, G., Davis, R.L., 2001. Molecular biology and anatomy of *Drosophila* olfactory associative learning. Bioessays 23, 571–581. Https://doi.org/10.1002/bies.1083

Roussel, B.D., Kruppa, A.J., Miranda, E., Crowther, D.C., Lomas, D.A., Marciniak, S.J., 2013. Endoplasmic reticulum dysfunction in neurological disease. Lancet Neurol. 12, 105–118. Https://doi.org/https://doi.org/10.1016/S1474-4422(12)70238-7

Schoemaker, M.H., Conde De La Rosa, L., Buist-Homan, M., Vrenken, T.E., Havinga, R., Poelstra, K., Haisma, H.J., Jansen, P.L.M., Moshage, H., 2004. Tauroursodeoxycholic acid protects rat hepatocytes from bile acid-induced apoptosis via activation of survival pathways. Hepatology 39, 1563–1573. Https://doi.org/10.1002/hep.20246

Skoulakis, E.M., Kalderon, D., Davis, R.L., 1993. Preferential expression in mushroom bodies of the catalytic subunit of protein kinase A and its role in learning and memory. Neuron 11, 197–208.

Strauss, R., Heisenberg, M., 1993. A higher control center of locomotor behavior in the *Drosophila* brain. J. Neurosci. 13, 1852–1861.

Synofzik, M., Gonzalez, M. A, Lourenco, C.M., Coutelier, M., Haack, T.B., Rebelo, A., Hannequin, D., Strom, T.M., Prokisch, H., Kernstock, C., Durr, A., Schöls, L., Lima-Martínez, M.M., Farooq, A., Schüle, R., Stevanin, G., Marques, W., Züchner, S., 2014. PNPLA6 mutations cause Boucher-Neuhauser and Gordon Holmes syndromes as part of a broad neurodegenerative spectrum. Brain 137, 69–77. Https://doi.org/10.1093/brain/awt326

Taylor, S.S., Kornev, A.P., 2011. Protein kinases: Evolution of dynamic regulatory proteins. Trends Biochem. Sci. 36, 65–77. Https://doi.org/10.1016/j.tibs.2010.09.006

Tenev, T., Zachariou, A., Wilson, R., Paul, A., Meier, P., 2002. Jafrac2 is an IAP antagonist that promotes cell death by liberating Dronc from DIAP1. EMBO J. 21, 5118–5129.

Topaloglu, A.K., Lomniczi, A., Kretzschmar, D., Dissen, G.A., Kotan, L.D., mcardle, C.A., Koc, A.F., Hamel, B.C., Guclu, M., Papatya, E.D., Eren, E., Mengen, E., Gurbuz, F., Cook, M., Castellano, J.M., Kekil, M.B., Mungan, N.O., Yuksel, B., Ojeda, S.R., 2014. Loss-of-function mutations in PNPLA6 encoding neuropathy target esterase underlie pubertal failure and neurological deficits in Gordon Holmes syndrome. J. Clin. Endocrinol. Metab. 99, E2067–E2075. Https://doi.org/10.1210/jc.2014-1836

Van Tienhoven, M., Atkins, J., Li, Y., Glynn, P., 2002. Human neuropathy target esterase catalyzes hydrolysis of membrane lipids. J. Biol. Chem. 277, 20942–20948. Https://doi.org/10.1074/jbc.M200330200

Verkhratsky, A., 2005. Physiology and Pathophysiology of the Calcium Store in the Endoplasmic Reticulum of Neurons. Physiol. Rev. 85, 201–279. Https://doi.org/10.1152/physrev.00004.2004

Walsh, D.A., Van Patten, S.M., 1994. Multiple pathway signal transduction by the camp-dependent protein kinase. FASEB J. Off. Publ. Fed. Am. Soc. Exp. Biol. 8, 1227–1236.

Wentzell, J.S., Cassar, M., Kretzschmar, D., 2014. Organophosphate-induced changes in the PKA regulatory function of Swiss Cheese/NTE lead to behavioral deficits and neurodegeneration. Plos One 9, e87526. Https://doi.org/10.1371/journal.pone.0087526

Wiethoff, S., Bettencourt, C., Paudel, R., Madon, P., Liu, Y.-T., Hersheson, J., Wadia, N., Desai, J., Houlden, H., 2017. Pure Cerebellar Ataxia with Homozygous Mutations in the PNPLA6 Gene. Cerebellum 16, 262–267. Https://doi.org/10.1007/s12311-016-0769-x

Winrow, C.J., Hemming, M.L., Allen, D.M., Quistad, G.B., Casida, J.E., Barlow, C., 2003. Loss of neuropathy target esterase in mice links organophosphate exposure to hyperactivity. Nat. Genet. 33, 477–85. Https://doi.org/10.1038/ng1131